UNIVERSITÀ DEGLI STUDI DI PADOVA

Dipartimento di Ingegneria dell'Informazione

Scuola di Dottorato di Ricerca in Ingegneria dell'Informazione

Indirizzo Scienza e Tecnologia dell'Informazione (I.C.T.)
XXII Ciclo

Efficient Management of HVAC Systems

Direttore della scuola: Ch.mo Prof. Matteo Bertocco

Supervisore: Ch.mo Prof. Alessandro Beghi

Dottorando: Mirco Rampazzo

Padova, 31 Gennaio, 2010

Efficient Management of HVAC Systems

Mirco Rampazzo

Ai miei genitori

"If being human is not simply a matter of being born of flesh and blood, if it is instead a way of thinking, acting and feeling, then I am hopeful that one day I will discover my own humanity. Until that, Commander Maddox, I will continue learning, changing, growing, and trying to become more than what I am."

Commander Data from *Star Trek*

Contents

Abstract

In HVAC (Heating, Ventilation and Air Conditioning) plants of medium-high cooling capacity, multiple-chiller systems are often employed. In such systems, chillers are independent of each other in order to provide standby capacity, operational flexibility, and less disruption maintenance. However, the problem of an efficiently managing of multiple-chiller systems is complex in many respects. In particular, the electrical energy consumption in the chiller plant markedly increases if the chillers are managed improperly, therefore significant energy savings can be achieved by optimizing the chiller operations of HVAC systems.

In this Thesis an unified method for Multi-Chiller Management optimization is presented, that deals simultaneously with the Optimal Chiller Loading and Optimal Chiller Sequencing problems. The main objective is that of reducing both power consumption and operative costs. The approach is based on a cooling load estimation algorithm, and the optimization step is performed by means of a multi-phase genetic algorithm, that provides an efficient and suitable approach to solve this kind of complex multi-objective optimization problem. The performance of the algorithm is evaluated by resorting to a dynamic simulation environment, developed in MATLAB™ and SIMULINK™, where the plant dynamics are accurately described. It is shown that the proposed algorithm gives superior performance with respect to standard approaches, in terms of both energy performance and load profile tracking.

Keywords: HVAC, energy saving, multiple chiller, optimization, optimal chiller loading, optimal chiller sequencing, genetic algorithm(s).

Sommario

Negli impianti HVAC di capacità frigorifera medio-grande vengono spesso impiegati sistemi con più refrigeratori di liquido (chiller) in parallelo. Il problema della gestione efficiente di tali sistemi è complesso sotto diversi punti di vista. In particolare, il consumo di energia elettrica dell'impianto aumenta notevolmente allorché i refrigeratori siano gestiti scorrettamente. In questa Tesi viene presentato un metodo unificato per l'ottimizzazione della gestione di chiller in parallelo che risolve simultaneamente i problemi del carico ottimo e della sequenza ottima di accensioni/spegnimenti relativi ai refrigeratori. L'obiettivo principale è quello ridurre il consumo energetico ed abbassare i costi di esercizio. L'approccio si basa su un algoritmo di stima del carico frigorifero richiesto e l'ottimizzazione è realizzata attraverso l'impiego di un algoritmo genetico multi-fase; quest'ultimo fornisce un approccio efficiente per risolvere questo genere di problema di ottimo multi-obiettivo. Le prestazioni dell'algoritmo sono valutate ricorrendo ad un ambiente di simulazione dinamico, sviluppato in MATLAB™ e SIMULINK™, dove le dinamiche del sistema sono accuratamente descritte. Si evince che l'algoritmo proposto fornisce prestazioni superiori, rispetto agli approcci standard, sia in termini di soddisfacimento del carico che di prestazione energetica.

Parole chiave: HVAC, risparmio energetico, chiller, ottimizzazione, ripartizione ottima del carico, sequenza ottima accensioni, algoritmi genetici.

Acknowledgements

First of all, I express my deepest gratitude to my advisor prof. Alessandro Beghi for his patient guidance, encouragement and excellent advice throughout this study at the Department of Information Engineer (DEI), University of Padova.

I am profound obliged with dr. Luca Cecchinato of the Department of Technical Physics, University of Padova, for his constant support. I would like to thank dr. Manuel Chiarello and dr. Massimiliano Scarpa.

I would like to express my gratitude to my Scholarship Sponsor Rhoss S.p.A for financing my studies. In particular, I thank dr. Michele Albieri, dr. Marco Pozzati and dr. Alessandro Scodellaro.

I am thankful to my colleagues Marco Bertinato, Paolo Ticozzi and Giovanni Cosi. A special thanks to the GROOD (a DEI Doctoral Students Group) and to Giulia, Alberto, Saverio, Francesca, Simone, Ruggero, Damiano, Lucia, Federica, Stefano, Alessandro, Enrico, Giulio, Mattia, Maura, Martina.

Also, I am thankful to my friends Francesco Gambato for his encouragement and Lorena Marchioro for her assistance on editing my Thesis writing.

And last but not least I would like to express my gratitude to prof. Mauro Bisiacco, since without his patient guidance and helpful encouragement my experience as a DEI Doctoral Student would has not been possible.

At the end of all, I take this opportunity to express my profound gratitude to my beloved parents and friends for their moral support and patience during all my studies.

Introduction

In Heating, Ventilation, and Air Conditioning (HVAC) systems equipped with vapour compression liquid chillers, the electrical energy consumption of the refrigerating unit far exceeds all that required by the other system components. Moreover, the electrical energy consumption in the chiller plant markedly increases if the chillers are managed improperly, therefore significant energy savings can be achieved by optimizing the chiller operation of HVAC systems.

In HVAC plants of medium-high cooling capacity, multiple-chiller systems [1] are more common than single-chiller systems (for the same reason that most commercial airplanes have more than one engine) and they are developed as a trade off between reliability and cost. In such system, every chiller is independent of each other to provide standby capacity, operational flexibility, and less disruption maintenance. Compared with a single-chiller system, the multiple-chiller system has a reduced starting in-rush current and a reduced power cost under part load conditions [2]. For instance, large chilled water plants at health-care and institutional facilities are excellent candidates for this type of solution. However, the capacity regulation and part load efficiency of each chiller (and therefore of the entire system) strongly depends on the refrigerating unit, refrigerant circuit design, type and number of compressors. For instance, multi-scroll chillers equipped with twin compressors on the same circuit present high part load Energy Efficiency Ratio values (EER, defined as the ratio of cooling capacity and total power absorption, fans included), whereas screw compressors units are strongly penalized, mainly because of the reduction of screw compressor isentropic efficiency at low cooling loads. Therefore, the problem of efficiently managing multiple-chiller systems is getting more and more important. A commonly used simple approach is to turn on/off chillers sequentially, following changes in demand, without considering any kind of performance measure associated with energy savings.

In [3] an optimal switch-point method is proposed for deciding whether or not another chiller must be switched on/off, based on the fact that the EER curve as a function of the part load ratio (PLR, defined as the cooling load ratio the chillers total cooling capacity) is a concave function. In this way, the load is distributed evenly on the chillers. This method assumes that capacities and characteristic curves of chillers are equal, and that only one chiller at a time can be connected/disconnected to the system. Since it is difficult to determine the switch point when cooling capacities of the chillers differ substantially, the resulting average loading amount is clearly non optimal. A simple workaround to this problem is presented in [4], where it is suggested to turn on the chiller with Maximal Peak Coefficient Of Performance (COP), when the activation of another chiller is required (MPCOP method). Again, this method is not optimal.

Recently, methods for Optimal Chiller Loading (OCL) and Optimal Chiller Sequencing (OCS) have been proposed. In [5] a genetic algorithm is employed to solve OCL problems with high accuracy and within a rapid frame rate. In [6] a simulated annealing approach is proposed for the same problem. In [7] a branch and bound method and the Lagrangian method are used to solve optimal chiller operations. In [8] a dynamic programming technique is proposed to solve the OCS problem and to eliminate the deficiencies of the conventional methods. However, most of these and other [9] [10] literature methods are heterogeneous: OCL and OCS problems are worked out differently. This can increase the complexity of the algorithms and decrease their accuracy and robustness, especially if the number of chillers involved is large and, more generally, if the involved systems are complex. Since Multi-Chiller Management (MCM) optimization is a nonlinear, constrained, combinatorial optimization with both continuous and discrete variables, and as such, it is a challenge to standard optimization methods. Moreover, in the HVAC literature are presented methods to do on-line optimization, but these usually ignore or disregard the system dynamics. The optimal control changes through time in response to uncontrolled variables including the ambient conditions and cooling loads.

In this Thesis[1] an unified method for MCM optimization is presented, which deals simultaneously with the OCL and OCS problems, with the overall objective of reducing both power consumption and operative costs. The use of a cooling load estimation algorithm is proposed in combination with a Multi-Phase Genetic Algorithm (MPGA). It is shown that the MPGA represents an efficient and suitable approach to solve this kind of complex multi-objective optimization problem. The performance of the algorithm is evaluated by resorting to a dynamic simulation environment developed in MATLAB™ and SIMULINK™, where the plant dynamics

[1] This Thesis work is carried out within an industrial partnership with Rhoss S.p.A., Codroipo (UD), Italy.

are accurately described. In fact, the MCM optimized method works dynamically, therefore it has been developed and tested under dynamic plant operation. The results of the simulations indicate that the proposed algorithm gives superior performance with respect to standard approaches (sequential strategy and symmetric strategy), in terms of both energy performance and load profile following.

Main contributions

As regards the study of multiple chiller systems, the contributions are twofold. First, an unified method for MCM optimization is developed, that deals simultaneously with the OCL and OCS problems, where energy analysis of the HVAC plant at part load condition is considered. The use of a cooling load estimation algorithm is proposed in combination with a Multi-Phase Genetic Algorithm. Second, we provide to design a dynamic simulation environment, where the plant dynamics are accurately described. This work achieved three papers and one patent:

- A. Beghi, M. Bertinato, L. Cecchinato, and M. Rampazzo. *A multi-phase genetic algorithm for the efficient management of multi-chiller systems.* In Proceedings of the 7th Asian Control Conference, Hong Kong, China, August 27-29, 2009.

- M. Albieri, A. Beghi, L. Cecchinato, and M. Rampazzo. G*estione ottima di sistemi con refrigeratori in parallelo mediante un algoritmo genetico multi-fase.* 47th AICARR Interational Conference, Roma-Tivoli, Ocotober 8-9, 2009.

- A. Beghi, L. Cecchinato, and M. Rampazzo. *A multi-phase genetic algorithm for the efficient management of multi-chiller systems.* Submitted to Energy Conversion and Management, May 9, 2009.

- M. Albieri, A. Beghi, M. Bertinato, L. Cecchinato, M. Rampazzo and A. Zen. *Metodo e sistema per controllare una pluralità di macchine frigorifere di un impianto di climatizzazione.* Submitted patent, Rhoss S.p.A. (Codroipo-Italy), 2009.

As concerns a collaboration with Carel S.p.A (Padova-Italy), an algorithm for evaporator control by means of electronic expansion valve is developed. This work carried out one paper:

- A. Beghi, L. Cecchinato and M. Rampazzo. *On-line, auto-tuning regulation of Electronic Expansion Valve for evaporator control.* In Proceedings of the 7th IEEE International Conference on Control & Automation (ICCA'09), December 9-11, 2009, Christchurch, New Zealand.

Thesis outline

In Chapter 1 a brief overview of Heating, Ventilation and Air Conditioning systems is presented.

In Chapter 2 the control and optimization of HVAC systems are dealt with reference to the thermal comfort and the energy aspects.

In Chapter 3 the multiple chiller systems are illustrated. In HVAC plants of medium-high cooling capacity, multiple chiller systems are more common than single-chiller systems.

In Chapter 4 the mathematical model of a multiple chiller system with primary-secondary architecture is derived.

In Chapter 5 the Optimal Chiller Loading (OCL) and the Optimal Chiller Sequencing problems are presented. Moreover, the energy analysis at part load condition is introduced.

In Chapter 6 an unified method for multiple chiller management is presented; it deals simultaneously with the OCL and OCS problems, with the overall objective of reducing both power consumption and operative costs. The use of a cooling load estimation algorithm is proposed in combination with a Multi-Phase Genetic Algorithm.

In Chapter 7 the proposed strategy is evaluated by resorting to a dynamic simulation environment developed in MATLAB™ and SIMULINK™. The simulations related to a case study are reported with performance analysis. Finally a brief analysis of the computational cost of the algorithm is illustrated by resorting to simulation examples.

1 HVAC systems

The mechanical heating or cooling load in a building is dependent upon the various heat gains and losses experienced by the building including solar and internal heat gains and heat gains or losses due to transmission through the building envelope and infiltration (or ventilation) of outside air. The primary purpose of the heating, ventilating, and air-conditioning (HVAC) system in a building is to regulate the dry-bulb air temperature, humidity and air quality by adding or removing heat energy. Due to the nature of the energy forces which play upon the building and the various types of mechanical systems which can be used in non-residential buildings, there is very little relationship between the heating or cooling load and the energy consumed by the HVAC system. There are many reasons why energy is consumed and wasted in HVAC systems for non residential buildings. These reasons fall into a variety of categories, including energy conversion technologies, system type selection, the use or misuse of outside air, and control strategies.

1.1 HVAC system types

The energy efficiency of systems used to heat and cool buildings varies widely but is generally a function of the details of the system organization. On the most simplistic level the amount of energy consumed is a function of the source of heating or cooling energy, the amount of energy consumed in distribution, and whether the working fluid is simultaneously heated and cooled. System efficiency is also highly dependent upon the directness of control, which can sometimes overcome system inefficiency. HVAC system types can be typically classified according to their energy efficiency as highly efficient, moderately efficient or generally inefficient. This terminology indicates only the comparative energy consumption of typical systems when compared to each other. Figure 1.1 shows the relative efficiency of the more commonly used types of HVAC systems discussed below. The range of actual energy

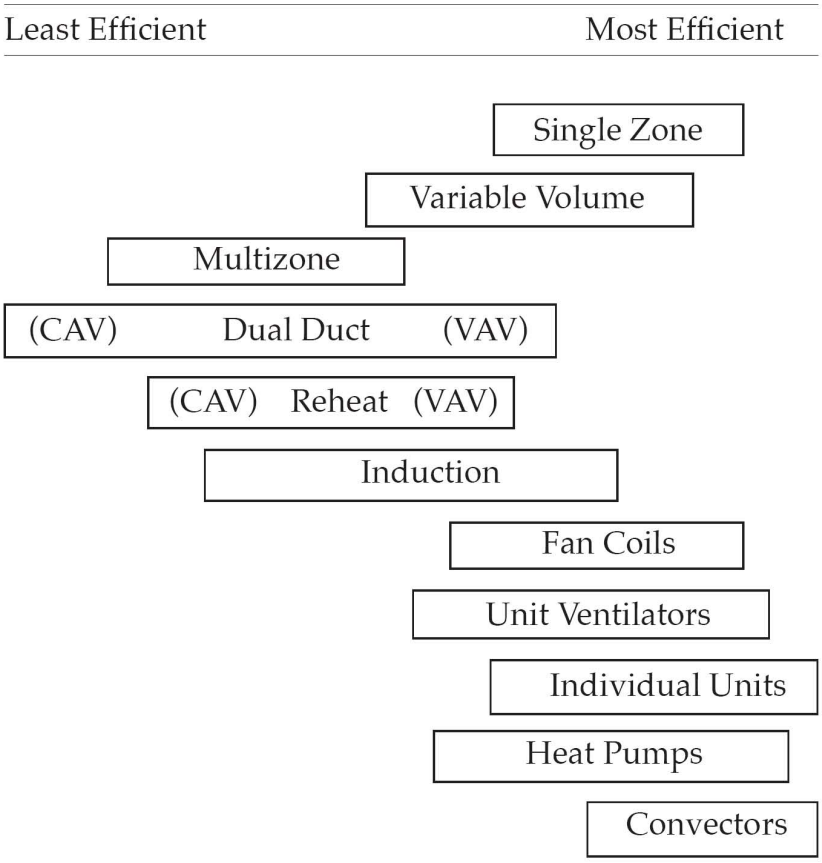

Figure 1.1: Relative energy efficiency of air-conditioning systems.

consumption for each system type is a function of other design variables including how the system is configured and installed in a particular building as well as how it is controlled and operated. To maximize the efficiency of any type of HVAC system, it is important to select efficient equipment, minimize the energy consumed in distribution and avoid simultaneous heating and cooling of the working fluid [11]. It is equally important that the control system directly controls the variable parameters of the system. Most HVAC systems include zones, which are areas within the building which may have different climatic and/or internal thermal loads and for which heat can be supplied or extracted independent of other zones.

1.1.1 All-air systems

The most common types of systems for heating and cooling buildings are those which moderate the air temperature of the occupied space by providing a supply of heated or cooled air from a central source via a network of air ducts. These systems, referred to as all-air systems, increase or decrease the space temperature by altering either the volume or temperature of the air supplied. Recalling that the most important

determinant of thermal comfort in a warm environment is air velocity, most buildings which require cooling employ all-air systems. Consequently, all-air systems are the system of choice when cooling is required. All-air systems also provide the best control of outside fresh air, air quality, and humidity control. An added benefit of forced air systems is that they can often use outside air for cooling interior spaces while providing heating for perimeter spaces. The advantages of all-air systems are offset somewhat by the energy consumed in distribution. All-air systems tend to be selected when comfort cooling is important and for thermally heavy buildings which have significant internal cooling loads which coincide with heating loads imposed by heat loss through the building envelope. The components of an all-air HVAC system include an air-handling unit (AHU) which includes a fan, coils which heat and/or cool the air passing through it, filters to clean the air, and often elements to humidify the air. Dehumidification, when required, is accomplished by cooling the air below the dew-point temperature. The conditioned air from the AHU is supplied to the occupied spaces by a network of supply-air ducts and air is returned from conditioned spaces by a parallel network of return-air ducts. The AHU and its duct system also includes a duct which supplies fresh outside air to the AHU and one which can exhaust some or all of the return air to the outside.

1.1.1.1 Single duct systems

The majority of all-air HVAC systems employ a single network of supply air ducts which provide a continuous supply of either warmed or cooled air to the occupied areas of the building.

- **Single Zone.** The single duct, single-zone system is the simplest of the all-air HVAC systems. It is one of the most energy-efficient systems as well as one of the least expensive to install. It uses a minimum of distribution energy[1], since equipment is typically located within or immediately adjacent to the area which it conditions. The system is directly controlled by a thermostat which turns the AHU on and off as required by the space temperature. Single zone systems can provide either heating or cooling, but provide supply air at the same volume and temperature to the entire zone which they serve. This limits their applicability to large open areas with few windows and uniform heating and cooling loads. Typical applications are department stores, factory spaces, arenas and exhibit halls, and auditoriums.

- **Variable Air Volume**. The variable air volume (VAV) HVAC system functions much like the single zone system, with the exception that the temperature

[1]Distribution energy includes all of the energy used to move heat within the system by fans and pumps. Distribution energy is typically electrical energy.

of individual zones is controlled by a thermostat which regulates the volume of air that is discharged into the space. This arrangement allows a high degree of local temperature control at a moderate cost. Both installation cost and operating costs are only slightly greater than the single-zone system. The distribution energy consumed is increased slightly over that of a single-zone system due to the friction losses in VAV control devices, as well as the fact that the fan in the AHU must be regulated to balance the overall air volume requirements of the system. Fan regulation by inlet vanes or outlet dampers forces the fan to operate at less than its optimum efficiency much of the time. Consequently a variable speed fan drive is necessary to regulate output volume of the fan. For the system to function properly, it is necessary that air be supplied at a constant temperature, usually about 13°C. This requires indirect control of the supply air temperature with an accompanying decrease in control efficiency. Single-duct VAV systems can often provide limited heating by varying the amount of constant temperature air to the space. By reducing the cooling airflow, the space utilizes the lights, people and miscellaneous equipment to maintain the required space temperature. However, if the space requires more heat than can be supplied by internal heat gains, a separate or supplemental heating system must be employed. Single-duct VAV systems are the most versatile and have become the most widely used of all systems for heating and cooling large buildings. They are appropriate for almost any application except those requiring a high degree of control over humidity or air exchange.

- **Reheat systems**. Both the single-zone and single duct VAV systems can be modified into systems which provide simultaneous heating and cooling of multiple zones with the addition of reheat coils for each zone. These systems are identical in design to the foregoing systems up to the point where air enters the local duct-work for each zone. In a reheat system supply air passes through a reheat coil which usually contains hot water from a boiler. In a less efficient option, an electrical resistance coil can also be used for reheat. A local thermostat in each zone controls the temperature of the reheat coil, providing excellent control of the zone space temperature. Constant air volume (CAV) reheat systems are typically used in situations which require precise control of room temperature and/or humidity, often with constant airflow requirements, such as laboratories and medical facilities. Both the CAV and VAV reheat systems are inherently inefficient, representing the highest level of energy consumption of the all-air systems. This is due to the fact that energy is consumed to cool the supply air and then additional energy is consumed to

reheat it. In VAV reheat systems, the reheat coil is not activated unless the VAV controls are unable to meet local requirements for temperature control, and they are therefore somewhat more energy efficient than CAV reheat systems. Both CAV and VAV reheat systems can also be used with specialized controls to condition spaces with extremely rigid requirements for humidity control, such as museums, printing plants, textile mills and industrial process settings.

- **Multi-zone**. In a multi-zone system, each zone is served by a dedicated supply duct which connects it directly to a central air handling unit. In the most common type of multi-zone system, the AHU produces warm air at a temperature of about 38°C as well as cool air at about 13°C which are blended with dampers to adjust the supply air temperature to that called for by zone thermostats. In a variation of this system, a third neutral deck uses outside air as an economizer to replace warm air in the summer or cool air in the winter. In another variation, the AHU produces only cool air which is tempered by reheat coils located in the fan room. In this case, the hot deck may be used as a preheat coil. Multi-zone systems are among the least energy efficient, sharing the inherent inefficiency of reheat systems since energy is consumed to simultaneously heat and cool air which is mixed to optimize the supply air temperature. Since a constant volume of air is supplied to each zone, blended conditioned air must be supplied even when no heating or cooling is required. In addition, multi-zone systems require a great deal of space for ducts in the proximity of the AHU which restricts the number of zones. They also consume a great deal of energy in distribution, due to the large quantity of constant volume air required to meet space loads. These drawbacks have made multi-zone systems nearly obsolete except in relatively small buildings with only a few zones and short duct runs.

1.1.1.2 Dual duct systems

Dual duct systems are similar to the multi-zone concept in that both cool supply air and warm supply air are produced by a central AHU. But instead of blending the air in the fan room, separate hot-air ducts and cold-air ducts run parallel throughout the distribution network and air is mixed at terminal mixing boxes in each zone. The mixing boxes may include an outlet for delivering air directly to the space, or a duct may connect a branch network with air mixed to a common requirement. Dual duct systems require the greatest amount of space for distribution duct-work. In order to offset the spatial limitations imposed by this problem, dual duct systems often employ high velocity/high pressure supply ducts, which reduce the size (and

cost) of duct work, as well as the required floor-to-floor height. However this option increases the fan energy required for distribution. Their use is usually limited to buildings with very strict requirements for temperature and or humidity control.

- **Constant Volume Dual Duct**. For a long time, the only variation of the dual duct system was a CAV system, which functioned very much like the multi-zone system. This system exhibits the greatest energy consumption of any all-air system. In addition to the energy required to mix conditioned air even when no heating or cooling is required, it requires a great amount of distribution energy even when normal pressure and low air velocities are used. For these reasons it has become nearly obsolete, being replaced with dual duct VAV or other systems.

- **Dual Duct VAV**. Although the dual duct VAV system looks very much like its CAV counterpart, it is far more efficient. Instead of providing a constant volume of supply air at all times, the primary method of responding to thermostatic requirements is through adjusting the volume of either cool or warm supply air. The properly designed dual duct VAV system functions essentially as two single duct VAV systems operating side by side; one for heating and one for cooling. Except when humidity control is required it is usually possible to provide comfort at all temperatures without actually mixing the two air streams. Even when humidity adjustment is required a good control system can minimize the amount of air mixing required. The dual-duct VAV system still requires more distribution energy and space than most other systems. The level of indirect control which is necessary to produce heated and cooled air also increases energy consumption. Consequently its use should be restricted to applications which benefit from its ability to provide exceptional temperature and humidity control and which do not require a constant supply of ventilation air.

1.1.2 All-water systems

Air is not a convenient medium for transporting heat. A cubic metre of air weighs only about 1 kg at standard conditions (21°C, 101.325 kPa). With a specific heat of about (1005 J/(kg °C)), one cubic metre can carry less than 1231 J/°C temperature difference. By comparison, a cubic metre of water weighs 1000 kg and can carry 4186 kJ/°C.

Water can be used for transporting heat energy in both heating and cooling systems. It can be heated in a boiler to a temperature of 60 to 120 °C or cooled by a chiller to 4 to 10°C, and piped throughout a building to terminal devices which take

in or extract heat energy typically through finned coils. Steam can also be used to transport heat energy. Steam provides most of its energy by releasing the latent heat of vaporization (about 2260 kJ/kg). Thus one mass unit of steam provides as much heating as fifty units of water which undergo a 11°C temperature change. However, when water vaporizes, it expands in volume more than 1600 times. Consequently liquid water actually carries more energy per cubic metre than steam and therefore requires the least space for piping. All-water distribution systems provide flexible zoning for comfort heating and cooling and have a relatively low installed cost when compared to all-air systems. The minimal space required for distribution piping makes them an excellent choice for retrofit installation in existing buildings or in buildings with significant spatial constraints. The disadvantage to these systems is that since no ventilation air is supplied, all-water distribution systems provide little or no control over air quality or humidity and cannot avail themselves of some of the energy conservation approaches of all-air systems. Water distribution piping systems are described in terms of the number of pipes which are attached to each terminal device:

1. *One-pipe systems:* use the least piping by connecting all of the terminal units in a series loop. Since the water passes through each terminal in the system, its ability to heat or cool becomes progressively less at great distances from the boiler or chiller. Thermal control is poor and system efficiency is low.

2. *Two-pipe systems:* provide a supply pipe and a return pipe to each terminal unit, connected in parallel so that each unit (zone) can draw from the supply as needed. Efficiency and thermal control are both high, but the system cannot provide heating in one zone while cooling another. Four-pipe systems provide a supply and return pipe for both hot water and chilled water, allowing simultaneous heating and cooling along with relatively high efficiency and excellent thermal control. They are, of course, the most expensive to install, but are still inexpensive compared to all-air systems. Three-pipe systems employ separate supply pipes for heating and cooling but provide only a single, common return pipe. Mixing the returned hot water, at perhaps 60°C, with the chilled water return, at 13°C, is highly inefficient and wastes energy required to reheat or recool this water. Such systems should be avoided.

1.1.2.1 Radiant heating

Radiant energy is undoubtedly the oldest method of centrally heating buildings, dating to the era of the Roman Empire. Recalling that the most important determinant of thermal comfort when environmental conditions are too cool is the radiant temperature of the physical surroundings, radiant heating systems are among the

most economical, so long as the means of producing heat is efficient. The efficiency of radiant heating is a function primarily of the temperature, area and emissivity of the heat source and the distance between the radiant source and the observer. It is therefore essential that radiant heat sources be located so that they are not obstructed by other objects. Emissivity is an object's ability to absorb and emit thermal radiation, and is primarily related to color. Dark objects absorb and emit radiation better than light colored objects. There are three categories of radiant heating devices, classified according to the temperature of the source of heat. All may employ electric resistance heating elements, but are more energy-efficient if they employ combustion as a heat source. Low temperature radiant floors employ the entire floor area as a radiating surface by embedding hot water coils in the floor. The water temperature is typically less than 50°C. By distributing the heat energy uniformly though the floor, surface temperature is normally below 40°C. By increasing the temperature of the radiant surface its area can be reduced. In medium temperature radiant panels, hot water circulates through metal panels, heating them to a temperature of about 60°C. Consequently the panels must be located out-of-reach, usually on the ceiling or on upper walls. High temperature infrared heaters are typically gas-fired or oil-fired and are discussed below under packaged systems. Because they are not dependent upon maintaining a static room air temperature, radiant heating systems provide excellent thermal comfort and efficiency in spaces subject to large influxes of outside air, such as factories and warehouses. However they are slow to respond to sudden changes in thermal requirements and malfunctions may be difficult or awkward to correct. Another drawback to radiant systems is that they promote the stratification of room air, concentrating warm air near the ceiling.

1.1.2.2 Natural convection

The simplest all-water system is a system of hydronic (hot-water) convectors. In this system hot water from a boiler or steam-operated hot water converter is circulated through a finned tube, usually mounted horizontally behind a simple metal cover which provides an air inlet opening below the tube and an outlet above. Room air is drawn through the convector by natural convection where it is warmed in passing over the finned tube. A variation on the horizontal finned-tube hydronic convector is the cabinet convector, which occupies less perimeter space. A cabinet convector would have several finned tubes in order to transfer additional heat to the air passing through it. When this is still insufficient a small electric fan can be added, converting the convector to a unit heater. Although an electric resistance element can be used in place of the finned tube, the inefficiency of electric resistance heating should eliminate this option. Hydronic convectors are among the least expensive heating systems to operate as well as to install. Their use is limited, however, to

heating only and they do not provide ventilation, air filtration, nor humidity control. Hydronic convectors and unit heaters may be used alone in buildings where cooling and mechanical ventilation is not required or to provide heating of perimeter spaces in combination with an all-air cooling system. They are the most suitable type of system for providing heat to control condensation on large expanses of glass on exterior wall systems.

1.1.2.3 Fan-coils

A fan-coil terminal is essentially a small air-handling unit which serves a single space without a ducted distribution system; the main difference other than size is that fan coils generally do not have outside air and exhaust provisions. One or more independent terminals are typically located in each room connected to a supply of hot and/or chilled water. At each terminal, a fan in the unit draws room air (sometimes mixed with outside air) through a filter and blows it across a coil of hot water or chilled water and back into the room. Condensate which forms on the cooling coil must be collected in a drip pan and removed by a drain. Although most fan-coil units are located beneath windows on exterior walls, they may also be mounted horizontally at the ceiling, particularly for installations where cooling is the primary concern. Technically, a fan-coil unit with an outside air inlet is called a unit ventilator. Unit ventilators provide the capability of using cool outside air during cold weather to provide free cooling when internal loads exceed the heat lost through the building envelope. Fan-coil units and unit ventilators are directly controlled by local thermostats, often located within the unit, making this system one of the most energy efficient. Drawbacks to their use is a lack of humidity control and the fact that all maintenance must occur within the occupied space. Fan-coil units are typically used in buildings which have many zones located primarily along exterior walls, such as schools, hotels, apartments and office buildings. They are also an excellent choice for retrofitting air-conditioning into buildings with low floor-to-floor heights. Although a four-pipe fan-coil system can be used for a thermally heavy building with high internal loads, it suffers the drawback that the cooling of interior zones in warm weather must be carried out through active air-conditioning, since there is no supply of fresh (cool) outside air to provide free cooling separately. They are also utilized to control the space temperature in laboratories where constant temperature make-up air is supplied to all spaces.

1.1.2.4 Closed-loop heat pumps

Individual heat pumps have a number of drawbacks in nonresidential buildings. However, closed-loop heat pumps, more accurately called water-to-air heat pumps,

offer an efficient option for heating and cooling large buildings. Each room or zone contains a water-source heat pump which can provide heating or cooling, along with air filtration and the dehumidification associated with forced-air air-conditioning. The water source for all of the heat pumps in the building circulates in a closed piping loop, connected to a cooling tower for summer cooling and a boiler for winter heating. Control valves allow the water to bypass either or both of these elements when they are not needed. The primary energy benefit of closed-loop heat pumps is that heat removed from overheated interior spaces is used to provide heat for under-heated perimeter spaces during cold weather. Since the closed-loop heat pump system is an all-water, piped system, distribution energy is low, and since direct, local control is used in each zone, control energy is also minimized, making this system one of the most efficient. Although the typical lack of a fresh-air supply eliminates the potential for an economizer cycle, the heat recovery potential discussed above more than makes up for this drawback. Heat pump systems are expensive to install and maintenance costs are also high. Careful economic analysis is necessary to be sure that the energy savings will be great enough to offset the added installation and maintenance costs. Closed-loop heat pumps are most applicable to buildings such as hotels which exhibit a wide variety of thermal requirements along with simultaneous heating requirements in perimeter zones and large internal loads or chronically overheated areas such as kitchens and assembly spaces.

1.1.3 Air and water systems

Once commonly used in large buildings, induction systems employ terminal units installed at the exterior perimeter of the building, usually under windows. A small amount of fresh outside ventilation air is filtered, heated or cooled, and humidified or dehumidified by a central AHU and distributed throughout the building at high-velocity by small ducts. In each terminal unit, this primary air is discharged in such a way that it draws in a much larger volume of secondary air from the room, which is filtered and passed through a coil for additional heating or cooling . The use of primary air as the motive force eliminates the need for a fan in the induction unit. The cooling coil is often deliberately kept at a temperature greater than the dew point temperature of the room air which passes through it, eliminating the need for a condensate drain. Although the standard air-water induction system is a cooling-only system, room terminals can employ reheat coils to heat perimeter zones. Despite the high pressures and velocities required for the primary air distribution, distribution energy is minimized by the relatively small volume of primary air. But the energy saved in primary air distribution is more than offset by the energy consumed in the indirect control and distribution of cooling water, making

air-water induction systems among the least energy efficient. Air-water induction units tend to be noisy and the system provides negligible control of humidity. The applicability of these systems is limited to buildings with widely varying cooling or heating loads where humidity control is not necessary, such as office buildings. Concerns about indoor air quality limits their use as well.

1.1.4 Packaged systems

All of the systems described above may be classified as central air-conditioning systems in that they contain certain central elements, typically including a boiler, chiller and cooling tower. Many large buildings provide heating and cooling with distributed systems of unitary or packaged systems, where each package is a stand-alone system which provides all of the heating and cooling requirements for the area of the building which it serves. Individual units derive their energy from raw energy sources typically limited to electricity and natural gas. Since large pieces of equipment usually have higher efficiencies than smaller equipment, it might be thought that packaged systems are inherently inefficient when compared to central air-conditioning systems. Yet packaged systems actually use much less energy. There are several reasons for this. First, there is much less energy used in distribution. Fans are much smaller and pumps are essentially non-existent. In addition, control of the smaller packaged units is local and direct. Typically, the unit is either on or off, which can be a disadvantage when the space use requires that ventilation air not be turned off. However there are some advantages associated with this control flexibility. It allows individual thermal control and accurate metering of use. In addition, if equipment failure occurs it does not affect the entire building. A third reason for the energy efficiency of packaged systems involves the schedule of operation. While large equipment is more efficient overall, it only operates at this peak efficiency when it is running at full load. Small packaged units, due to their on/off operation, run at full load or not at all. In a central air-conditioning system, the central equipment must run whenever any zone requires heating or cooling, often far from its peak load, optimum efficiency conditions. A secondary advantage to the use of packaged systems is the advantage of diversity. The design of a large central air-conditioning system sometimes requires that a compromise be made between the ideal type of system for one part of a building and a different type of system for another. When packaged systems are employed, parts of a building with significantly different heating and cooling requirements can be served by different types of equipment. This will always provide improved thermal comfort, and often results in improved efficiency as well.

1.1.4.1 Packaged terminal air-conditioners

The most common type of packaged equipment is the packaged terminal air conditioner, often called a PTAC or incremental unit, due to the fact that increases in equipment can be made incrementally. Examples of PTACs are through-the-wall air-conditioners and single-zone rooftop equipment. Their use is limited to about 50 m^2 per unit. Individual air-to-air (air-source) heat pumps can also be installed as a packaged system. A heat pump is essentially a vapor-compression air-conditioner which can be reversed to extract heat from the outdoor environment and discharge it into the occupied space. A significant drawback to air-source heat pumps is that vapor compression refrigeration becomes inefficient when the evaporator is forced to extract heat from a source whose temperature is 0°C or below. In large systems, heat pumps can utilize a source of circulating water from which to extract heat during cold weather, so that the evaporator temperature never approaches 0°C. The circulating water would be heated in the coldest weather, and could be cooled by a cooling tower to receive rejected heat during warm weather. These closed-loop heat pumps are discussed under all-water systems above.

1.1.4.2 Unit heaters

Packaged heating-only units typically utilize electricity or natural gas as their primary source of energy. Electricity is the most expensive source of heat energy and should be avoided. Natural gas (or liquefied propane) provides a more economical source of heat when used in packaged unit heaters. Fan-forced unit heaters can disperse heat over a much larger area than packaged air-conditioners. They can distribute heat either vertically or horizontally and respond rapidly to changes in heating requirements. High temperature infrared radiant heaters utilize a gas flame to produce a high-temperature (over 260°C) source of radiant energy. Although they do not respond rapidly to changes in heating requirements, they are essentially immune to massive intrusion of cold outside air. Because they warm room surfaces and physical objects in the space, thermal comfort returns within minutes of an influx of cold air. HVAC systems may be central or distributed; all-air, all-water, or air-water (induction). Each system type has advantages and disadvantages, not the least important of which is its energy efficiency. An economic analysis should be conducted in selecting an HVAC system type and in evaluating changes in HVAC systems in response to energy concerns.

1.2 HVAC equipment

The elements which provide heating and cooling to a building can be categorized by their intended function. HVAC equipment is typically classified as heating equipment, including boilers, furnaces and unit heaters; cooling equipment, including chillers, cooling towers and air-conditioning equipment; and air distribution elements, primarily air-handling units (AHUs) and fans. Figure 1.2 depicts the typical energy cost distribution for a large commercial building which employs an all-air reheat-type HVAC system. Excluding the energy costs associated with lighting, kitchen and miscellaneous loads which are typically 25-30 percent of the total, the remaining energy can be divided into two major categories: the energy associated with heating and cooling and the energy consumed in distribution. The total energy consumed for HVAC systems is therefore dependent on the efficiency of individual components, the efficiency of distribution and the ability of the control system to accurately regulate the energy consuming components of the system so that energy is not wasted. The size (and heating, cooling, or air-moving capacity) of HVAC equipment is determined by the mechanical designer based upon a calculation of the peak internal and envelope loads. Since the peak conditions are arbitrary (albeit well-considered and statistically valid) and it is likely that peak loads will not occur simultaneously throughout a large building or complex requiring all equipment to operate at its rated capacity, it is common to specify equipment which has a total capacity slightly less than the peak requirement. This diversity factor varies with the function of the space. For example, a hospital or classroom building will use a higher diversity multiplier than an office building. In sizing heating equipment however, it is not uncommon to provide a total heating capacity from several units which exceeds the design heating load by as much as fifty percent. In this way it is assured that the heating load can be met at any time, even in the event that one unit fails to operate or is under repair. The selection of several boilers, chillers, or air-handling units whose capacities combine to provide the required heating and cooling capability instead of single large units allows one or more components of the system to be cycled off when loads are less than the maximum. This technique also allows off-hours use of specific spaces without conditioning an entire building.

1.2.1 Equipment efficiency

Efficiency, by definition, is the ratio of the energy output of a piece of equipment to its energy input, in like units to produce a dimensionless ratio. Since no equipment known can produce energy, efficiency will always be a value less than 1.0 (100%). Heating equipment which utilizes electric resistance appears at first glance to come closest to the ideal of 100 percent efficiency. In fact, every kilowatt of electrical power

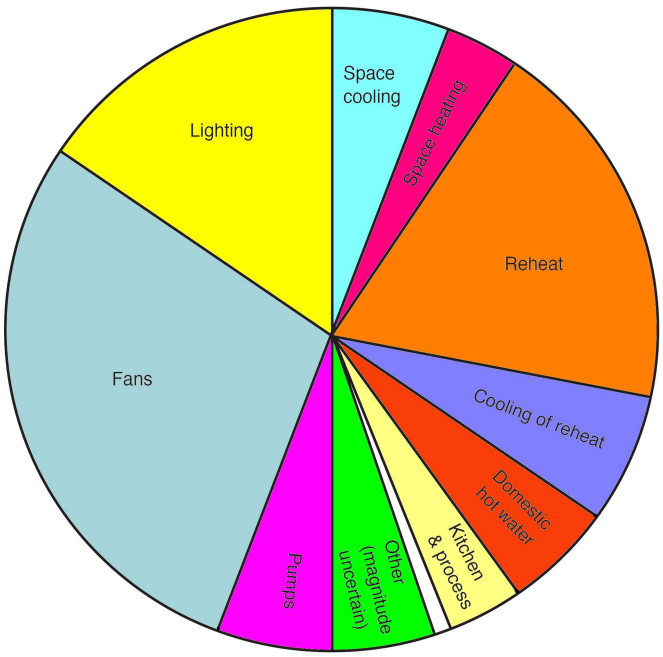

Figure 1.2: Energy cost distribution for a typical non-residential building using an all-air reheat HVAC system.

consumed in a building is ultimately converted to 3600 kJ per hour of heat energy. Since this is a valid unit conversion it can be said that electric resistance heating is 100 percent efficient. What is missing from the analysis however, is the inefficiency of producing electricity, which is most commonly generated using heat energy as a primary energy source. Electricity generation from heat is typically about 30 percent efficient, meaning that only 30 percent of the heat energy is converted into electricity, the rest being dissipated as heat into the environment. Energy consumed as part of the generation process and energy lost in distribution use up about ten percent of this, leaving only 27 percent of the original energy available for use by the consumer. By comparison, state-of-the-art heating equipment which utilizes natural gas as a fuel is more than eighty percent efficient. Distribution losses in natural gas pipelines account for another 5 percent, making natural gas approximately three times as efficient as a heat energy source than electricity. The relative efficiency of cooling equipment is usually expressed as a coefficient of performance (COP), which is defined as the ratio of the heat energy extracted to the mechanical energy input in like units. Since the heat energy extracted by modem air conditioning far exceeds the mechanical energy input a COP of up to 6 is possible. Air-conditioning equipment is also commonly rated by its energy efficiency ratio (EER) or seasonal energy efficiency ratio (SEER). EER is defined as the ratio of heat energy extracted[2] to the mechanical energy input in watts. Although it should have dimensions of

[2]Sometime expressed as Btu/hr; where Btu is the British thermal unit:$1\,\mathrm{Btu} \approx 1005\,J$

Btu/hr/watt, it is expressed as a dimensionless ratio. The EER efficiency term typically includes the energy requirement of auxiliary systems such as the indoor and outdoor fans.

Although neither COP nor EER is the efficiency of a chiller or air-conditioner, both are measures which allow the comparison of similar units. The term air-conditioning efficiency is commonly understood to indicate the extent to which a given air-conditioner performs to its maximum capacity. As discussed below, most equipment does not operate at its peak efficiency all of the time. For this reason, the seasonal energy efficiency ratio (SEER), which takes varying efficiency at partial load into account, is a more accurate measure of air-conditioning efficiency than COP or EER. In general, equipment efficiency is a function of size. Large equipment has a higher efficiency than small equipment of similar design. But the rated efficiency of this equipment does not tell the whole story. Equipment efficiency varies with the load imposed. Equipment operates at its optimum efficiency when operated at or near its design full-load condition. Both overloading and under-loading of equipment reduces equipment efficiency. This fact has its greatest impact on system efficiency when large systems are designed to air-condition an entire building or a large segment of a major complex. Since air-conditioning loads vary and since the design heating and cooling loads occur only rarely under the most severe weather or occupancy conditions, most of the time the system must operate under-loaded. When selected parts of a building are utilized for off-hours operation this requires that the entire building be conditioned or that the system operate far from its optimum conditions and thus at far less than its optimum efficiency. Since most heating and cooling equipment operates at less than its full rated load during most of the year, its part-load efficiency is of great concern. Because of this, most state-of-the-art equipment operates much closer to its full-load efficiency than does older equipment. A knowledge of the actual operating efficiency of existing equipment is important in recognizing economic opportunities to reduce energy consumption through equipment replacement.

1.3 Control and management

Control systems play a large part in the energy conservation potential of a HVAC system. To be effective at controlling energy use along with thermal comfort they must be used appropriately, work properly and be set correctly. Overheated or overcooled spaces not only waste energy, they are uncomfortable [12].

Computerized energy management and control systems provide an excellent means of reducing utility costs associated with maintaining environmental conditions in buildings. These systems can incorporate advanced control strategies that

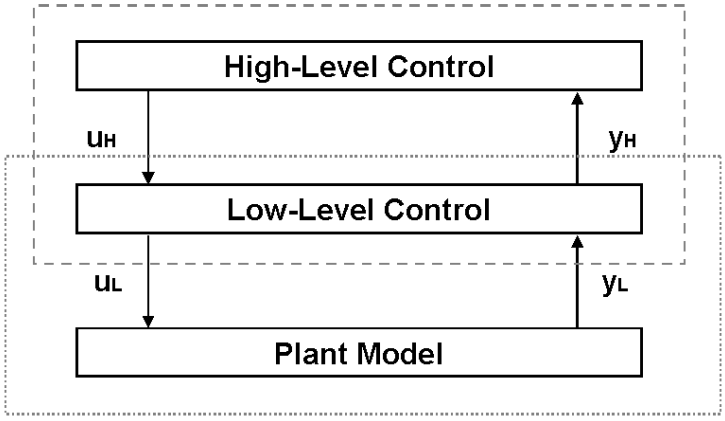

Figure 1.3: Two-level control structure.

respond to changing weather and building conditions and minimize operating costs.

HVAC systems are typically controlled using a two-level control structure (Figure 1.3). Low-level local-loop control of a single set point is provided by an actuator. For example, the supply air temperature from a cooling coil is controlled by adjusting the opening of a valve that provides chilled water to the coil[3]. The upper control level, supervisory control, specifies set points and other time-dependent modes of operation. The performance of large, commercial HVAC systems can be improved through better local-loop and supervisory control. Proper tuning of local-loop controllers can enhance comfort, reduce energy use, and increase component life. Set points and operating modes for cooling plant equipment can be adjusted by the supervisor to maximize overall operating efficiency. Dynamic control strategies for ice or chilled-water storage systems can significantly reduce on-peak electrical energy and demand costs to minimize total utility costs. Similarly, thermal storage inherent in a building's structure can be dynamically controlled to minimize utility costs. In general, strategies that take advantage of thermal storage work best when forecasts of future energy requirements are available.

Several local-loop controllers respond to load change to maintain specified set points. A supervisory controller establishes modes of operation and chooses (or resets) values of set points. At any given time, cooling or heating needs can be met with various combinations of modes of operation and set points.

[3]In Appendix D another example of low-level controller is reported. This work was carried out in collaboration with Carel S.p.A (Padova-Italy) during the author's PhD period and it deals with control algorithms for evaporator control by means of EEV (Electronic Expansion Valve).

2

Control and optimization of HVAC systems: comfort and energy aspects

Control systems are an integral part of many energy related processes. Control systems can be as simple as a residential thermostat, to very complex computer controlled systems for multiple buildings, to industrial process control. Their diligence and repeatability can also serve to maintain the savings of the project improvements for years, further justifying their existence by providing economic return to the customer.

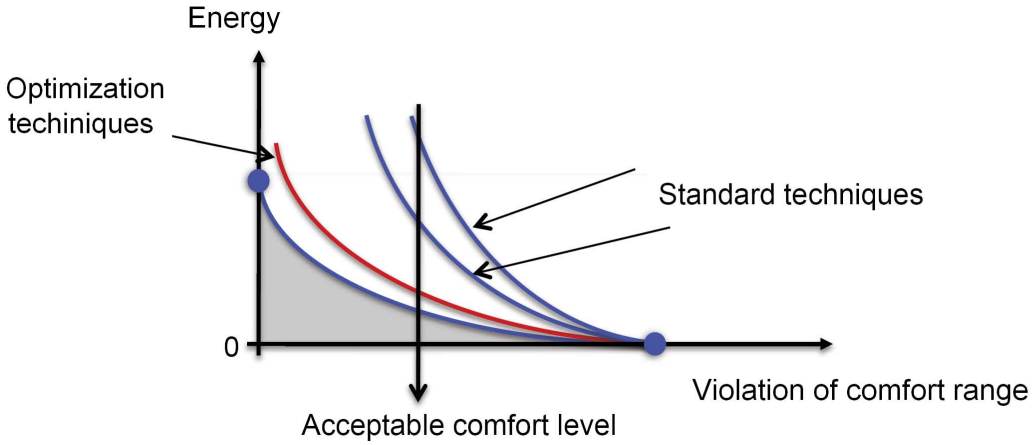

Figure 2.1: Energy-Violation of comfort

Heating, ventilating and air conditioning systems represents one of the most complex challenges for control and optimization. Non-stationary plant operating conditions resulting from low-frequency (seasonal) and high-frequency (diurnal) climate changes coupled with complex patterns of user demand combine with the intrinsically non linear characteristics endemic in HVAC plant to give one of the

more complex control applications known. Combined with the infinitely variable combination of user needs at the human interface, these swings in energy demand contribute to highly dynamic "environment" within control takes place. It comes as no surprise then much of HVAC control is about compromise: a balance that usually results in reasonable comfort at minimum energy use (Figure 2.1) and financial costs [11], [12].

2.1 Why control?

Control is important for many reasons:

- Regulation: many things need attention and adjustment to compensate for changing conditions, or varying demands. Examples of this are common in living organisms, such as body temperature, blood pressure, etc. Process control regulation is really just emulating the concepts of such natural processes. The field of automatic control is similar in that we *"continually adjust some device to cause a particular measured variable to remain at a desired state."* Examples:
  - The need to throttle heating and cooling equipment sized for maximum load that is effectively oversized at part load conditions.
  - Varying occupancy, and systems attendant to the occupants (lighting, ventilation).
  - Varying product throughput rate through manufacturing facilities.
  - Varying demands, and the need to maintain level or full state for water or fuel reservoirs, feed or coal bins, etc.
- Coordination: organizing or sequencing multiple processes in a logical and efficient manner is an important aspect of automatic control applications.
- Automation: human beings can make very good manual controllers because we can think on our feet and consider many variables together, but most control tasks are repetitive and suitable for mechanization. Automatic operation allows people to provide oversight of system operations and more effectively utilize their time.
- Consistency: manual control by people can be effective, although we are not all that repeatable and are sometimes forgetful. Using machinery for automatic control adds the improvement of consistent, repeatable operations. The repeatability and consistency feature of automatic control is very important in manufacturing.

- Conservation: supplemental enhancement control routines can be incorporated to reduce energy use while still maintaining good control. It is important to note that control systems do not necessarily reduce energy consumption, unless specifically applied and designed for that purpose.

2.2 Why optimization?

The Pareto principle (also known as 80-20 Rule) reminds us that we can usually hope to achieve 80 percent of the measure's potential with 20 percent of the difficulty, but the remaining portion requires much more effort. Optimization can be characterized as taking over where the basic controls left off and working on the remaining opportunities, the ones that are not as easy to attain. The appropriate use of optimization depends upon the customer's priorities, and these should be tested before the decision to optimize is made. Of course, from an energy conservation or ecology standpoint, we should all press for that last 20 percent. But if maximum simplicity controls that require only basic skills are a main focus of the customer, optimization may not be a good application. Similarly, projects where reliability is the first priority may be better served with basic control routines, allowing the extra 20 percent potential to slip away to gain the advantages of simplicity. Economics always comes into play, and some optimization projects (chasing the last 20 percent) may not have the attractive payback periods of their 80 percent counterparts. Most projects represent some balance of these interests, depending upon the needs of the customer. It is important to understand that optimization for maximum benefit will not be for everyone. A case in point for optimization is the subject of fixed set points, which are often a matter of convenience or approximation, and usually represent a compromise in optimal energy use. The more factors we can take into account, the closer to optimal will be the result, as stated by Liptak: *"... multivariable optimization is the approach of common sense. It is the control technique applied by nature, and frequently it is also the simplest and most elegant method of control."*[13]. To summarize, the desires for maximum simplicity and maximum efficiency are at odds with each other. A system that is perceived as being too complex will likely fall into disrepair and be bypassed or unplugged. If the customer is committed to squeezing their energy costs through optimization, they will need to also embrace the technology and be willing to adapt and change along with the process. It is almost a given that pushing the envelope of optimization requires the operations personnel to accept additional complication and raise the bar of required operational skill. This concept should be discussed in advance to be sure the project isn't set up to fail by being unacceptably complex.

2.3 Human thermal comfort

The ultimate objective of any heating, cooling and ventilating system is typically to maximize human thermal comfort. Due to the prevalence of simple thermostat control systems for residential and small-scale commercial HVAC systems, it is often believed that human thermal comfort is a function solely, or at least primarily, of air temperature. But this is not the case. Human thermal comfort is actually maximized by establishing a heat balance between the occupant and his or her environment. Since the body can exchange heat energy with its environment by conduction, convection and radiation, it is necessary to look at the factors which affect these heat transfer processes along with the body's ability to cool itself by the evaporation of perspiration. All living creatures generate heat by burning food, a process known as metabolism. Only 20 percent of food energy is converted into useful work; the remainder must be dissipated as heat. This helps explain why we remain comfortable in an environment substantially cooler than our internal temperature of nearly 37°C. In addition to air temperature, humidity, air motion and the surface temperature of surroundings all have a significant influence on the rate at which the human body can dissipate heat. At temperatures below about 27°C most of the body's heat loss is by convection and radiation. Convection is affected mostly by air temperature, but it is also strongly influenced by air velocity. Radiation is primarily a function of the relative surface temperature of the body and its surroundings. Heat transfer by conduction is negligible, since we make minimal physical contact with our surroundings which is not insulated by clothing. At temperatures above 27°C the primary heat loss mechanism is evaporation. The rate of evaporation is dependent on the temperature and humidity of the air, as well as the velocity of air which passes over the body carrying away evaporated moisture. In addition to these environmental factors, the rate of heat loss by all means is affected by the amount of clothing, which acts as thermal insulation. Similarly, the amount of heat which must be dissipated is strongly influenced by activity level. Thus, the degree of thermal comfort achieved is a function of air temperature, humidity, air velocity, the temperature of surrounding surfaces, the level of activity, and the amount of clothing worn. In general, when environmental conditions are cool the most important determinant of human thermal comfort is the radiant temperature of the surroundings. In fact, a five degree increase in the mean-radiant temperature of the surroundings can offset a seven degree reduction in air temperature. When conditions are warm, air velocity and humidity are most important. It is not by accident that the natural response to being too warm is to increase air motion. Similarly, a reduction in humidity will offset an increase in air temperature, although it is usually necessary to limit relative humidity to no more than 70% in

summer and no less than 20% in winter. There is, of course, a human response to air temperature, but it is severely influenced by these other factors. The most noticeable comfort response to air temperature is the reaction to drift, the change of temperature over time. A temperature drift of more than 0.5°C per hour will result in discomfort under otherwise comfortable conditions. Temperature stratification can also cause discomfort, and temperature variation within the occupied space of a building should not be allowed to vary by more than 3°C. Modern control systems for HVAC systems can respond to more than just the air temperature. One option which has been around for a long time is the humidistat, which senses indoor humidity levels and controls humidification. However, state-of-the-art control systems can measure operative temperature, which is the air temperature equivalent to that affected by radiation and convection conditions of an actual environment[1]. Another useful construct is that of effective temperature, which is a computed temperature that includes the effects of humidity and radiation[2]. The location and type of air distribution devices play a role equal in importance to that of effective controls in achieving thermal comfort. The discomfort caused by stratification can be reduced or eliminated by proper distribution of air within the space. In general terms, thermal comfort can be achieved at air temperatures between about 20°C and 27°C, and relative humidities between 20% and 70%, under varying air velocities and radiant surface temperatures. Figure 2.2 shows the generalized "comfort zone" of dry bulb temperatures and humidities plotted on the psychrometric chart. However it should not be forgotten that human thermal comfort is a complex function of temperature, humidity, air motion, thermal radiation from local surroundings, activity level and amount of clothing.

2.4 Energy aspects

Electricity consumption in the European Union (EU) has continued to grow in the last years despite numerous energy efficiency polices and programmes at EU and national level [14]. Total electricity consumption in the residential sector in the EU-25 has grown by 10.8% in the period 1999-2004, at almost the same rate as the economy (GDP). Similar trends are also observed in the tertiary sector and to a lesser extend in industry. The electricity consumption in the tertiary sector has grown by 15.6% in the period 1999-2004 and by 2.0% in the period 2003-2004.

[1]Operative temperature is technically defined as the uniform temperature of an imaginary enclosure with which an individual experiences the same heat by radiation and convection as in the actual environment.

[2]Effective temperature is an empirical index which attempts to combine the effect of dry bulb temperature, humidity and air motion into a single figure related to the sensation of thermal comfort at 50% relative humidity in still air.

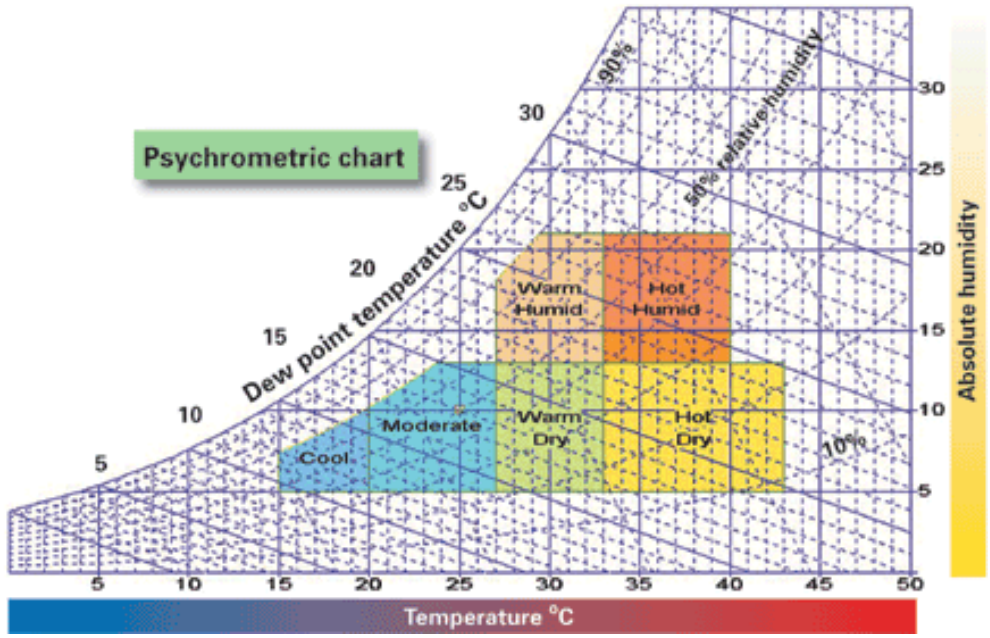

Figure 2.2: Psychrometric chart.

Despite this increase and the consequent impact on CO_2 emissions, there is little knowledge at European level, where the electricity is used, what is the status of efficiency of the installed and sold equipment and what is the likely impact of the past, present and planned policies. For the tertiary sector there is even much less data available for individual electricity end-uses than for the residential sector, and only a few sources or countries attempted to split the total electricity consumption among the different end-uses. The energy consumption of the industrial sector has continued to grow in the period 1999 to 2004 in the EU-25 with an increase of 6.6%, while the yearly growth rate in the period 2003- 2004 has been 1,3. The electricity in the industrial sectors has grown by 9.5% in the period 1999-2004 and by 1.7% in the period 2003-2004.

2.4.1 Air-conditioning appliances

In the 'southern' countries (Italy, Spain, Portugal, Greece and Southern France) one of the main drivers to increases in electricity consumption and more important to electricity peak demand is the fast penetration of small residential air-conditioners (less then 12 kW output cooling power) and their extensive use during the summer months. Due to the heat wave in the summer of 2003 in Italy during that year all small air-conditioners available on the market were sold and installed. For Italy, the manufacturer trade association reported the sale trends, as depicted in Fig. 2.1.

The impact of 2003 summer heat wave had also a big effect on sales for year 2004. Cooler summers in 2004 and 2005 reduced the sales levels in 2005. There is also

Table 2.1: Sales of small air-conditioners Italy.

Year	Sales (thousand)	Annual increase
2001	950	
2002	1067	12%
2003	1550	45%
2004	2100	35%
2005	1367	-35%

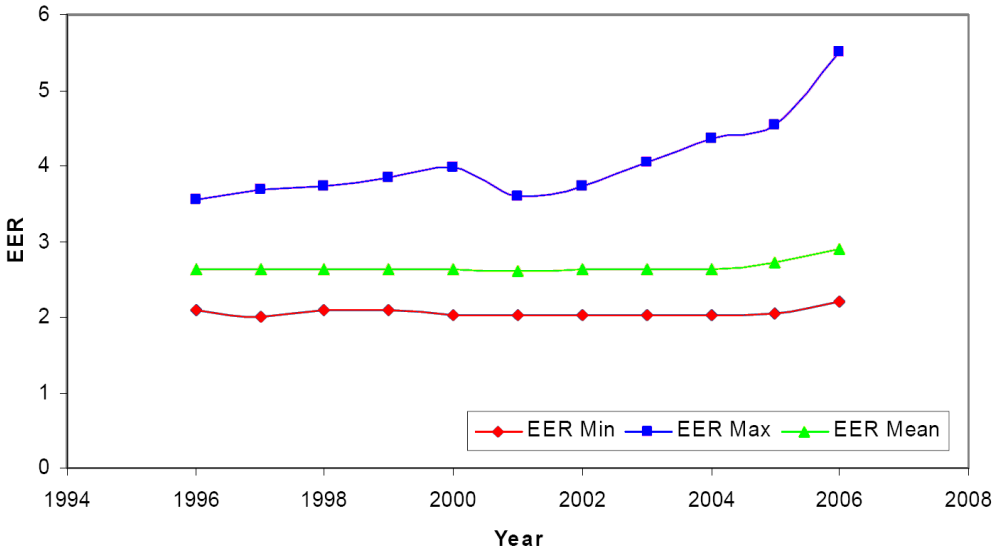

Figure 2.3: Evolution of the EER (minimum, maximum and model weighted average) for split, non ducted, air-cooled Air conditioners up to 12 kW.

some saturation effect as almost 20% of Italian household own an air-conditioner. Although at European level the penetration of small air-conditioners is still small (about 4% of residential space), in some countries such as Italy and Spain the penetration of small air-conditioners reached in 2005 significant penetration levels similar to the US where there is a penetration of about 20%. Total residential air-conditioners' electricity consumption in EU-25 in year 2005 was estimated to be between 7-10 TWh per year. For room air-conditioners (up to 12 kW output power), the Labelling Directive (2002/31/EC) has been adopted by the European Commission and was published in March 2002.

The full mandatory application of this Directive was fixed for 30 June 2003. However the relevant test standard needed to serve as the reference document was missing; the new revised standard EN 14511 covering all products in the scope of the Directive has not been finalized before May 2004. The European Commission in agreement with the Labelling Committee decided to postpone the application till just before the summer 2004. The A class limit for the split, non ducted, air-cooled air conditioners up to 12kW is set at EER of 3.2; some new models have been

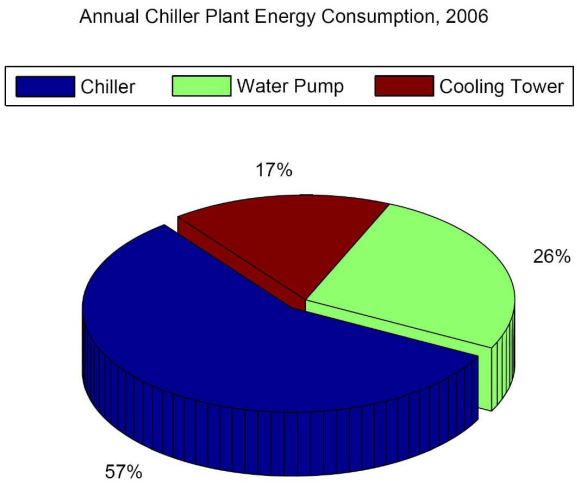

Figure 2.4: Annual chiller plant energy consumtion, 2006.

introduced on the market with EER above 4, the best models on the market having an EER of 5.51.

2.4.2 HVAC and refrigeration in tertiary sector

For tertiary sector end-use equipment (e.g. central air conditioners, chillers, commercial refrigeration, pumps, etc.) there is even less information on market penetration of efficient equipment. Air-conditioners in non residential buildings are estimated to consume about 70 to 80 TWh of electricity [15]. In the UK the MTP (Market Transformation Programme [16]) has calculated approximately 14.4 TWh for non-domestic and domestic air conditioning (the residential share being almost negligible) [17].

Chillers are a key components of air conditioning systems for large buildings. In HVAC system equipped with vapour compression liquid chillers, the electrical energy consumption of the refrigerating unit far exceeds all that required by the other system components, Figure 2.4 (chillers usually consume about 40-60% of the total energy consumed in a chilled water system).

Eurovent [18] established classification for full load Energy Efficiency Ratio of each type of chillers. The classification follows the A to G approach used in the European Energy Label for household appliances but the limits between classes have been defined for the existing chillers as listed in Eurovent directory, see Table 2.2 for cooling mode.

The classification has been implemented in February 2005; the distribution of number of units in each class is shown in Table 2.3.

It is too early to see the influence of this classification on energy efficiency. However, the distribution shows that 7% of certified chillers are in Eurovent Class A and

Table 2.2: Chillers Energy Classification in Cooling Mode.

EER	Air Cooled	Water cooled	Remote condenser
Class			
A	EER≥3.1	EER≥5.05	>=3.55
B	2.9≤ EER< 3.1	4.65≤ EER<5.05	3.4≤ EER<3.55
C	2.7≤ EER< 2.9	4.25≤ EER<4.65	3.25≤ EER<3.4
D	2.5≤ EER< 2.7	3.85≤ EER<4.25	3.1≤ EER<3.25
E	2.3≤ EER< 2.5	3.45≤ EER<3.85	2.95≤ EER<3.1
F	2.1≤ EER< 2.3	3.05≤ EER<3.45	2.8≤ EER<2.95
G	<2.1	<3.05	<2.8

Table 2.3: Distribution of units in each class.

Class/kW	0-50	50-100	100-150	150-200	200-500	500-1000	>1000	Total
A	85	12	4	7	72	85	115	380
B	114	51	46	21	142	179	112	665
C	203	75	76	40	206	229	137	966
D	244	143	106	80	295	213	80	1161
E	283	131	121	84	432	246	98	1495
F	287	62	54	52	125	68	29	677
G	152	14	10	8	41	31	19	275
Total	1468	488	417	292	1313	1051	590	5619

in total only 5% of the certified chillers are in Eurovent Class G. Another important share of electricity is consumed by fans for ventilation systems (including fans) which results in about 94 TWh in the. For the time being there are no existing European polices to improve efficiency of ventilation systems. A similarly important sector in term of consumption is commercial refrigeration. Estimate for the total European consumption range from 70 to 100 TWh per year. Only a few national data are available, in Germany it has been estimated a consumption of 13TWh for commercial refrigeration in the service sector by one expert, while another estimate that is around 8TWh in the wholesale, retail trade, hotels and restaurants. In the UK, the MTP estimates that the consumption of commercial refrigeration equipment represent 8.5% of the total non domestic energy consumption. The specific refrigeration products covered by commercial refrigeration equipment, are: process chillers, refrigerated display and service cabinets, cellar cooling, ice making machines (non domestic), walk-in cold stores, refrigerated vending machines, refrigeration compressors, air-cooled condensing units, heat exchangers (process/industrial applications).

3 Multiple chiller system

In HVAC plants of medium-high cooling capacity, multiple chiller systems [1] are more common than single-chiller systems (for the same reason that most commercial airplanes have more than one engine) and they are developed as a trade-off between reliability and cost. Multiple chillers are normally configured in parallel. In such system, every chiller is independent of each other to provide standby capacity, operational flexibility, and less disruption maintenance. Compared with a single-chiller system, the multiple-chiller system has a reduced starting in-rush current and a reduced power cost under part load conditions [2]. For instance, large chilled water plants at health-care and institutional facilities are excellent candidates for this type of solution. However, the capacity regulation and part load efficiency of each chiller (and therefore of the entire system) strongly depends on the refrigerating unit, refrigerant circuit design, type and number of compressors. For instance, multi-scroll chillers equipped with twin compressors on the same circuit present high part load Energy Efficiency Ratio values (EER, defined as the ratio of cooling capacity and total power absorption, fans included), whereas screw compressors units are strongly penalized, mainly because of the reduction of screw compressor isentropic efficiency at low cooling loads. Therefore, the problem of efficiently managing multiple-chiller systems is getting more and more important.

3.1 Chilled-water-plant basics

Chilled-water plants [19] consist of these functional parts:

- Chillers that produce chilled water.
- Loads, often satisfied by coils, that transfer heat from air to water.
- Chilled-water distribution pumps and pipes that send chilled water to the previously mentioned loads.

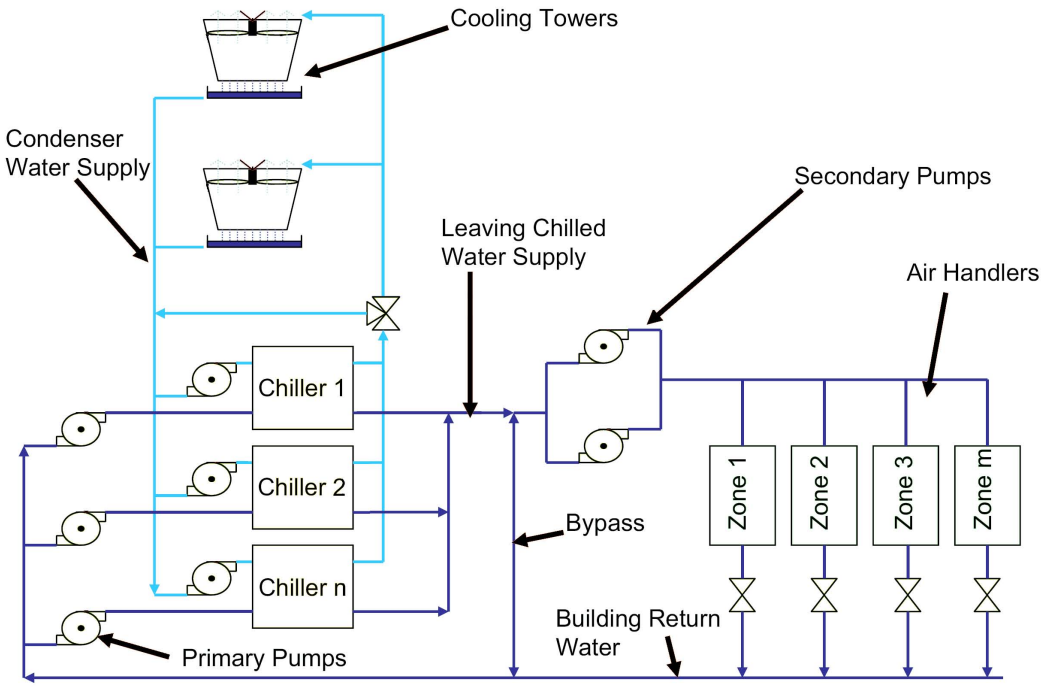

Figure 3.1: Chilled water system.

- Condenser-water pumps, pipes, and cooling towers that reject heat (for water-cooled chillers).
- Controls that coordinate the operation of the mechanical components together as a system.

3.2 Chiller

Chillers are a key component of most centralized air-conditioning systems. The function of a chiller is to generate chilled water, which is distributed to large spaces for cooling. Most commonly, they are reciprocating, screw, scroll and centrifugal. Chillers can be either air or water cooled. Major vapor-compression chiller components include an evaporator, a compressor, a condenser, and an expansion device.

3.2.1 Vapour-compression cycle

The vapour-compression cycle is used in most household refrigerators as well as in many large commercial and industrial refrigeration systems. Figure 3.2 provides a schematic diagram of the components of a typical vapor-compression refrigeration system.

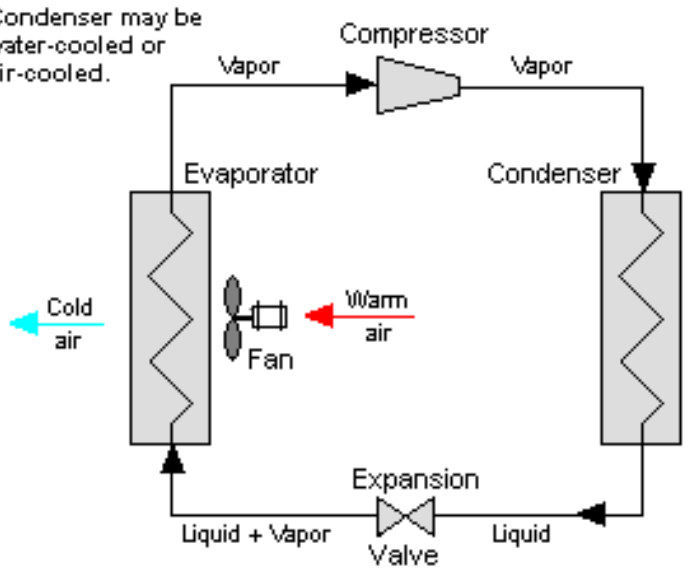

Figure 3.2: Typical vapor-compression refrigeration system.

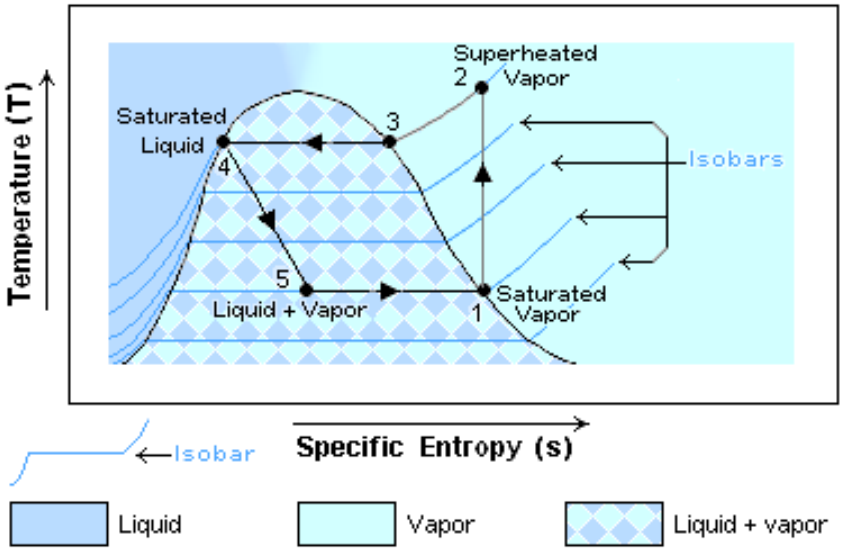

Figure 3.3: Thermodynamics of the vapour-compression cycle.

The thermodynamics of the cycle can be analyzed on a diagram as shown in Figure 3.3. In this cycle, a circulating refrigerant enters the compressor as a vapor. From point 1 to point 2, the vapor is compressed at constant entropy and exits the compressor superheated. From point 2 to point 3 and on to point 4, the superheated vapor travels through the condenser which first cools and removes the superheat and then condenses the vapor into a liquid by removing additional heat at constant pressure and temperature. Between points 4 and 5, the liquid refrigerant goes through the expansion valve (also called a throttle valve) where its pressure abruptly decreases, causing flash evaporation and auto-refrigeration of, typically, less than half of the liquid.

That results in a mixture of liquid and vapor at a lower temperature and pressure as shown at point 5. The cold liquid-vapor mixture then travels through the evaporator coil or tubes and is completely vaporized by cooling the warm air (from the space being refrigerated) being blown by a fan across the evaporator coil or tubes. The resulting refrigerant vapor returns to the compressor inlet at point 1 to complete the thermodynamic cycle.

The above discussion is based on the ideal vapor-compression refrigeration cycle, and does not take into account real-world effects like frictional pressure drop in the system, slight thermodynamic irreversibility during the compression of the refrigerant vapor, or non-ideal gas behavior (if any).

3.2.2 Compressors

At the heart of the vapour compression cycle is the mechanical compressor. A compressor has two main functions:

1. to pump refrigerant through the cooling system;
2. to compress gaseous refrigerant in the system so that it can be condensed to liquid and absorb heat from the air or water that is being cooled or chilled.

Different types of chillers are also used depending upon the type of compressor used as part of the refrigeration circuit. A set of different types of compressors are illustrated below.

3.2.2.1 Reciprocating

A reciprocating compressor uses the reciprocating action of a piston inside a cylinder to compress refrigerant (Figure 3.4). As the piston moves downward, a vacuum is created inside the cylinder. Because the pressure above the intake valve is greater than the pressure below it, the intake valve is forced open and refrigerant is sucked into the cylinder. After the piston reaches its bottom position it begins to move

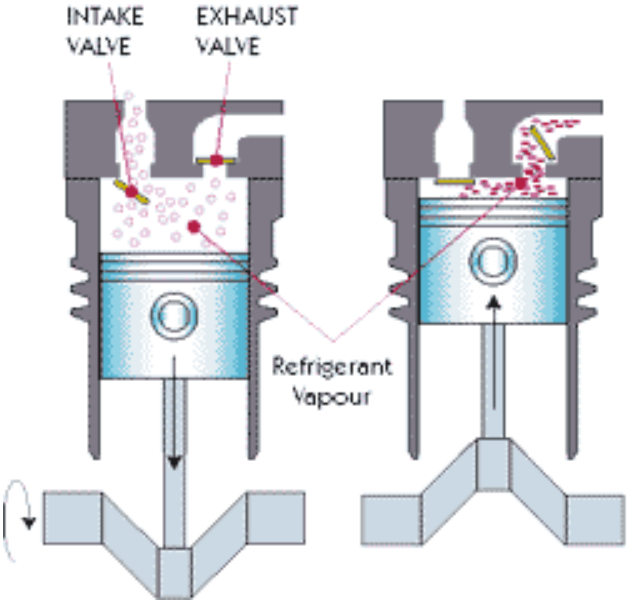

Figure 3.4: Reciprocating compressor schematic.

upward. The intake valve closes, trapping the refrigerant inside the cylinder. As the piston continues to move upward it compresses the refrigerant, increasing its pressure. At a certain point the pressure exerted by the refrigerant forces the exhaust valve to open and the compressed refrigerant flows out of the cylinder. Once the piston reaches it top-most position, it starts moving downward again and the cycle is repeated. These compressors are available in two basic types: hermetically sealed units and units of open construction. In hermetically sealed units, the motor and the compressor are direct-coupled and housed in a single casing that is sealed to the atmosphere. In open construction units, the motor and the compressor are in separate housings. In general, open construction units have a longer service life, lower maintenance requirements and higher operating efficiencies. The hermetically sealed units are most common particularly in small capacities.

Single stage reciprocating machines have an ability to operate at compression ratios[1] of 10 to 12. The capacity control in a reciprocating machine is achieved through 'On-Off' or 'Loading- Unloading' of compressor cylinders. Reciprocating machines are manufactured in capacities from 0.5 to 150 TR[2]. The main factor favoring reciprocating machines is low cost. The other advantage is that multiple reciprocating machines can be installed to closely match the building loads. Multiple units allow flexibility to operate machines per the need. If properly managed this could contribute to significant energy savings during low loads. A major drawback

[1]The compression ratio being absolute output (head) pressure divided by the absolute input (suction) pressure.

[2]The standard unit of refrigeration in vogue is Ton Refrigeration (TR): 1 TR =3.5167 kW. This is approximately the power required to melt one short ton (2000 lb, 907 kg) of ice at 0 °C in 24 hours, thus representing the delivery of 1 ton of ice per day.

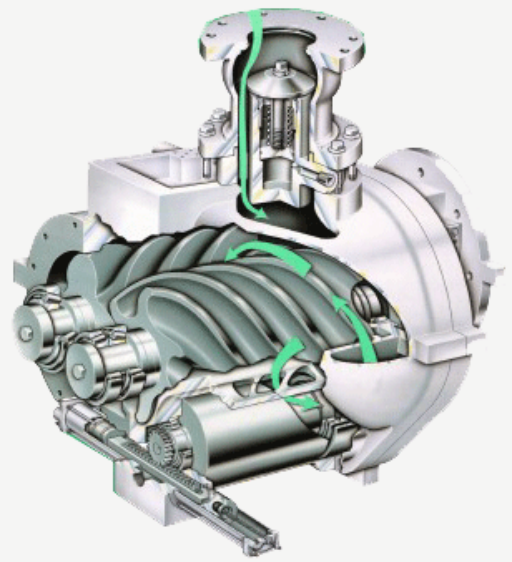

Figure 3.5: Screw compressor.

is a high level of maintenance requirements, noise and vibration. Since the capacity is limited to 150 TR, multiple units cost more than other options. Multiple chiller configurations require large space and consume more energy per ton of refrigeration.

3.2.2.2 Screw

Screw compressors use a pair of helical rotors. As the rotors rotate they intermesh, alternately exposing and closing off interlobe spaces at the ends of the rotors. When an interlobe space at the intake end opens up, refrigerant is sucked into it. As the rotors continue to rotate the refrigerant becomes trapped inside the interlobe space and is forced along the length of the rotors. The volume of the interlobe space decreases and the refrigerant is compressed. The compressed refrigerant exists when the interlobe space reaches the other end (Figure 3.5).

The commercial refrigeration installation relies more on screw machines. Screw compressors are available in several designs, both single screw and twin screw, with oil-free and oil-injected designs in both types. Twin-screw oil-injected compressors are slightly more energy efficient at moderate compression ratios. Twin-screw compressors have an ability to operate at a compression ratio of 30. Units are available in both hermetically sealed and open construction. Screw compressors are used in the mid-range of unit sizes, around 20-1000 TR. They are compact and have less moving parts, hence lower maintenance costs and longer life spans. Continuously variable loading can also be provided, improving partial load efficiencies. The capacity control in a screw compressor is achieved thorough a moveable slide stop valve, which will vary the compressor internal volume ratio to achieve optimum energy consumption during part load operation. The major drawback is their high cost.

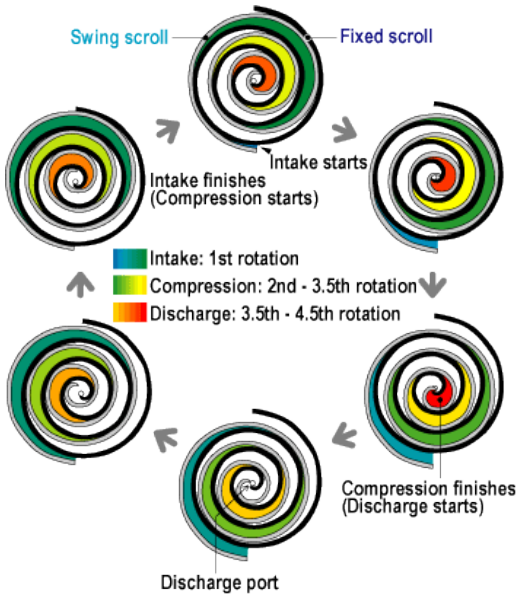

Figure 3.6: Scroll compressor.

For smaller loads, reciprocating machines are less expensive to purchase and for large loads centrifugal machines cost less.

3.2.2.3 Scroll

In a scroll compressor refrigerant is compressed by two offset spiral disks that are nested together. The upper disk is stationary while the lower disk moves in orbital fashion (Figure 3.6). The orbiting action of the lower disk inside the stationary disk creates sealed spaces of varying volume. Refrigerant is sucked in through inlet ports at the perimeter of the scroll. A quantity of refrigerant becomes trapped in one of the sealed spaces. As the disk orbits the enclosed space containing the refrigerant is transferred toward the centre of the disk and its volume decreases. As the volume decreases, the refrigerant is compressed. The compressed refrigerant is discharged through a port at the centre of the upper disk. Scroll compressors are quiet, smooth-operating units with the highest efficiency ratio of all compressor types.

Scroll compressors have been used in commercial practice for systems that have capacities less than 30 TR. Scroll compressors are used in smaller units such as unitary heat pumps, and may be up to 10% more efficient than an equivalently sized reciprocating unit. On such small sizes, these do not affect the life cycle economics drastically.

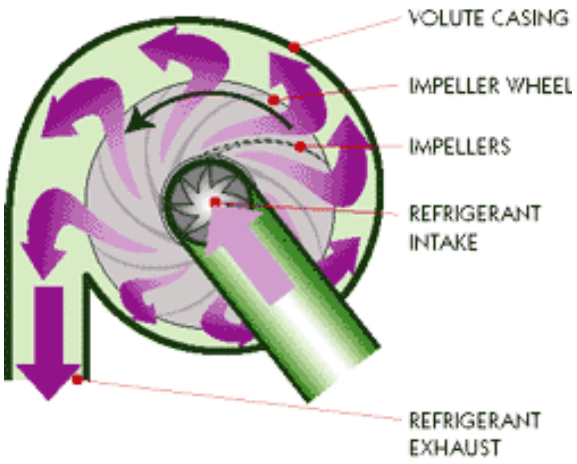

Figure 3.7: Centrifugal compressors.

3.2.2.4 Centrifugal

Centrifugal compressors use the rotating action of an impeller wheel to exert centrifugal force on refrigerant inside a round chamber (volute). Refrigerant is sucked into the impeller wheel through a large circular intake and flows between the impellers. The impellers force the refrigerant outward, exerting centrifugal force on the refrigerant (Figure 3.7). The refrigerant is pressurized as it is forced against the sides of the volute. Centrifugal compressors are well suited to compressing large volumes of refrigerant to relatively low pressures. The compressive force generated by an impeller wheel is small, so chillers that use centrifugal compressors usually employ more than one impeller wheel, arranged in series. Centrifugal compressors are desirable for their simple design and few moving parts.

Centrifugal chillers for refrigeration applications are generally designed for a fixed compression ratio of 18. The capacity control is achieved through the use of inlet vanes on the impellers that restrict refrigerant flow. The centrifugal chillers are manufactured in capacities from 90 to 2000 TR and are generally used for capacities above 200 TR. The main factor favoring centrifugal machines is their high operational efficiency at full load, compact size and availability in large sizes. The biggest drawback of centrifugal machines is a very poor part load performance and inability to operate at low cooling loads.

3.2.3 Evaporator

The evaporator section of a water chiller is a shell-and-tube, refrigerant-to-water heat exchanger. Depending on the chiller's design, either the refrigerant or the water is contained within the tubes.

- In a flooded shell-and-tube evaporator, cool, liquid refrigerant at low-pressure enters the distribution system inside the shell and moves uniformly over the

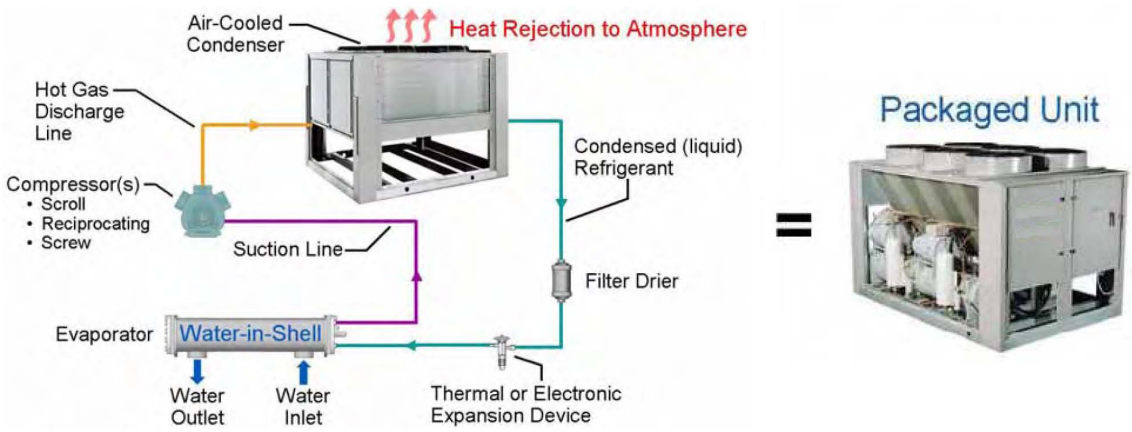

Figure 3.8: Refrigeration cycle components of an air-cooled chiller.

tubes, absorbing heat from warmer water that flows through the tubes.

- In a direct-expansion (DX) shell-and-tube evaporator, warmer water fills the shell while the cool, lower-pressure liquid refrigerant flows through the tubes.

In either design, there is an approach temperature, which is the temperature difference between the refrigerant and exit water stream. The approach temperature is a measure of the heat transfer efficiency of the evaporator.

3.2.3.1 Water-cooled condenser

To cool a building or process, the transferred heat must ultimately be rejected. The total amount of heat rejected includes the sum total of the evaporator load, the compressor work, and the motor inefficiency. In a hermetic chiller, where the motor and compressor are in the same housing, these loads are all rejected through the condenser. In an open chiller, where the motor is separate from the compressor and connected by a shaft, the motor heat is rejected directly to the surrounding air. The evaporator load and the compressor work are rejected through the condenser and the motor heat must be taken care of by the air-conditioning system.

3.2.3.2 Air-cooled condenser

Obviously, air-cooled chillers do not use condenser-water, since they reject their heat by having ambient air passed across refrigerant-to-air heat exchangers (Figure 3.8). In packaged air-cooled chillers, the manufacturers attempt to provide optimal performance by staging fans in response to chiller load and ambient, dry-bulb temperature.

Air cooled chillers are generally located outside the building and reject heat directly to the atmosphere, while water cooled chillers are generally located within

the building and use cooling towers located outside the building to reject the heat.

3.2.3.3 Air-Cooled versus Water-Cooled Chillers

Circumstances favoring Air-cooled Systems

Air cooled chillers are favored over the water cooled systems under following circumstances:

1. Where water is scarce or quality water is not available.
2. Where the system is not required to operate 24 hours.
3. Where the system is not to be located in or around noise restricted areas.
4. Where there is adequate and accessible roof top or ground space for the system equipment.
5. Where sitting of cooling tower is restricted due to Legionella risk minimization constraints.
6. Where air-conditioning requirement is less than 200 TR.
7. Where statutory requirements for health and safety may not permit use of cooling towers in certain areas.
8. Where a high humidity climatic condition in tropical areas exists that significantly reduces the effectiveness of cooling towers.

Circumstances favoring Water-cooled Systems

Water-cooled chillers are generally favorable over the air-cooled systems under the following circumstances:

1. Where the system is required to operate 24 hours.
2. Where there is limited roof top or ground space for the system equipment.
3. Where noise minimization and aesthetics are of relative importance.
4. Where there are larger system capacity requirements, typically above 200 TR.

The present trend leans towards the use of air-cooled condensers. Results from recent generic studies on comparative life cycle costs of air cooled and water cooled systems indicate that each system is considered to be more favorable than the other over a certain range of plant capacity.

3.3 Loads

In comfort-cooling applications, loads are usually satisfied by air handlers equipped with coils to transfer heat from conditioned space air to circulating chilled-water. Air is thus cooled and dehumidified as it passes across the finned surface of the cooling coils. Since the psychrometric process of conditioning air takes place at the coils, selection of the optimum coil size and type from the wide variety available is important for proper system performance.

Some specialized process loads do not involve cooling air. Instead, they may involve heat transfer directly within a piece of process equipment, such as the cooling jacket of an injection-molding machine. Heat transferred from the loads can be controlled in a number of ways:

- Three-way valve.
- Two-way valve.
- Variable-speed pump
- Uncontrolled coils

3.3.1 Three-way valve load control

A three-way control valve regulates the amount of water passing through a coil in response to loads. The valve bypasses unused water around the coil and requires a constant flow of water in the system, regardless of load. A drawback of this bypass is that the temperature of the water leaving the three-way valve is reduced at part-load conditions. This can be a major cause of so-called "low ΔT syndrome"[3]. Three-way valves are used in many existing systems.

3.3.2 Two-way valve load control

A two-way, water modulating valve at the coil performs the same water throttling function as the three-way valve. The coil sees no difference between these two methods. The chilled-water system, however, sees a great difference. In the case of the two-way valve, all flow in the coil circuit is throttled. No water is bypassed. Consequently, a system using two-way valves is a variable-flow chilled-water system. The temperature of the water leaving the coil is not diluted by bypass water so at part-load conditions, the system return-water temperature is higher than with three-way valve control.

[3]During the past several years the "low ΔT syndrome" debate has raged. The symptom of the problem is that, in large systems, return-water temperature is too low, thus not allowing the chillers to fully load.

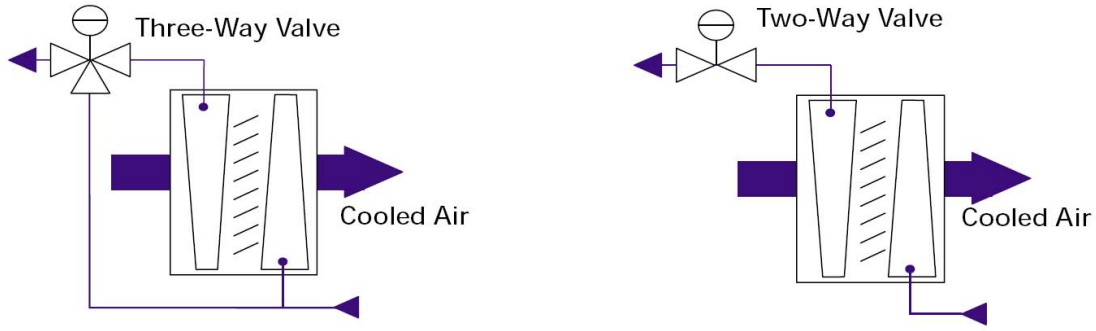

Figure 3.9: Valve-controlled loads.

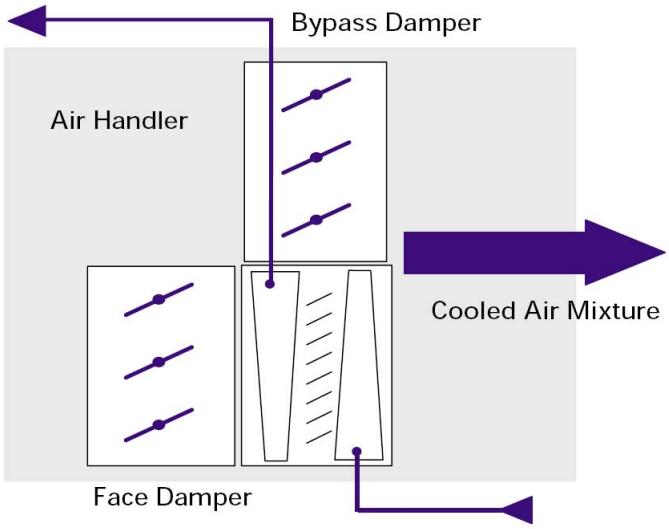

Figure 3.10: Uncontrolled coil.

3.3.3 Variable-speed pumping load control

By using a pump for each coil, the flow may be controlled by varying the pump speed. In such systems, there may be no control valves at the coil. This can reduce both the valve and the valve installation costs.

3.3.4 Uncontrolled coils

Figure 3.10 shows a control variation using an uncontrolled or "wild"coil. In this system, control of the conditioned air supply is executed by face-and-bypass dampers that permit a portion of the air to bypass the coil surface. Advantages of the strategy are the elimination of control valves and improved part-load dehumidification. A disadvantage is that all the water is pumped all the time; however, in systems with very small water pressure drops, this system arrangement may work economically.

3.4 Chilled-water distribution system

Chilled water is circulated through fixed piping most commonly steel, copper, or plastic that connects the chiller with various load terminals. Piping is sized to meet a project's pressure loss, water velocity, and construction cost parameters. Pressure drop is overcome by the use of a chilled-water pump.

3.4.1 Chilled-water pump

The purpose of the chilled-water pump is to circulate chilled water within the loop. Generally, the pump must overcome the frictional pressure losses caused by the piping, coils, and chiller and the pressure differential across open control valves in the system. The pump, while working at the system static pressure, does not need to overcome this static pressure.

The pump is typically located upstream of the chiller, however it may be anywhere in the system, provided that the pump:

- meets the minimum pump net positive suction-head requirements. That is, the system pressure at the pump inlet must be both positive and high enough to allow the pump to operate properly;
- maintains the minimum dynamic pressure head at critical system components (usually the chiller). If the dynamic pressure head is not high enough at these components, proper flow will not be established through them;
- accommodates the total pressure (static head plus dynamic head) on system components such as the chiller's evaporator, valves, etc.

Note that the pump heat is added to the water and must be absorbed by the chiller. Generally, this represents a very small temperature increase. Multiple pumps are often used for redundancy. Depending on the terminal control devices and system configurations, the chilled-water pumps may be either constant or variable-flow.

3.4.2 Distribution piping

By itself, the distribution system is easy to understand. Figure 3.11 shows a simplified distribution system consisting of multiple cooling coils, each controlled by a thermostat that regulates the flow in its respective coil. The valves may be either three-way or two-way. As previously discussed, three-way valves require constant water flow, while two-way valves allow the water flow in the system to vary. As flow varies, the pump may simply ride its curve or use a method of flow control such as a variable-speed drive.

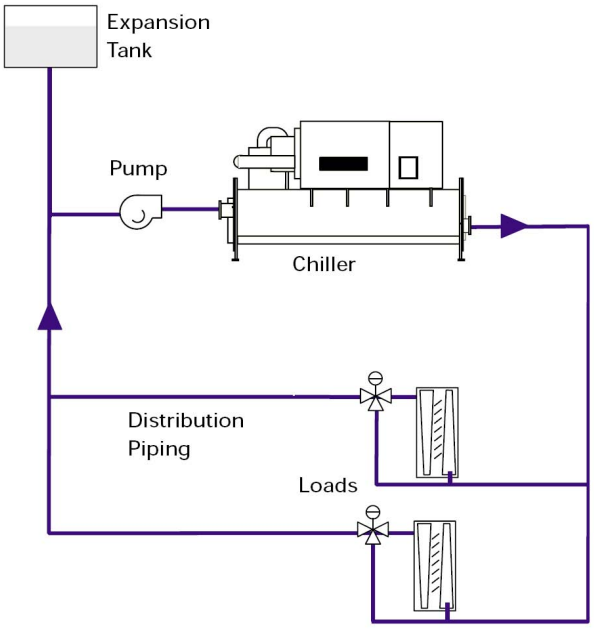

Figure 3.11: Simplified distribution system.

The distribution system may contain other components, such as an expansion tank, control valves, balancing valves, check valves, and an air separator, to name a few. The density, and therefore the volume, of the water in a "closed" chilled-water distribution system varies as it undergoes changes in temperature. The expansion tank allows for this expansion and contraction of water volume.

3.5 Condenser-water system

As in chilled-water distribution systems, condenser-water system piping most commonly steel, copper, or plastic is sized to meet a project's operating pressure, pressure loss, water velocity, and construction cost parameters. Pressure drop through piping and the chiller's condenser, plus the cooling tower static lift, is overcome by use of a condenser-water pump.

3.5.1 Cooling tower

To reject heat, water is passed through a cooling tower where a portion of it evaporates, thus cooling the remaining water. A particular cooling tower's effectiveness at transferring heat depends on water flow rate, water temperature, and ambient wet bulb. The temperature difference between the water entering and leaving the cooling tower is the range. The temperature difference between the leaving water temperature and the entering wet-bulb temperature is the approach.

- Effect of load: as the building load, or heat rejection, decreases, range and approach also decrease. This means that when the building is at part load, the cooling tower can provide colder water at the same ambient wet-bulb temperature.
- Effect of ambient conditions: as ambient wet-bulb temperature drops, the approach, at a constant load, increases. This must be considered when cooling-tower-control strategies are developed.

3.6 Controls

The chilled-water supply temperature is usually controlled at the chiller. Most commonly, supply water temperature is used as the sensed variable to permit control of chiller capacity to meet system load demand. Supply-temperature control strategies may be used on either constant, or variable, flow systems. As previously discussed, flow control is executed at the load terminals using three-way or two-way valves, or separate pumps for each coil. Control capabilities run the gamut from slow-acting pneumatic controls, to electromechanical controls, to sophisticated digital controls that use algorithms tuned to give superior performance.

3.6.1 Chiller control

Today's chiller controls are capable of doing more than simply turning the chiller on and off. At a minimum, these controls should monitor:

- Safety points such as bearing temperatures and electrical points that, when out of range, may cause motor failure.
- Data points that may cause operational problems if corrective action is not taken. An example is low chilled-water or refrigerant temperature, which may result in freezing in or around the evaporator tubes.
- General points that should be logged daily to ensure proper chiller performance.

In addition to monitoring data, it is vital that the chiller controls alert operators to possible problems. Diagnostic messages are necessary for the operator to respond to safety issues and data points that are outside normal operating ranges. While communicating these diagnostic messages is a requirement, some chiller controls include factory-installed programming that responds to the diagnostic messages. For example, when the chilled-water temperature nears freezing, the chiller sends a diagnostic message and adapts its operation by reducing the compressor capacity,

raising the chilled-water temperature to a safer condition. Finally, the chiller controls should communicate with a system-level controller. There are many system aspects that are outside the chiller's direct control, such as condenser-water temperature and the amount of fluid flowing through the evaporator and condenser. To minimize the system energy costs, the system controls must coordinate chiller, pump, cooling-tower, and terminal-unit controls. This can only be done if adequate information is communicated from each system component to the system-level controls.

3.6.2 Pump control

In so-called constant flow systems, the pumps are either on or off, providing relatively constant flow when in the on position. In practice, some flow variation will occur as system pressure drop changes. In a variable-flow system, pump control is most often performed by maintaining a pressure differential at a selected point in the system. For example, a variable-speed drive will increase its speed if the sensed pressure differential is too low, or slow down if the pressure differential is too high. The control point is selected to minimize overpressuring the system and to assure adequate flow at all critical loads.

4

Multiple chiller with primary-secondary architecture

In Figure 4.1 the block structure of the basic system taken as a reference in this Thesis is reported. Three basic blocks can be pointed out:

1. The energy production section: a packaged air-cooled water chiller.

2. The hydraulic section: a common primary-secondary pumping arrangement is adopted with constant water flow rate on the secondary, thus decoupling the chiller section from the distribution one. Separate pumps are dedicated to production and distribution. While the same water is pumped twice (by different pumps), there is no duplication of pumping energy. This is because the production pumps overcome only the chiller and production-side pressure drop, while the distribution pumps overcome only the distribution system pressure drops. The unrestricted bypass line hydraulically decouples the production and distribution pumps so that they cannot operate in a series coupled pumping arrangement. Although the two pumping systems are independent, they share the bypass piping. Changes in flows or pressures, due to variations in dynamic head or the number of chillers operating, cannot cross the bypass line.

3. The load section: the building thermal load and capacity is represented in the simulation scheme by cooling coils and a water tank of suitable capacity.

4.1 Mathematical model

The thermal behavior of such a plant can be usefully analyzed by a lumped formulation of the conservation equations ([20]). The elements of the plant are simulated

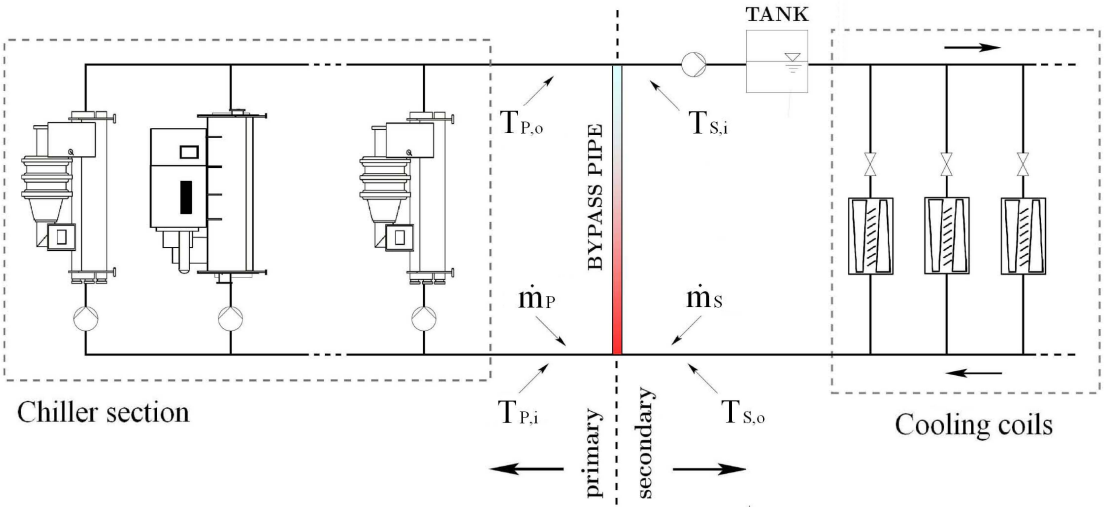

Figure 4.1: Decoupled system: primary-secondary architecture.

Table 4.1: Some symbols used throughout the paper.

c_p	specific heat at constant pressure [J/(kgK)]
e	specific energy [J/kg]
e_c	specific kinetic energy [J/kg]
e_p	specific potential energy [J/kg]
f	well-mixed volume fraction [-]
L	mechanical energy [J]
$\dot{m}$	mass flow rate [kg/s]
Q	thermal energy [J]
s	Laplace variable [-]
t_c	water tank or piping time constant [s]
T	temperature [^{o}C]
V	volume [m^3]
ρ	density [kg/ m^3]
τ	integration time [s]
Subscripts	
f	water tank or piping well-mixed section outlet
H	hydraulic section
L	load section
C	chiller section
i	block inlet
o	block outlet
k	block index

through blocks, and the heat transfer processes are considered as concentrated inside the blocks. Furthermore, the following hypotheses are introduced:

- The water thermal properties are considered constant.
- The water is considered incompressible.
- The three sections have constant water mass flow.
- There is no mass accumulation inside blocks.
- Piping and water tanks are considered adiabatic.

The system dynamics are governed by the mass, momentum, and energy conservation laws. The mass and energy equations are implemented as block equations for each component of the plant, where each block is modelled as a thermodynamic open system. The dynamic behavior of the plant is thus obtained solving the fluid flow problem and the energy balance. No solution of the momentum equation is needed because of the constant water mass flow assumption in the three sections. Thus the fluid flow problem consists only in the determination of the mass flow rate and the equations for the k-th block may be simply written as follows:

$$\dot{m}_{k,i} - \dot{m}_{k,o} = 0\,. \tag{4.1}$$

and therefore, for all k,

$$\dot{m}_{k,i} = \dot{m}_{k,o} = \dot{m}_k\,. \tag{4.2}$$

where dependence on the time variable t is omitted for notational convenience, when possible. The thermal problem consists in the determination of the temperature values at the outlet of the k-th block. The energy equation at time t can be written as follows:

$$\begin{aligned} \frac{dQ_k}{d\tau} - \frac{L_k}{d\tau} \;=\; & -\dot{m}_{k,i}\left(c_p T_{k,i} + e_{p,k,i} + e_{c,k,i}\right) \\ & +\dot{m}_{k,o}\left(c_p T_{k,o} + e_{p,k,o} + e_{c,k,o}\right) \\ & +\frac{\partial}{\partial\tau}\int_0^{V_k} e\rho dv\,. \end{aligned} \tag{4.3}$$

4.1.1 Water storage tank

Since the model has to be used for control design of systems with low capacity water storage tank, it is not possible to proceed under the well-mixed hypothesis for the

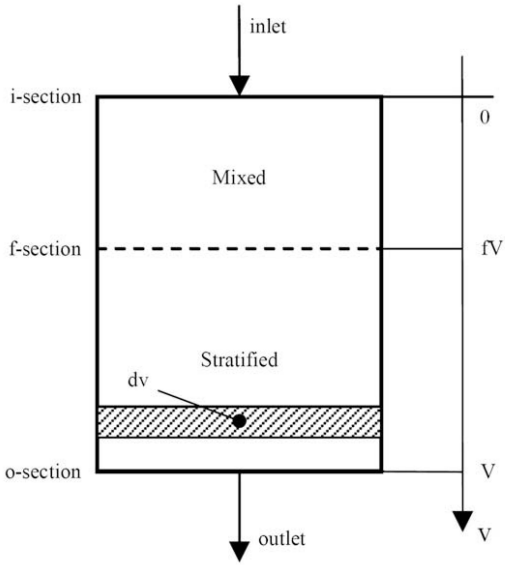

Figure 4.2: Water tank and piping scheme.

water inside the system components as in Jian's model ([21]). In fact, the water contents and the dynamics of the water tanks strongly influence the behavior of the chiller control system. Therefore, each water tank is modelled as two separate parts connected in series (see Figure 2). In the first part a well-mixed condition is assumed, while in the second part a perfect stratification condition is considered. For the well-mixed section, with the above mentioned simplifying hypotheses and neglecting kinetic and potential energy variations, Equation (4.3) at time τ becomes:

$$-\dot{m}_{k,i}c_pT_{k,i} + \dot{m}_{k,o}c_pT_{k,f} + f_k\rho V_k c_p\frac{dT_{k,f}}{d\tau} = 0\,, \tag{4.4}$$

where f_k is the well-mixed section fraction of the tank total volume. This parameter is given as a function of a cylindrical tank geometric dimension and of the water velocity by means of FVM (Finite Volume Method) three-dimensional simulation. For the stratified section of the water tank, the temperature in each infinitesimal volume dv depends only on the inlet time t of the associated infinitesimal water mass at the integration time τ, and Equation (4.4) becomes:

$$-\dot{m}_{k,i}c_pT_{k,f}(\tau) + \dot{m}_{k,o}c_pT_{k,o}(\tau) + \frac{\partial}{\partial\tau}\int_{f_kV}^{V_k}\rho c_pT_{k,i}(t)dv = 0\,. \tag{4.5}$$

Since no mixing occurs inside the stratified section of the water tank, the volumetric coordinate v associated to the position of an infinitesimal water mass inside the tank can be expressed as a function of the time instant t when the water mass entered the stratified portion of the tank. The resulting expression for v with reference to the actual integration time τ:

$$v = f_k V_k + (\tau - t)\frac{(1 - f_k)V_k}{t_{c,k}}\,, \tag{4.6}$$

where t_c is the tank section time constant defined as:

$$t_{c,k} = (1 - f_k)\frac{\rho V_k}{\dot{m}_{k,i}}\,. \tag{4.7}$$

Differentiating Equation (4.6) and substituting in Equation (4.5), the following equation is obtained:

$$-\dot{m}_{k,i}c_p T_{k,f}(\tau) + \dot{m}_{k,o}c_p T_{k,o}(\tau) + \frac{\partial}{\partial \tau}\int_{\tau}^{\tau - t_c} -\rho c_p \frac{(1 - f_k)V_k}{t_{c,k}} T_{k,f}(t)dt = 0\,, \tag{4.8}$$

and integrating Equation (4.8), the final equation for the stratified section is determined:

$$\dot{m}_{k,o}c_p T_{k,o}(\tau) = \dot{m}_{k,i}c_p T_{k,f}(\tau - t_c)\,. \tag{4.9}$$

Combining Equations (4.9) and (4.4) at each time step, the water tank block energy equation is solved and the outlet temperature is determined. The two equations can also be merged using Laplace transforms, thus obtaining the following first-order transfer function for the tank:

$$W_k(s) = \frac{T_{k,o}(s)}{T_{k,i}(s)} = \frac{e^{-st_c}}{1 + s\dfrac{f_k \rho V_k}{\dot{m}_k}}\,. \tag{4.10}$$

The same approach is used to model piping blocks, although the FVM analysis indicated that water mixing is negligible for typical water velocity design conditions.

4.1.2 Chiller and cooling coil

For the particular system under consideration, chiller and cooling coils water content can be neglected and the energy equation for these two $k-$th blocks at time τ can be written as follows:

$$-\dot{m}_{k,i}c_p T_{k,i} + \dot{m}_{k,o}c_p T_{k,o} = \frac{dQ_k}{d\tau} = P_k\,, \tag{4.11}$$

where for the chiller, the RHS (Right Hand Side) term, as well as the electrical absorbed power, is determined on the basis of data provided by the manufacturer as a function of water inlet temperature, mass flow, and external air temperature. Thus, the dynamic phenomena associated with heat and mass transfer, especially during start-ups, are neglected.

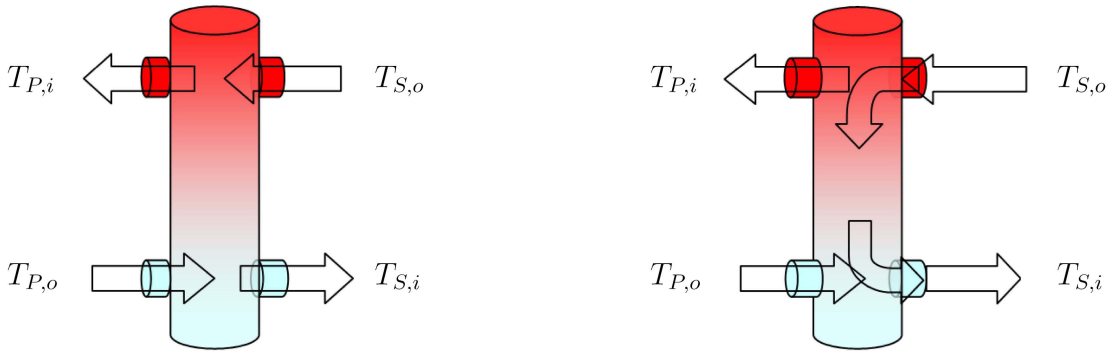

Figure 4.3: Hydraulic bypass: (a) $\dot{m}_P = \dot{m}_S$ and (b) $\dot{m}_P < \dot{m}_S$.

4.1.3 Bypass line and collector

Inside the plant a bypass arm is used: a pipe connecting the chiller outgoing arm with the returning arm coming from users. The hydraulic section with chiller machines is defined as primary circuit; the secondary circuit is the hydraulic section with distribution systems (pumps, collectors) and the final users. In relation with the water load ratio between primary and secondary circuit, it is possible to evaluate qualitatively and quantitatively the effect of inserting a bypass. This bypass, even called decoupler arm, allows a general manage of losses and exceeds on the flow coming from parallel chillers. In details, if on the secondary there's a demand through the various fan-coil circuits pumps of a flow greater than those feeded by the primary active arms, then a portion of the water coming back from users is forced, through bypass pipes, to go back on the outgoing tube. On the other hand, in case of an exceeding flow from chillers, the outgoing water is forced through bypass pipes to go to the returning arm without passing through the users circuit. In this Thesis, conditions analyzed are focused on balanced flows cases or even with the case of a secondary load greater than that on primary.

Let $\dot{m}_{Ch_1}, ..., \dot{m}_{Ch_n}$the masses flow rate of the n-chillers. Let constant mass flow rate at the secondary $\dot{m}_S = \dot{m}_{Ch_1} + ... + \dot{m}_{Ch_n}$.[1]

On the primary side, when a chiller is in the OFF state even the dedicated respective pump is unlighted, therefore the primary circuit load can assume the following values: $\dot{m}_P \in \left\{0, \dot{m}_{Ch_1}, \dot{m}_{Ch_1} + \dot{m}_{Ch_2}, ..., \sum_{i \in ON} \dot{m}_{Ch_i}\right\}$when are in ON state none, one or two or more chillers respectively. In conclusions, thanks to the given simplified hypothesis, comes $\dot{m}_P \leq \dot{m}_S$.

On Figure 4.3(a) condition ($\dot{m}_P = \dot{m}_S$), given a steady state regime, with the hypothesis of no thermal losses towards the ambient, the powers at primay and

[1]It is a simplified hypothesis because it does not consider the exclusion of some distribution sections, on the users side, by the means of zone valves or valves of the fan-coils themselves.

secondary comes (for notational simplicity are omitted the time temperature dependence) :

$$P_P = \dot{m}_P c_p (T_{P,o} - T_{P,i}) \,, \tag{4.12}$$

$$P_S = \dot{m}_S c_S (T_{S,o} - T_{S,i}) \,, \tag{4.13}$$

$$P_P = P_S \,. \tag{4.14}$$

From devices geometrical considerations, not too much restrictive, it can be assumed:

$$T_{P,o} = T_{S,i} \,, \tag{4.15}$$

and, considering the equal loads hypothesis, it comes out from the Equation 4.14 that the chiller returning water temperature is the same coming back from users.

$$T_{P,i} = T_{S,o} \,. \tag{4.16}$$

On the other side, when at least one of the two chillers is in OFF state, the Figure 4.3(b) condition ($\dot{m}_P < \dot{m}_S$) is entered: part of the water coming from users goes back as an outgoing to the load. With the previous remaining hypothesis still valid, in this case it comes:

$$(T_{P,i} - T_{P,o})\dot{m}_P = (T_{S,o} - T_{S,i})\dot{m}_S \,, \tag{4.17}$$

and, if relative positions of outgoing and coming back from primary and secondary are honored, considering the coming flow from the secondary returning is much greater than that returning from primary:

$$T_{P,i} = T_{S,o} \,. \tag{4.18}$$

Combining (4.17) with (4.18), expression (4.19) is obtained for the users circuit outgoing water temperature (secondary circuit), given the temperatures coming out from chillers and going back from users.

$$T_{S,i} = T_{S,o} - \frac{\dot{m}_P}{\dot{m}_S} (T_{S,o} - T_{P,o}) \equiv T_{S,o} - \frac{\dot{m}_P}{\dot{m}_S} (T_{P,i} - T_{P,o}) \,. \tag{4.19}$$

The (4.19) second formulation shows intuitively the decoupling functioning when flows are unpaired: the users outgoing water temperature is equal to the coming back temperature to which is subtracted a part, proportional to the loads ratio, of the thermal gap to the primary circuit. The formulation obtained in (4.19) remains

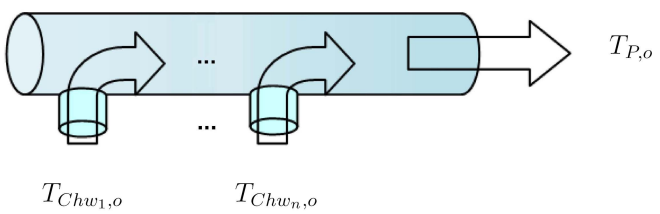

Figure 4.4: Collector.

valid even in the case of loads equilibrium, Figure 4.3 (a), since it gives exactly the (4.15).

Referring to the Figure 4.1 basic scheme, are seen on the primary circuit nodes where each chiller outgoing water flows into the circuit itself outgoing mass. Physically, the device executing that operation is commonly known as collector: for the present plant the 4.4 example figure is reported.

Given the stationary regime, it is imposed that the thermal power entering the collector is equal to that going out

$$\dot{m}_{Ch_1} c_p T_{chw_1,o} + ... + \dot{m}_{Ch_n} c_p T_{chw_n,o} = \dot{m}_P c_p T_{P,o} \,, \tag{4.20}$$

from which

$$T_{P,o} = \frac{\dot{m}_{Ch_1} c_p T_{chw_1,o} + ... + \dot{m}_n c_p T_{chw_n,o}}{\dot{m}_P} \,. \tag{4.21}$$

4.1.4 Remark

The dynamic behaviors that are relevant for controller design and optimization have been taken into account (see, e.g., the modelling of water tanks),while neglecting or simplifying other dynamic phenomena that contribute only marginally to the assessment of the overall controller-plant performance. Aim to develop an efficient management strategy for multiple chiller system and to evaluate its performance, we have resorted to a dynamic simulation environment developed in MATLAB™ and SIMULINK™, where the plant dynamics are accurately described, by the formulation described above.

4.2 Simulation model validation

In this Section an experimental test facility for single chiller unit that has been used to validate the model is described, some results of the validation tests are presented, showing a satisfactory agreement between test and simulation. A more extensive validation test campaign, for multiple chiller system, is nowadays under implementation.

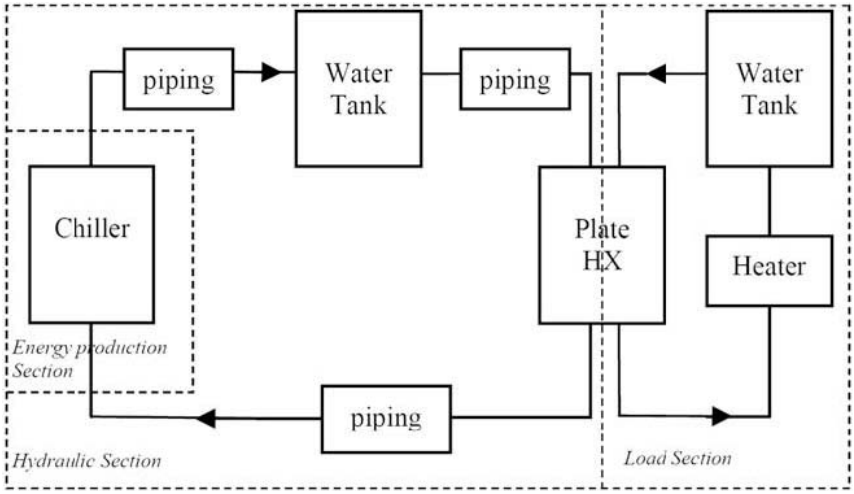

Figure 4.5: Model: single chiller system. For the plate heat exchanger block, the energy term is determined as a function of inlet temperatures defining a heat exchanger efficiency ϵ and evaluating the heat-exchanger performance using the number-of-transfer-units method [22].

4.2.1 The test facility

In Figure 4.6 the experimental test facility used to validate the simulation model (Figure 4.5) is schematically shown. The energy production section is equipped with a Rhoss TCAEY 130 packaged air-cooled water chiller with R410A refrigerant, cooling capacity of 29.1 kW and COP (coefficient of performance defined as the ratio of cooling capacity and compressor power absorption) of 2.44 in the following operating conditions: condenser input air temperature, 35 °C; chilled water temperature, 7 °C; and temperature differential at evaporator, 5 °C. The chiller is equipped with a single scroll compressor without capacity control. The hydraulic section has a 45 l water tank and a piping total volume of 36 l. The pump constant water flow rate is 1.28 kg/s. The load section has an electrical heater, with a heating capacity in the range 0–50 kW and a 480 l water tank. A brazed plate heat exchanger (BHE) is installed.

Thermocouples and pressure transducers are placed as shown in Figure 4.6. Water temperatures are measured with Pt100 thermometers placed inside mixing chambers at the inlet and outlet of each heat exchanger. The refrigerant temperatures are measured with Pt100 thermometers placed on the pipe wall. A 0.3 °C accuracy is estimated for all the temperature measurements. The R410A mass flow rate is measured by a Coriolis mass flow meter placed upstream of the throttling valve. The claimed accuracy is 0.1% of reading. Water volumetric flow rates are measured by electromagnetic meters (accuracy 0.2% of reading). The R410A pressures are recorded with strain-gauge transducers at compressor suction and discharge. The accuracy is 10 kPa according to the calibration report from the manufacturer. Elec-

trical absorbed power is recorded with an electronic transducer (with an accuracy 0.5% of the reading value). Tests have been carried out with the condenser positioned in a climatic room maintained at 35 °C air temperature. By controlling the heater thermal power, the chiller has been tested in full load conditions and at 25%, 50%, 75% part load conditions. The mean system efficiencies in terms of EER (energy efficiency ratio defined as the ratio of cooling capacity and total power absorption, fans included) have been obtained by integrating the power absorption and the cooling capacity, computed from the instantaneous values of refrigerant mass flow, condenser outlet and evaporator outlet enthalpies, which are computed from pressure and temperature values on the basis of refrigerant properties as represented in the NIST Reference Fluid Thermodynamic and Transport Properties – REFPROP, Version 7.0 [23]. The computed cooling capacity on the refrigerant side has been compared and validated with the computed capacity on the water side.

4.2.2 Validation test campaign

A wide validation test campaign for the developed simulation environment has been carried out on the test facility described above (Figure 4.6). Tests have been performed on the chiller with inlet water temperature control, for different values of the electrical heat load, condenser supply air temperature, water mass flow, temperature set-point and differential. The system dynamics and energy performances obtained from experimental tests have been compared to those obtained in the virtual simulation environment. As an example, in Figures 4.7 and 4.8, real and virtual absorbed power, chiller and water tank outlet temperatures are compared at 20% and 75% part load ratio. It is worth noticing that the chiller cooling capacity and absorbed power model are based on manufacture data which do not consider energy losses during compressor start-ups. As a consequence, the expected absorbed power is not exactly predicted, especially during the first period of the compressor working cycle. From Figure 4.8 it can be observed that the simplified, mono dimensional model for the water tank is only partially in agreement with the experimental data, as expected, in particular at high thermal load. However, it is fully adequate for the purpose of controller design reproducing the main dynamic behaviours that are relevant for controller design.

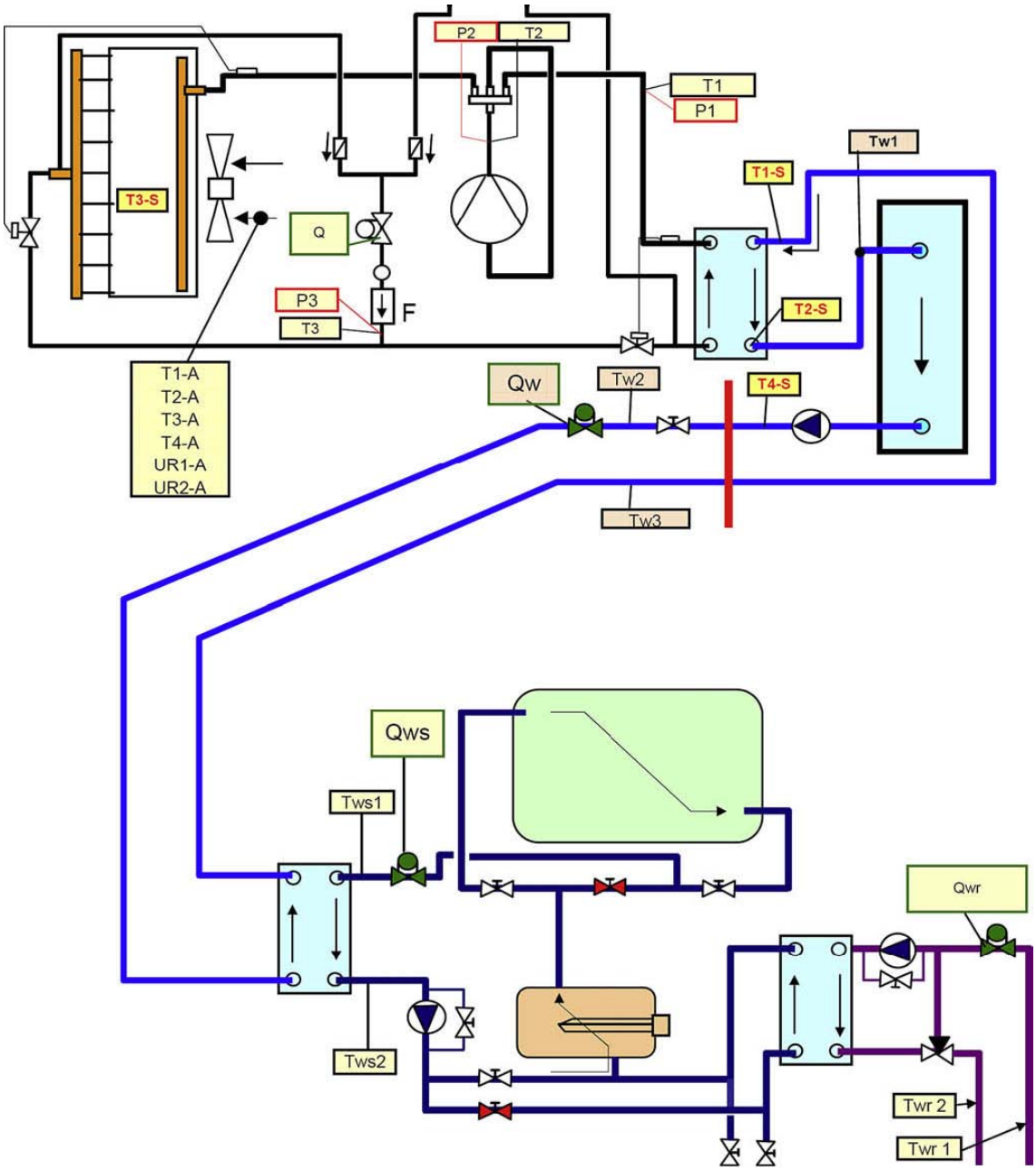

Figure 4.6: System test facility.

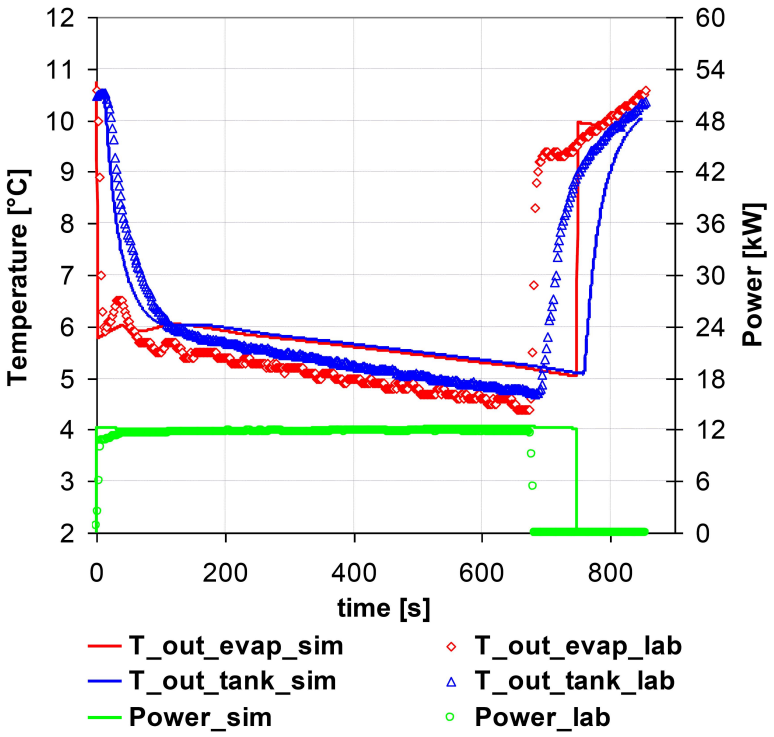

Figure 4.7: Comparison between experimental and virtual system at 20% part load ratio.

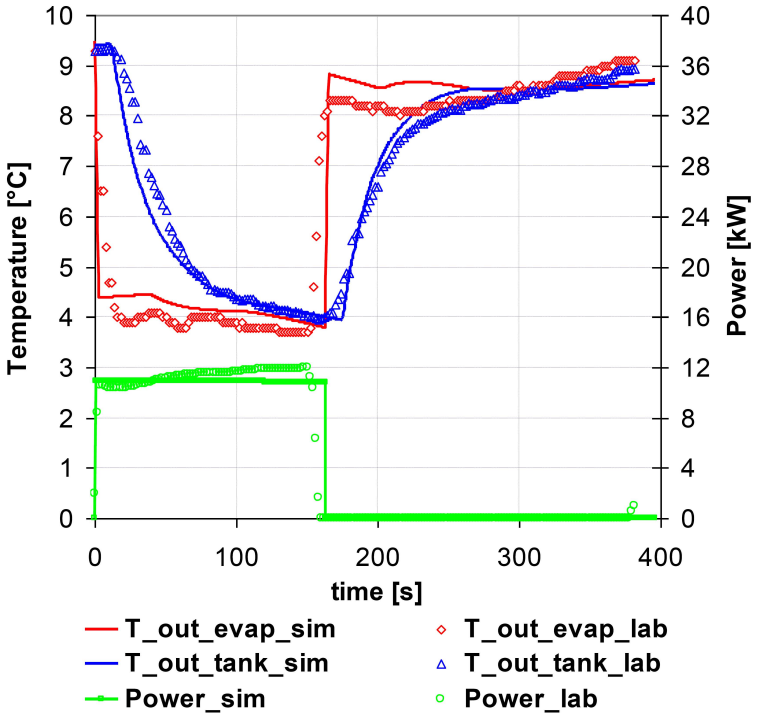

Figure 4.8: Comparison between experimental and virtual system at 75% part load ratio.

5

Multiple chiller optimization and performance

The problem of efficiently managing multiple-chiller systems is complex in many respects. The electrical energy consumption in the chiller plant markedly increases if the chillers are managed improperly therefore significant energy savings can be achieved by optimizing the chiller operation of HVAC systems. In particular, the performance of a system increases if chiller's EER is maximized while the load is satisfied (EER is defined as the ratio of cooling capacity and total power absorption). In general, the cooling load is expressed as a Part Load Ratio (PLR), which is the chiller cooling load divided by its design capacity.

Since Multiple Chiller Management optimization is a nonlinear, constrained, combinatorial optimization with both continuous and discrete variables, and as such, it is a challenge to standard optimization methods.

5.1 Optimal chiller operation

The problem of optimal chiller operation has been ignored because the systems cooling load and the number of chillers have not been large. A commonly used simple approach is to turn on/off chillers sequentially, following changes in demand, without considering any kind of performance measurement associated with energy savings. In [3] an optimal switch-point method is proposed for deciding whether or not another chiller must be switched on/off, based on the fact that, often, the EER curve as a function of the part load ratio is a concave function. In this way, the load is distributed evenly on the chillers. This method assumes that capacities and characteristic curves of chillers are equal, and that only one chiller at a time can be connected/disconnected to the system. Since it is difficult to determine the switch point when cooling capacities of the chillers differ substantially, the resulting average loading amount is clearly non optimal. A simple workaround to this problem

is presented in [4], where it is suggested to turn on the chiller with maximal peak COP, when the activation of another chiller is required (MPCOP method). Again, this method is not optimal.

Since the multi-chiller system consists of chillers of varying performance characteristics and capacities, its optimal operation, that is, its minimum energy consumption during various load demands, is of major concern in efficient multiple chiller management. Specifically, this Thesis attempts to investigate on the distribution of, for instance, the status (on-line or off-line) and the loading ration of chillers in a given load demand and how that distribution best meets the minimum energy consumption. To do so, the Optimal Chiller Loading (OCL) and the Optimal Chiller Sequencing (OCS) are solved to minimize energy consumption.

5.1.1 The OCL problem

The performance of a system with all electric cooling is best when the EER of a chiller is maximized with the load being satisfied. The cooling load is generally expressed as a PLR, which is the chiller cooling load divided by its designed capacity. The EER of a chiller is a function of its PLR for a given wet bulb temperature:

$$EER = f(PLR)\,. \tag{5.1}$$

The Optimal Chiller Loading (OCL) problem is to find a set of chiller output which does not violate the operating limits while maximizing the EER and keeping the cooling demand satisfied (i.e. the sum of cooling load of each chiller, Q_i, have to satisfy the system cooling load Q_{CL}). The constrained maximization problem results:

$$\arg\max_{PLR_i} \sum_i EER_i\,, \tag{5.2}$$

subjected to:

$$\sum_i Q_i = Q_{CL}\,, \tag{5.3}$$

where $i \in \{1, ..., n_{ch}\}$ and n_{ch} is number of chillers of the system.

5.1.2 The OCS problem

Multiple chillers system permits staging equipment to meet the changing loads. The term "sequencing" refers to activating or deactivating chiller units in a chiller water system. Hence, it is beneficial to select the optimal combination of available chillers that maximize the operating system efficiency. The main requirement from a practical standpoint is to avoid excessive number of switches (activation/deactivation) in

order to eliminate chiller start-up and shutdown times and increase equipment life. A common strategy for sequencing chillers is typically accomplished by the "capacity" method in which additional chillers are activated when the operating units have insufficient capacity to meet the current load, and chillers are deactivated when the current load can be met with one fewer machines operating [24], [25]. Given a bank of chillers, choosing the optimal combination of chillers and optimal distribution of cooling load among those chillers can be seen as a dynamic resource allocation problem. Consider a large commercial facility with 15 chillers with different capacities and efficiency curves, leading to 2^{15}combinations. For each discrete combination, there is an optimal selection of its continuous operational variables, including chilled water flow and temperature set-points, that distribute a given thermal load optimally among the participating chillers. This becomes a nonlinear mixed integer optimization problem with potentially multiple solutions. Since it is desirable to minimize the number of switches, it is important to identify solution clusters which remain close as the building loads vary. The Optimal Chiller Sequencing (OCS) problem is to determine which chillers should be on-line or off-line, while minimizing the input power and satisfying the chiller operating constraints during stage working. The constrained minimization problem can assume the form:

$$\arg\min_{status_i} \sum_i InputPower_i\,, \qquad \text{status}_i \in \{\text{on,off}\} \tag{5.4}$$

subjected to, for instance, the following operational constraints:

- *Cooling load balance equation:*

$$\sum_i Q_i = Q_{CL}\,. \tag{5.5}$$

- *Loading limit:*

$$PLR_{min,i} \leq PLR_i \leq PLR_{Max,i}\,, \tag{5.6}$$

  where $PLR_{min,i}$ and $PLR_{Max,i}$ are the lower and upper limits on PLR_i, respectively. The maximal output of a chiller is its designed capacity, so $PLR_{Max,i}$ is one.

- *Minimal up time (MUT) constraints:* a chiller should not be turned off immediately after it has been running, to prevent the chiller from damage caused by frequent start-up and shut downs.

- *Minimal down time (MDT) constraints:* when the chiller is shut down, the pressure between the charge side and the discharge side is very high, and the compressor may not be restarted and maintain its mechanical performance. That is, once a chiller has been disconnected, a minimal period must pass before it can be reconnected.

5.1.3 Remark

Recently, methods for Optimal Chiller Loading and Optimal Chiller Sequencing have been proposed. To solve OCL problem, the Lagrangian method has been adopted in [15] based on the convex function of the kW–PLR curve. The Lagrangian method which uses lambda-iteration method, however, can cause a problem to not reach convergence at low demand. In [5] a genetic algorithm is employed to solve OCL problems with high accuracy and within a rapid frame rate. In [6] a simulated annealing approach is proposed for the same problem. In [7] a branch and bound method and the Lagrangian method are used to solve optimal chiller operations. In [8] a dynamic programming technique is proposed to solve the OCS problem and to eliminate the deficiencies of the conventional methods. However, most of these and other [12] [13] literature methods are heterogeneous: OCL and OCS problems are worked out differently. This can increase the complexity of the algorithms and decrease their accuracy and robustness, especially if the number of chillers involved is large and, more generally, if the involved systems are complex. Moreover, in the HVAC literature are presented methods to do on-line optimization, but these usually ignore or disregard the system dynamics. The optimal control changes through time in response to uncontrolled variables including the ambient conditions and cooling loads.

Since Multi-Chiller Management (MCM) optimization is a nonlinear, constrained, combinatorial optimization with both continuous and discrete variables, and as such, it is a challenge to standard optimization methods. In this Thesis an unified method (MCM) to do on-line optimization is presented, that deals simultaneously with the OCL and OCS problems, with the overall objective of reducing both power consumption and operative costs.

5.2 Energy analysis of air condensed chiller

In the hypothesis of using air condensed chillers, for each one, the electric power consumption $P_{e_{full}}$ and the cooling power $P_{c_{full}}$, in the case of continuous working at full capacity, are expressed as a function of water return temperature, external air temperature and water mass flow rate:

$$\begin{aligned} P_{e_{ful}}(t) &= a_e + b_e T_{chwr}(t) + c_e T_{air}(t) + d_e \dot{m}_w(t) + e_e T_{chwr}(t)\dot{m}_w(t)\,. \\ P_{c_{full}}(t) &= a_c + b_c T_{chwr}(t) + c_c T_{air}(t) + d_c \dot{m}_w(t) + e_c T_{chwr}(t)\dot{m}_w(t)\,. \end{aligned} \tag{5.7}$$

The coefficients a_e, b_e, c_e, d_e, e_e, a_c, b_c, c_c, d_c, e_c, are obtained by a regression procedure on manufacturer's data.

The mean coefficient of performance EER_{full} at full load operating conditions

is defined, in the time step $\Delta\tau$, as:

$$EER_{full} = \frac{P_{c,full}}{P_{e,full}}\,, \tag{5.8}$$

Then a mean part load ratio PLR is calculated as the ratio of the load requirement really supplied by the machine in the time step to the maximum energy which could be supplied in the same time interval in the case of continuous working at full capacity:

$$PLR = \frac{P_c}{P_{c,full}}\,, \tag{5.9}$$

In order to carry out a correct energy analysis of the HVAC plant an evaluation of the effect of operating at part load conditions is required.

The part load influence is taken into account by dividing the full load EER_{full} for a part load factor (PLF) calculated as a function of PLR. The ARI standard suggests a generalized use of the following equation to calculate PLF ([26]):

$$PLF = 1 - c_d(1 - PLR) \tag{5.10}$$

where c_d is a degradation coefficient specified by the manufacturer or taken to be 0.25 as a default value.

Under these assumptions, for a chiller, in part load condition, cooling energy supply and the electric energy consumption on the time interval $\Delta\tau$, are:

$$P_{c,PLF} = PLR \cdot P_{c,full}\,, \tag{5.11}$$

$$P_{e,PLF} = \frac{PLF}{PLR} \cdot P_{e_{full_i}}\,. \tag{5.12}$$

In Figure 5.1 an example of PLF as function of PLR is depicted. Moreover, power consumption as well as cooling power and performance are illustrated, for THAEY120 scroll chiller, in Figure 5.2. It is worth noticing that the effective power absorption of the chiller unit (during ON status) increases when PLR decrease due to discontinue working of the compressor (to obtain load partialisation).

However, the results of tests recently carried out have shown how much unacceptable is the approximation of this simple correlation depicted above and its application for refrigeration machines also very different for operating and control modes. The need to have a correct algorithm, verified for each type of unit, leads to the elaboration of a standard which specifies the test conditions for the rating of commercial machines in order to estimate their behavior also in part load working conditions. For this aim in Italy a new standard, UNI 10963 [27], has been recently

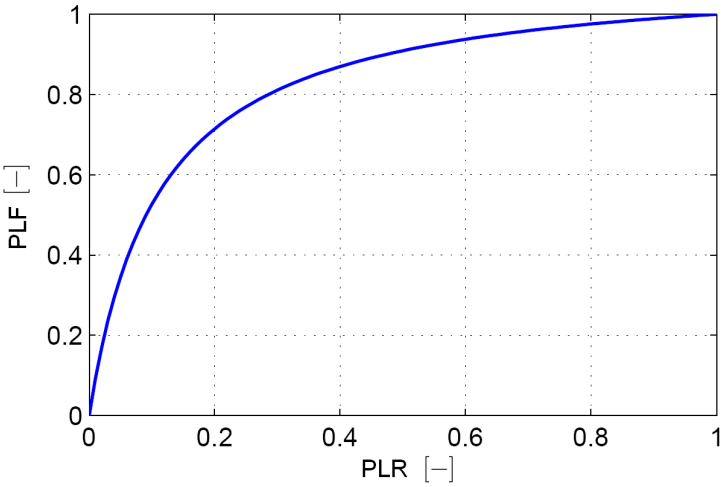

Figure 5.1: THAEY120 scroll chiller: Part Load Factor.

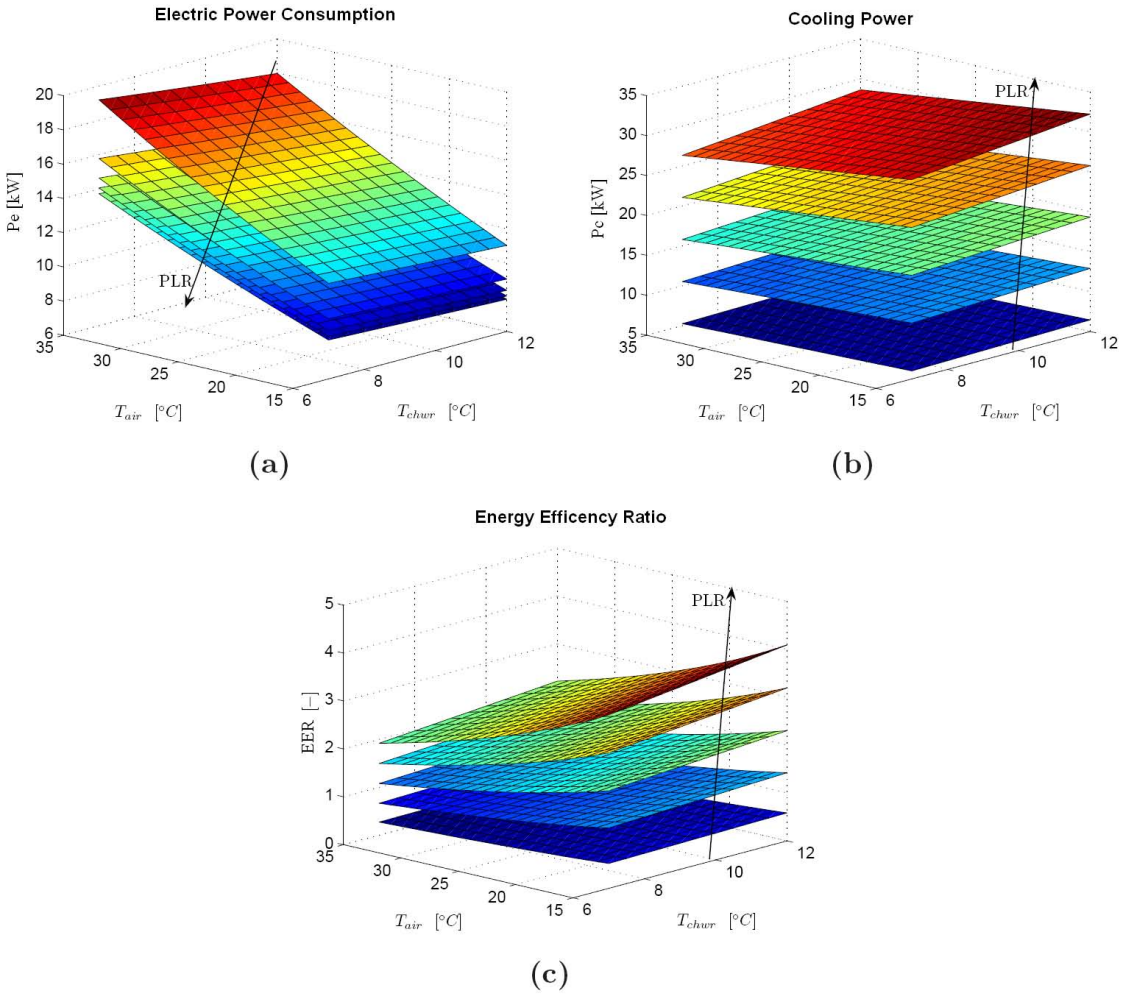

Figure 5.2: THAEY120 scroll chiller: electric power consumption (a), cooling power(b), EER (c) as functions of PLR, air temperature T_{air} and chiller water return temperature T_{chwr}.

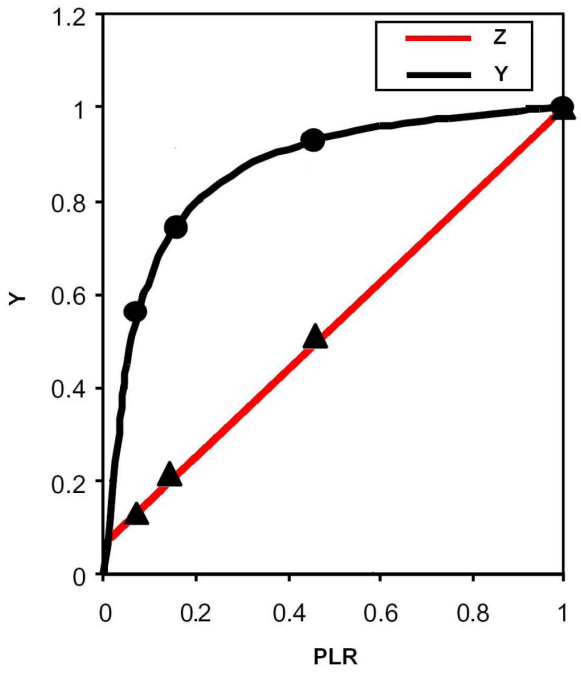

Figure 5.3: Y and Z curves (functions of PLR, fixed T_{air}).

introduced and also proposed to ISO. The UNI 10963 "Air conditioners, chillers and heat pumps. Determination of the part load performances has the merit of the novelty not only in Italy but also at international level.

In order to carry out a correct energy analysis of the HVAC plant, when the refrigerant machines are working at part load conditions a procedure based on this standard, as suggested in [28], is here adopted.

For the chiller unit the part load rating is obtained by the cycling of the compressor. In this case:

$$Y = \frac{EER_{cyc}}{EER_{full}} \tag{5.13}$$

where EER_{cyc} is the coefficient of performance at part load working (cycling conditions) and EER_{full} is the full load EER.

In the same way:

$$PLR_{cyc} = \frac{P_{c,cyc}}{P_{c,full}} \tag{5.14}$$

where $P_{c,cyc}$ is the part load capacity and $P_{c,full}$ is the full capacity at the same operative temperatures. Moreover, a parameter called Z is also introduced as the ratio of the electric consumption of the machine at part load working $P_{e,cyc}$ to that

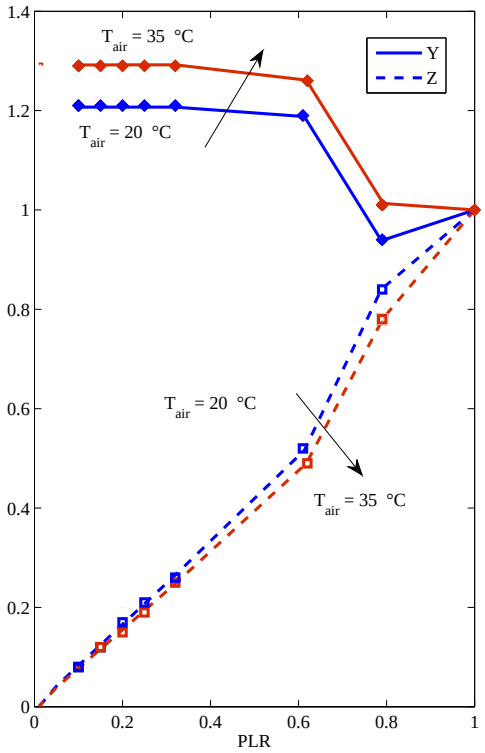

Figure 5.4: Y and Z curves (functions of PLR and T_{air}).

one at full capacity $P_{e,full}$:

$$Z = \frac{P_{e,cyc}}{P_{e,full}} \tag{5.15}$$

The relation between Y and Z results:

$$Y = \frac{PLR_{cyc}}{Z} \tag{5.16}$$

The Y and Z part load factors, for a specified chiller model, are obtained from the Y_{curve} and Z_{curve} that are derived as a function of PLR , for a fixed air temperature, from laboratory tests (Figure 5.3).

Nevertheless, the simulations done during this work suggest that for a correct energy and performance analysis the influence of the external air temperature T_{air} is not negligible. Therefore, The Y and Z part load factors, for a specified chiller model, are obtained from the Y_{curve} and Z_{curve} that are derived as a function of PLR and T_{air} (Figure 5.4).

For a chiller, in part load condition, cooling power supply and the electric power consumption can be obtained (for instance, exploiting Z_{curve}) as :

$$P_{c,cyc} = PLR_{cyc} \cdot P_{c,full} \, , \tag{5.17}$$

$$P_{e,cyc} = Z \cdot P_{e,full} \,. \tag{5.18}$$

The EER for a single chiller is defined, in the time step $\Delta\tau$, as:

$$EER = \frac{P_{c,cyc}\Delta\tau}{P_{e,cyc}\Delta\tau} \,. \tag{5.19}$$

6 Multiple chiller management

Better performance of HVAC systems can be achieved by optimizing the supervisor control strategy. One significant improvement in efficient chiller operation is the development of chiller management and maintenance software.

6.1 Common strategies

A commonly used simple approach is to turn on/off chillers sequentially, following changes in demand, without considering any kind of performance measure associated with energy savings. For a set of n-parallel chillers with m-discrete capacity steps system two common strategies are considerated[1]:

1. *sequential strategy (MS):* chillers are represented as a sorted sequence $Ch_{1,j}, ..., Ch_{i,j}, ..., Ch_{n,j}$ with $1 \leq j \leq m$; if, at a given instant t, chillers $Ch_{1,m}, ..., Ch_{i-1,m}, Ch_{i,s}$ are operating and load demand is unsatisfied, then chiller $Ch_{i,s+1}$ is switched on. Only the last chiller, potentially, operates at part load condition, the others operate at full capacity (Figure 6.1a) ;

2. *symmetric strategy (SS):* if, at given instant t, chillers $Ch_{1,s}, ..., Ch_{i,s}, Ch_{i+1,s-1}, ..., Ch_{n,s-1}$ are operating and load demand is unsatisfied, then chiller $Ch_{i+1,s}$ is switched on (Figure 6.1b).

6.2 MCM strategy

With reference to Figure 6.2 a two-level control structure is used. At the low-level, each chiller set-point is maintained using a local controller (for instance as presented in [22]). At the higher control level, a supervisor specifies the modes of operation and

[1] See Appendix C for a pseudocode example.

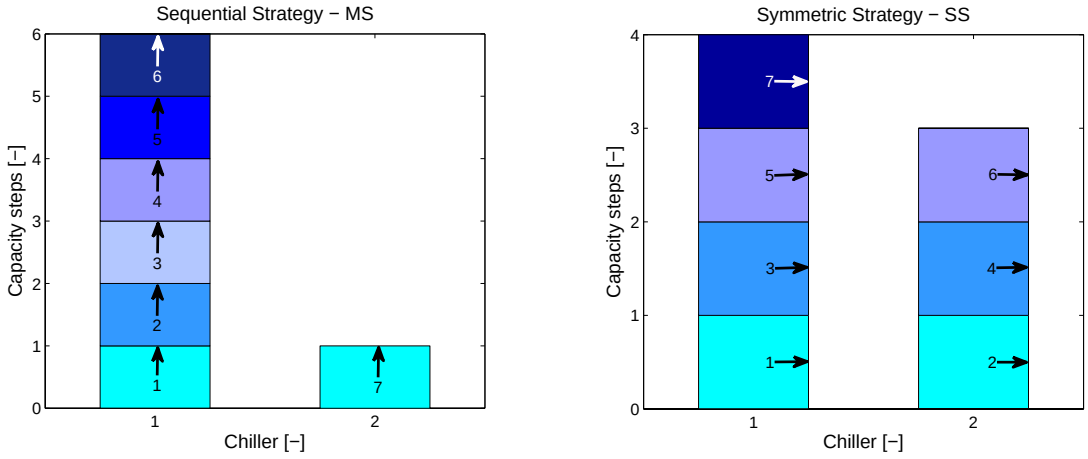

(a) The MS strategy.

(b) The SS strategy.

Figure 6.1: Example: common strategies for 2-parallel chillers with 4-discrete capacity steps system.

the set-points for each chiller. If the set points, and thus the individual cooling loads of the units, are determined without resorting to a global system optimization, the system does not perform at its full potential because the OCL and OCS problems are not solved.

6.2.1 Low-level controller

Typically, a chiller without capacity control can be regulated in two different ways, namely by controlling the chiller evaporator water outlet or the chiller evaporator water inlet. In both cases, a relay control law is used, where the compressor is switched on and off when the controlled temperature reaches given threshold values. The difference between the upper and lower threshold values is called water temperature differential, and its value clearly affects the width of the oscillations of the supply water temperature as well as the number of start-ups of the compressor.

Summarizing, the regulation parameters affecting chiller performance are three: the imposed set-point, its temperature differential (DM or DR when controlling the chiller evaporator water outlet or the chiller evaporator water inlet, respectively) and the thermal gap (ΔT) of the water within the exchanger (evaporator) or by the difference between the input and output water temperatures.

A low value of the water temperature differential grants a higher control bandwidth and allows to obtain a more constant water temperature. On the other hand, there is an upper bound to the number of compressor start-ups per hour, which is set by the compressor manufacturer. As a consequence, there is an upper bound to the achievable control bandwidth. Also, the value of differential cannot be decreased arbitrarily, but there is a lower limit value which depends on the plant water content

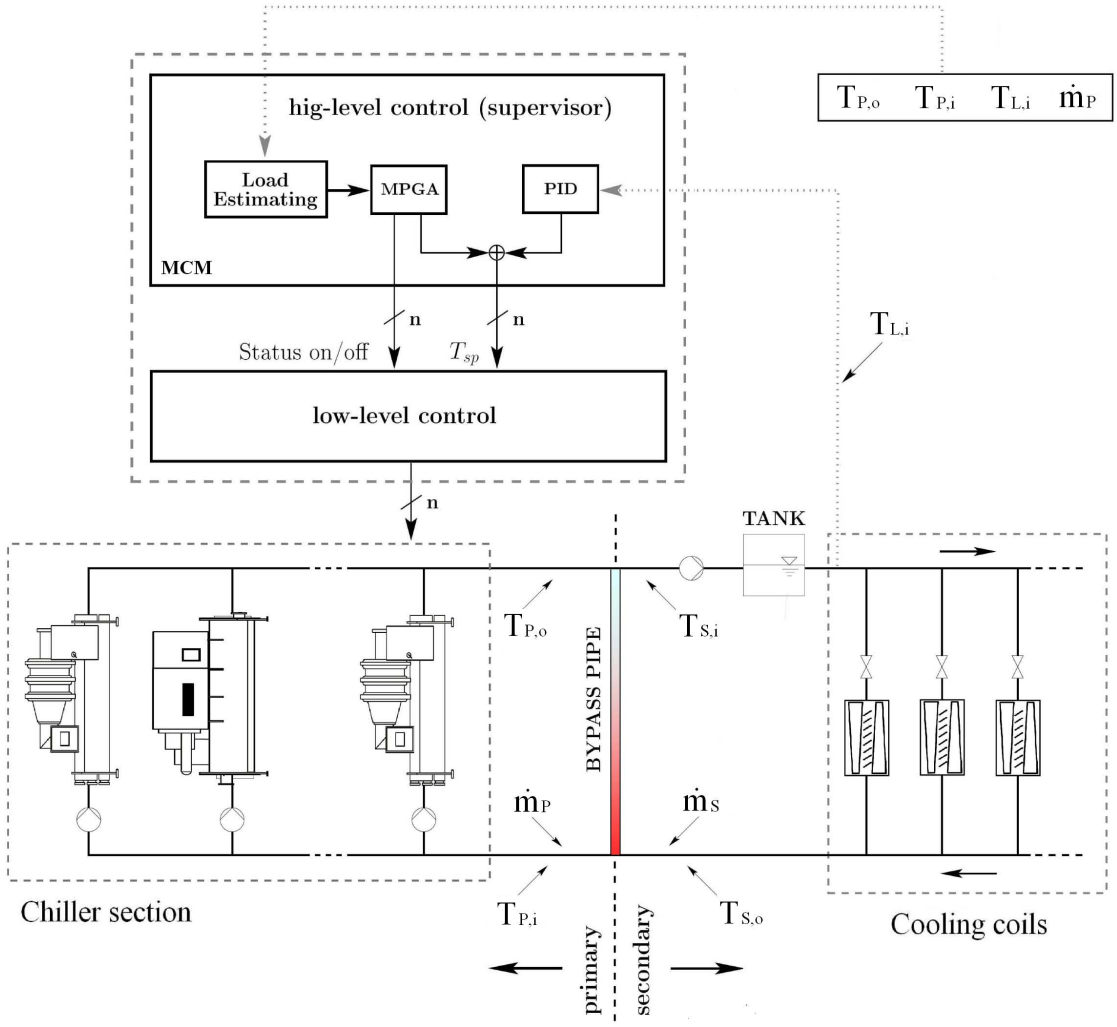

Figure 6.2: Decoupled system.

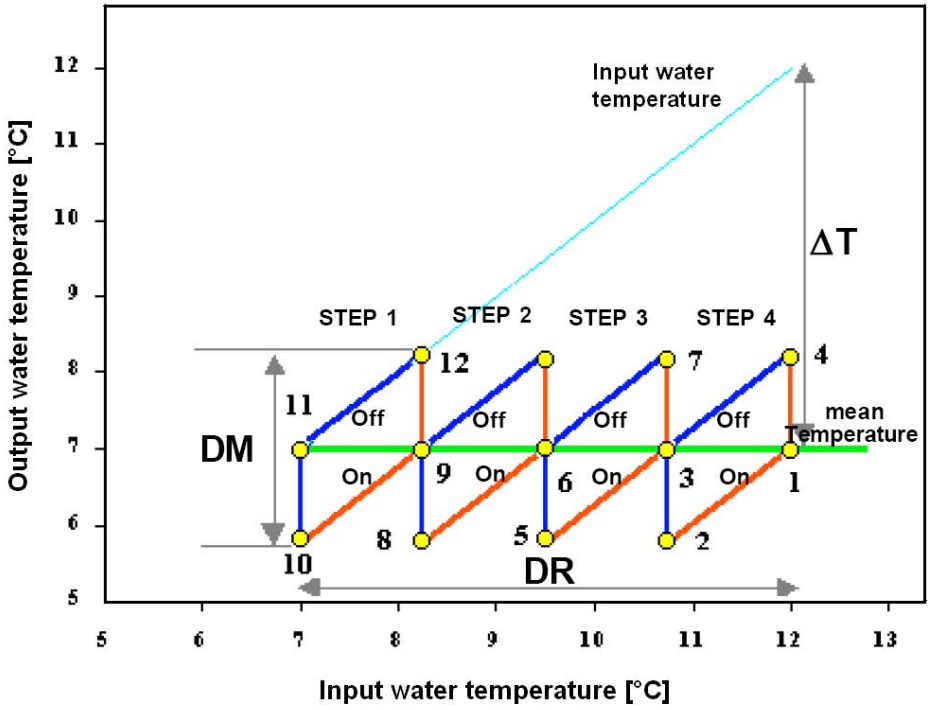

Figure 6.3: Logic regulation for cooling machine with four capacity partialization steps.

([4]).

Most machines are equipped with several steps of regulation. The temperatures behavior can be depicted on a diagram showing on abscissa the exchanger input temperature and on ordinates its output temperature. Figure 6.3 proposes an example of temperatures behavior on a machine with four regulation steps.

When the machine works at full load condition, with input temperature at 12°C, whenever the thermal gap ΔT is of 5 °C the output temperature is equal to 7 °C (Figure 6.3, point 1). If the load of the plant is less than the power provided by the chiller group, then the evaporator input temperature diminishes and, consequently, so does the output one. When the input temperature is equal to 10.75 °C, the output temperature is equal to 5.75 °C (point 2) and the first partialization step is switched off. Power is reduced by a quarter and consequently, remaining unchanged the water throughput, even the thermal gap is reduced from 5 °C to 3.75 °C. The output temperature becames again 7°C (point 3).

If the power furnished by the group continues to be greater than the one requested by the plant, then the temperature tends to go down again towards point 5, where another step is deactivated, therefore reducing the thermal load ΔT to only 2.5 °C (point 6). Instead, if the power is lesser than requested, then the temperature tends to go up until point 4 is achieved, where the partialization step is reactivated and the thermal gap ΔT becames again 5 °C.

Therefore, every partialization step draws a quadriside over whose sides output temperatures move as a function of the input temperatures: when the connected step is activated (step ON) temperatures are moving over the red sides, when it is deactivated (step OFF) they are moving over blue sides. As the load diminishes the various steps are deactivated and the work point is moved towards quadrisides more on the left.

The rule is simple: a load diminishing moves points to the left, an augment to the right. The way of moving is always clockwise. Further pairs of points are not possible, if not modifying the water throughput, then the thermal gap ΔT, that is the external parameter.

Obviously, when a partialization step is being deactivated the thermal gap to the evaporator diminishes in proportion. If with four steps activated the difference between the input and output temperature is equal to 5 °C, then with three becames equal to 3.75 °C, with two is equal to 2.5 °C and 1.25 °C with one.

While both control strategies maintain constant water supply temperature in full load conditions, outlet water temperature control grants better performance during chiller part load operations since it maintains the mean water supply temperature fairly constant during on/off operations. Chillers evaporator water outlet control is here adopted.

6.2.1.1 Virtual Tank

Integrated controllers of chillers on Market usually implements logics limiting the number of hourly ignitions, besides the duration itself of the compressor ON and OFF intervals. An accurate control, from the point of view of single processor functionality, goes beyond this paper aims; nevertheless, even for chiller evaporator water outlet control needs, an artifice used in [29] is introduced in order to complete the relay logic: the virtual tank. The basic principle of the virtual gathering is that of simulating the presence of a tank in order to increase the inertia "seen" by the hysteresis chiller controller. As discussed in Section (4.1.1), the transfer function of an (actual) accumulator can be assimilated to a low-pass filter plus a delay function: likewise, for the virtual tank a time continuous function is employed:

$$W_{vt}(s) = \frac{e^{-s\tau_{vt}}}{1 + s\mathcal{T}_{vt}} \,. \tag{6.1}$$

A discrete form of (6.1) is obtained by the means of the impulsive answer invariant method as follows:

$$H_{vt}(z) = \frac{k_1}{1 + z^{-1}k_2} z^{-\frac{\tau_{vt}}{\mathcal{T}_s}} \,. \tag{6.2}$$

Usually, a generic accumulation inserted on a plant (like that on scheme (4.1))

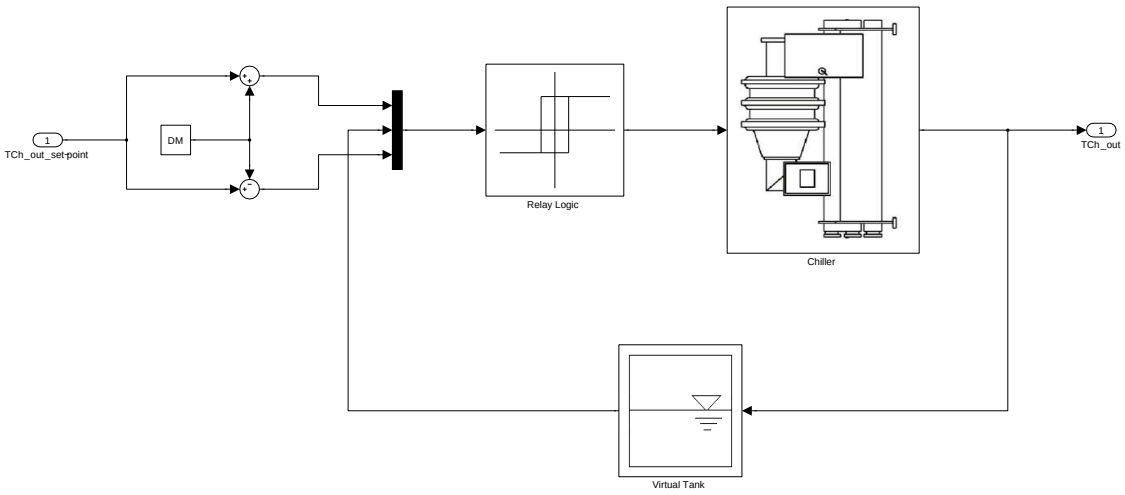

Figure 6.4: Relay logic with virtual tank.

Table 6.1: Values for τ_{vt} , $\mathcal{T}_{vt}$ and k_1 and k_2 corresponding to $1 \div 10$ l/kW water content.

l/kW	τ_{vt}	$\mathcal{T}_{vt}$	k_1	k_2
1	7.69	13.99	$3.511 \cdot 10^{-2}$	0.9649
2	13.71	28.41	$1.745 \cdot 10^{-2}$	0.9826
3	19.73	42.82	$1.161 \cdot 10^{-2}$	0.9884
4	26.61	56.38	$8,83 \cdot 10^{-3}$	0.9912
5	32.62	70.80	$7.04 \cdot 10^{-3}$	0.9930
6	38.64	85.21	$5.855 \cdot 10^{-3}$	0.9941
7	44.66	99.63	$5.001 \cdot 10^{-3}$	0.9950
8	50.67	114.05	$4.375 \cdot 10^{-3}$	0.9956
9	56.67	128.47	$3.885 \cdot 10^{-3}$	0.9961
10	62.64	142.89	$3.493 \cdot 10^{-3}$	0.9965

is dimensioned in terms of litres installed per kilo-Watt of total chilling power. In Table 6.1 some values for τ_{vt} , $\mathcal{T}_{vt}$ and consequently for k_1 and k_2 are given for the range from 1 to 10 l/kW water content (for further reading, see [29] and [30]).

6.2.2 High-level controller: supervisor

The architecture of the supervisor, Multi-Chiller Management (MCM) [31] consists of three main components (Figure 6.2):

- a load estimation algorithm;
- a Multi-phase genetic algorithm for solving the OCL and OCS problems;
- a PID controller.

At each supervision period (i.e. 10 minutes) the system cooling demand is estimated and is passed to the MPGA that solves, simultaneously, the OCL and OCS prob-

lems and provides the cooling load, in the form of local set-points, and the status (on/off) to each chiller. Moreover the supervisor is equipped with a supplementary control loop, with a PID controller, in order to regulate the inlet load-side water temperature. The computations required by the optimization process are well performed within a time length of five minutes on a personal computer, thus granting an on-line implementation.

6.3 Problem Formulation

The aim of the optimization problem is to minimize chillers energy consumption keeping the cooling demand satisfied; as a matter of fact, the performance of the system increases if chiller's EER is maximized while the load is satisfied. In order to minimize the input electric power and satisfying the chiller operating constraint, at each supervision period, OCL and OCS problems are solved, simultaneously, to determine for each chiller:

- the status: on-line or off-line;
- the fraction of the total cooling load to be supplied;
- the water outlet set-point temperature.

6.3.1 Constrained formulation

The problem is nonlinear, constrained, combinatorial optimization with both continuous and discrete variables. In relation to a $\Delta\tau$ time step, the problem can be formulated as follows:

find

$$\arg \min_{(PLR_i,\, status_i)} \sum_i P_{e,i}\,, \tag{6.3}$$

subjected to:

$$\sum_i P_{c,i} = \hat{P}_L\,, \tag{6.4}$$

$$\left|PLR_i - PLR_{i_{prev}}\right| \leqq \kappa_i\,, \qquad i = 1, ..., n\,. \tag{6.5}$$

In (6.3) and (6.4), $P_{e,i}$ and $P_{c,i}$ are the $i-$th chiller power consumption and cooling capacity, respectively. $\hat{P}_L$ is the estimated cooling demand on the $\Delta\tau$ time step and PLR_i is the i-th chiller cooling load divided by its design capacity. The constraint (6.5) describes the gap between PLR_i and $PLR_{i_{prev}}$, assigned to the $i-$th chiller at the previous supervisor time-step. It avoids that the cooling load attributed to a single chiller varies too much between two successive supervision

periods in order to reduce the need of actuating the unit and as a consequence reducing the mechanical stress. In symbols:

$$PLR_i = \left.\frac{P_{c,cyc}}{P_{c,full}}\right|_i \tag{6.6}$$

$$Z_i = \left.\frac{P_{e,cyc}}{P_{e,full}}\right|_i \tag{6.7}$$

$$P_{c,i} = PLR_i \cdot P_{c,full}|_i \ , \tag{6.8}$$

$$P_{e,i} = Z_i \cdot P_{e,full}|_i \ . \tag{6.9}$$

The EER_i for a single chiller is defined on the time step $\Delta\tau$ as:

$$EER_i = \frac{P_{c,i}\Delta\tau}{P_{e,i}\Delta\tau} \tag{6.10}$$

6.3.1.1 Remark: thermal comfort model

The ultimate objective of any energy management program is the identification of energy conservation opportunities which can be implemented to produce a cost saving. However, it is important to recognize that the fundamental purpose of an HVAC system is to provide human thermal comfort, or the equivalent environmental conditions for some specific process.

As concern the thermal comfort, the model proposed by Fanger is the most diffused [32]. Fanger identify a model in which the main factors involved in the heat exchange are strictly dependent only on environment condition(the heat lost in convection phenomena and the energy lost for the irradiation phenomena) and on an insulating battier between body surface and the air. This model was accepted by the International Standard Organization and introduced in the ISO 7730 norm [33] for the comfort inside moderate thermal environments. Fanger created an index that express the satisfaction of people in the well-defined situations: the predicted mean vote (PMV) that describes, with the seven different discrete level of the ASRHAE comfort scale, the feelings of the considered subjects (e.g. -3 cold, -2 slightly cool, +3 hot).

We would maintain that there is no necessity to specify comfort, and thereby PMV, with more precise scale, because considering the psycho physics connotation, a thermal comfort index has to be intrinsically at low resolution. The second parameter proposed, the PPD (percent of dissatisfied), is a function of PMV and indicates the number of people who are not in a comfort condition at that PMV, thereby it completes the scenario proposed for an automatic and personalized thermal comfort,

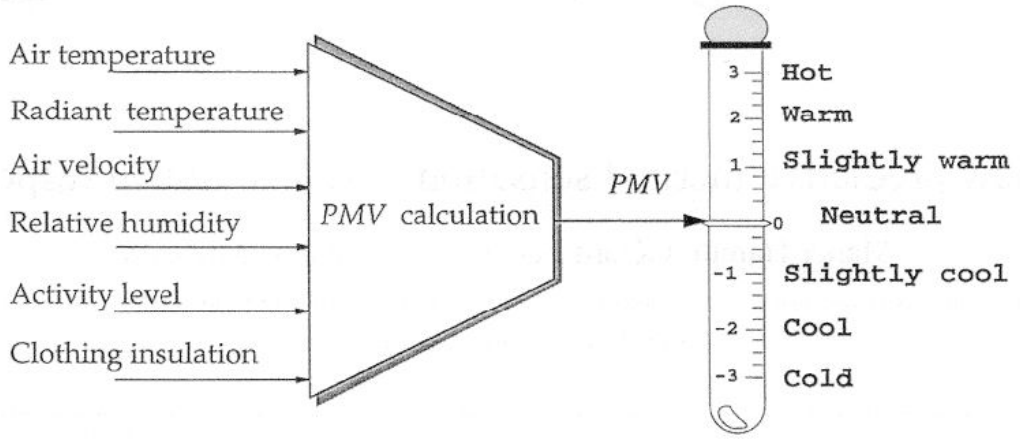

Figure 6.5: PMV calculation.

forcing the system to also obtained a specific PPD (typically 10% of the population). In more detail, Fanger proposed to quality thermal comfort using Equation 6.11:

$$\begin{aligned} PMV = \; & \left(0.303 \cdot e^{-0.036M} + 0.028\right) \{(M-W) - 3.05 \cdot 10^{-3} [5733+ \\ & -6.99\,(M-W) - p_a] - 0.42\,[(M-W) - 58.15] + \\ & -1.7 \cdot 10^{-5} M\,(5867 - p_a) - 1.4 \cdot 10^{-3} M\,(34 - T_a) + \\ & -3.96 \cdot 10^{-8} f_{cl} \left[(T_{cl}+273)^4 - (T_{mrt}+273)^4\right] + \\ & -f_{cl} h_c\,(T_{cl} - T_a)\,\} \; ; \end{aligned} \tag{6.11}$$

where:

$$\begin{aligned} T_{cl} = \; & 35.7 - 0.028(M-W) - 0.155 I_{cl} \{3.96 \cdot 10^{-3} f_{cl} [(T_{cl}+273)^4 - \\ & -(T_{mrt}+273)^4] - f_{cl} h_c (T_{cl} - T_a)]\,, \end{aligned} \tag{6.12}$$

and,

$$h_c = \begin{cases} 2.38(T_{cl} - T_a)^{0.25} & \text{if } 2.38(T_{cl} + T_a)^{0.25} \geq 12.1\sqrt{V_{air}} \\ \\ 12.1\sqrt{V_{air}} & \text{if } 2.38(T_{cl} + T_a)^{0.25} \leq 12.1\sqrt{V_{air}} \end{cases}, \tag{6.13}$$

with:

- M is the metabolic energy produced (met, $1\,met = 58.2\ W/m^2$);
- W is the free energy production (external work, W/m^2);

- p_a is the partial vapour pressure of water vapor (P_a);
- t_a is the air temperature ($°C$);
- f_{cl} is the ratio between covered and free surface of body;
- h_c is the convective heat exchange coefficients ($W/m^2/°C$);
- T_{cl} is the clothes temperature of the external surface ($°C$);
- I_{cl} is the clothing thermal resistance value (clo, $1\,clo = 0.155 K m^2/W$);
- T_{mrt} is the mean radiant temperature ($°C$).
- V_{air} is the air velocity (m/s)

It is worth noting that this formula is composed of many terms that are not easy to calculatem such as M, W, t_{cl}, h_c and t_r and we consequently have to consider the possibilitty to extrapoalte these in an automatic way.

In this way a penalty term, based on PMV and PPD, can be add to the contrained problem 6.3. A test is presently under development.

6.3.2 Unconstrained formulation

In this work, in order to solve the constrained problem 6.3, a genetic algorithm approach is employed (see Appendix A). One of the advantages of genetic algorithms is that it is parallel because they have multiple offspring thus making it ideal for large problems where evaluation of all possible solutions in sequence would be too time taking, if not impossible. They perform well in problems where the fitness landscape is complex, where the fitness function is discontinuous, noisy, changes over time or has many local optima.

However, Genetic Algorithms are most directly suited to unconstrained optimization. Application of Genetic Algorithms to constrained optimization problems is often a challenging effort. In this paper, a penalty-based methods is used (see Appendix B).

In this way, in relation to the $\Delta\tau$ time step, the constrained problem 6.3 can be reduced to an unconstrained minimization problem by an objective nonlinear function with penalty:

$$\arg \min_{(PLR_i,\, status_i)} \quad F_{obj}\,, \tag{6.14}$$

with:

$$F_{obj} \triangleq h_{obj}\left[\sum_i P_{e,i}\Delta\tau\right]^{\nu_{obj}} + h_{err}\left|\sum_i \left(P_{c,i} - \hat{P}_L\right)\Delta\tau\right|^{\nu_{err}} + \\ + h_{reg}\left[\sum_i \max\left(0,\ \left|PLR_i - PLR_{i_{prev}}\right| - \kappa_i\right)\right]^{\nu_{reg}} \qquad (6.15)$$

$i = 1, ..., n\,,$

where the first term of 6.15 is associated with the energy minimization and coefficients h_{obj} and ν_{obj} are the corresponding coefficients, the second term is associated with the load penalty function and h_{err} and ν_{err} are the corresponding load penalty coefficient and the last term of 6.15 is associated with regularity penalty function and h_{reg} and ν_{reg} are the corresponding regularity penalty coefficient.

6.4 Load estimation algorithm

On the secondary side of the hydronic circuit is supposed the presence of an accumulator followed by the block dedicated to work as a load-user. Clearly the supervisor does not have any a priori knowledge about the amount of the instantaneous total cooling load in order to solve the OCL and properly distribute the load to chillers. Therefore, there is the want to study which is the effect of using an estimate instead of the actual load value: in particular, the system is modelled so that the load is seen as a disturbance.

The thermal load estimation algorithm is designed under the key assumption that information on the plant is available in terms of measurements of the inlet and supply water temperatures ($T_{P,i}$ and $T_{P,o}$) and the inlet load-side water temperature ($T_{L,i}$). Therefore, although there are many different thermal loads affecting the plant, it is appropriate to consider a mean-value approach as follows. The energy equation for the hydraulic circuits are obtained under the assumptions that the bypass line is adiabatic and the liquid inside it is negligible, that is:

$$\dot{m}_P c_p (T_{P,i}(t) - T_{P,o}(t)) + \rho c_p V_{tank}\frac{dT_{L,i}(t)}{dt} - P_L = 0 \qquad (6.16)$$

where it has been assumed that the bypass should be an adiabatic device and that the hydrionic liquid amount contained within it is negligible: the latter should not be considered in the energy balance pattern. Note how the accumulation modeling is simpler than what is depicted in 4.1.1: in the following simulations only the device fully mixed part is modelled, ignoring the section involved on stratification phenomena; even the water content of the primary circuit is neglected while that of the secondary is added to the accumulator.

The thermal load dynamics are slow with respect to the chillers dynamics, because they are associated both with the units and individual compressors switching

frequency. As a consequence, as is common in standard disturbance estimation schemes, it is assumed that P_L has constant dynamics. The resulting overall state space model is the following:

$$\begin{cases} \dot{P}_L = 0 \\ \\ \dot{T}_{L,i} = \dfrac{1}{\rho c_p V_{tank}} P_L + \dfrac{\dot{m}_P}{\rho V_{tank}} T_{P,o} - \dfrac{\dot{m}_P}{\rho V_{tank}} T_{P,i} \end{cases} \tag{6.17}$$

Since it is assumed that the supervisor algorithm (with the part devoted to load estimation) will have a micro controller card or an industrial PC as a hardware support, from now on a discrete-time approximate equation of the load balance equation will be used; with the Euler discretization[2] of the (6.16), yields the following equation:

$$P_L(n)\mathcal{T}_s = \dot{m}_P c_p (T_{P,i}(n) - T_{P,o}(n))\mathcal{T}_s + \rho c_p V_{tank}(T_{L,i}(n+1) - T_{L,i}(n)), \tag{6.18}$$

where $\mathcal{T}_s$ is the sampling time and $n \in \mathbb{Z}(\mathcal{T}_s)$. The load is assumed to be slowly varying, in particular it is supposed to remain constant during the sampling period: therefore the equation 6.18 can be represented as a bi-dimensional LTI[3] system Σ, whose states are the heat load and the temperature of water coming out from accumulator and entering load on the secondary.

On the basis of state space model (6.19), a standard Luenberger [34] observer is designed in order to obtain the estimated load $\hat{P}_L$.

$$\begin{cases} P_L(n+1) = P_L(n) \\ \\ T_{L,i}(n+1) = \dfrac{\mathcal{T}_s}{\rho c_p V_{tank}} P_L(n) + T_{L,i}(n) + \dfrac{\dot{m}_P \mathcal{T}_s}{\rho V_{tank}} T_{P,o} - \dfrac{\dot{m}_P \mathcal{T}_s}{\rho V_{tank}} T_{P,i} \end{cases} \tag{6.19}$$

Considering the temperatures $\begin{bmatrix} T_{P,o} & T_{P,i} \end{bmatrix}'$ as inputs of the system Σ and $T_{L,i}$ as the output, matrices describing Σ can be defined : $\Sigma(A, B, C, D)$ with:

$$A = \begin{bmatrix} 1 & 0 \\ \frac{\mathcal{T}_s}{\rho c_p V_{Tank}} & 1 \end{bmatrix}, \qquad B = \begin{bmatrix} 0 & 0 \\ \frac{\dot{m}_P \mathcal{T}_s}{\rho V_{Tank}} & -\frac{\dot{m}_P \mathcal{T}_s}{\rho V_{Tank}} \end{bmatrix},$$

$$C = \begin{bmatrix} 0 & 1 \end{bmatrix}, \qquad D = \begin{bmatrix} 0 \end{bmatrix}.$$

Also, the asymptotic discrete order state estimator can be seen as an LTI system

[2]Forward Euler discretization: $\dfrac{dx(t)}{dt} \approx \dfrac{x_{n+1} - x_n}{\mathcal{T}_s}$

[3]Linear Time-Invariant system.

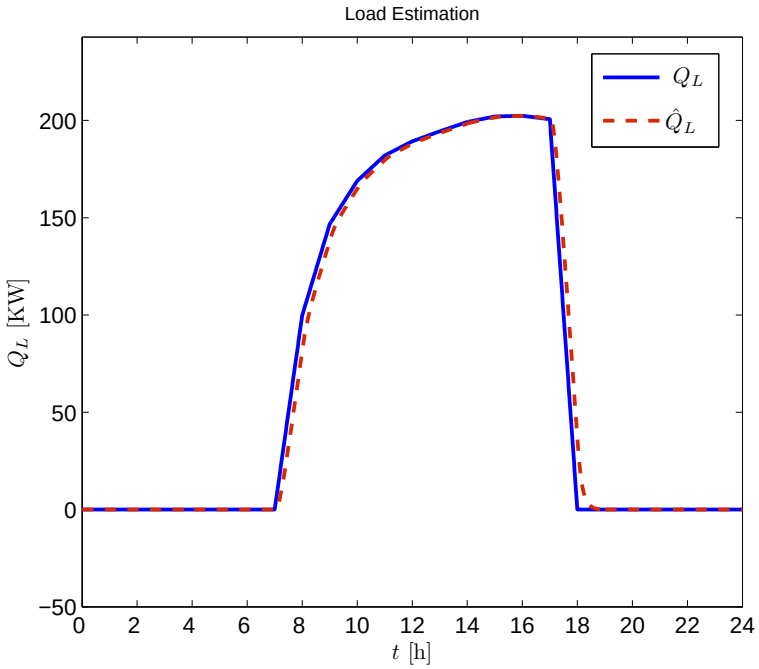

Figure 6.6: Load estimation.

in the state-space form $\Sigma(F, G, H, J)$ with input $u_{\hat{\Sigma}} = \begin{bmatrix} T_{P,o} & T_{P,i} & T_{L,i} \end{bmatrix}'$ (i.e. inputs and output of the system Σ); the output, instead, is represented by the whole estimated load $y_{\hat{\Sigma}} = \begin{bmatrix} \hat{P}_L & \hat{T}_{L,i} \end{bmatrix}'$. Therefore, the estimator matrices are hence:

$$F = [A - LC] \,, \qquad G = \begin{bmatrix} B & L \end{bmatrix} \,, \qquad H = I_{2\times 2} \,, \qquad J = 0_{2\times 3} \,. \tag{6.20}$$

Regarding the correction gain matrix L, several case studies are taken into account: the error dynamics matrix eigenvalues positions obviously affect the estimation error rate, at the expense of the disturbances rejection. The determination of L, once are known the error dynamics matrix eigenvalues, is done via the command MATLAB™ *place*. The latter, however, implements the algorithm [35] for a state feedback system eigenvalues allocation. In Figure 6.6 an example of the load estimation, over a day, is depicted.

6.5 Multi-Phase Genetic Algorithm (MPGA)

Genetic Algorithms (GAs) are a family of computational models inspired by evolutionary schemes and operating through non-deterministic, randomized search. These algorithms encode a specific problem potential solution on a simple chromosome-like data structure and apply recombination operators to these structures in order to preserve critical information. GAs are intelligent search techniques, which are

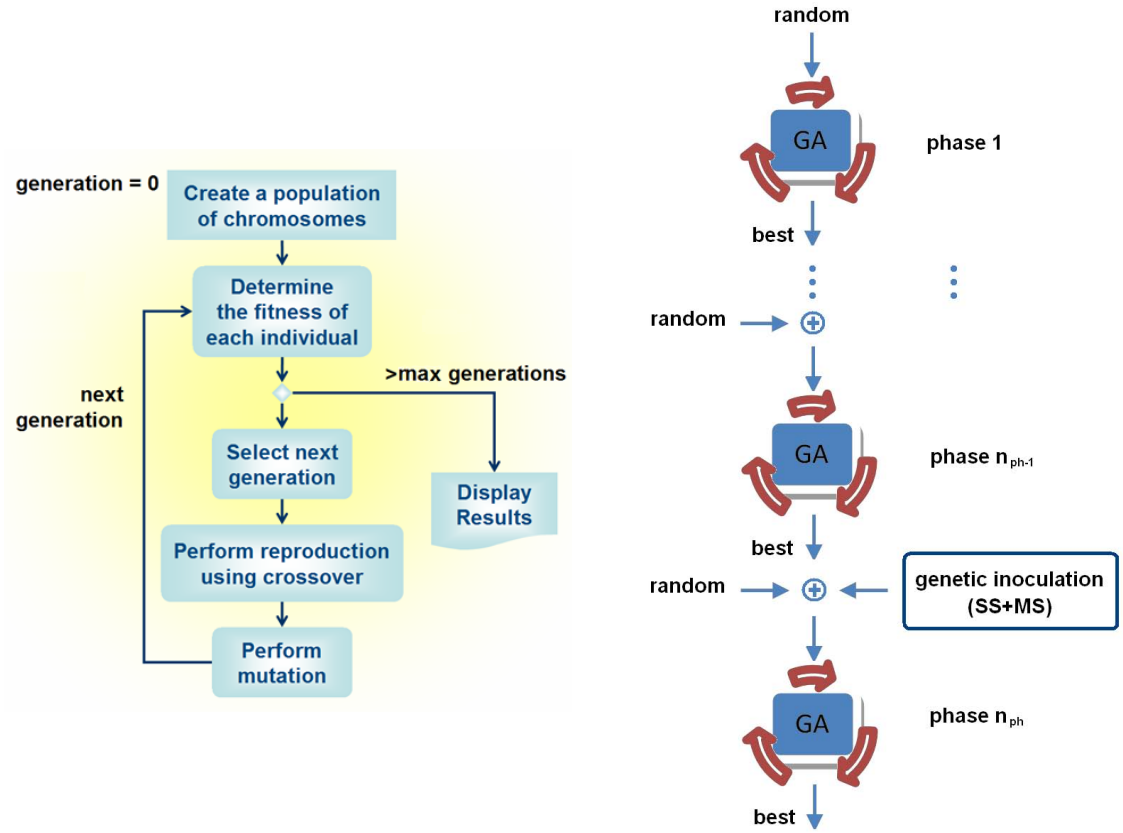

(a) (b)

Figure 6.7: a) Simple GA . b) MPGA.

capable to scan over large search spaces with multiple peaks. They are efficient in searching for the global optimum because of their inherent parallel ability. Moreover, it is worth noticing that mutation prevents the algorithm to be trapped in a local minimum (see appendix A).

However, conventional GAs suffer from bad initializations and it is widely accepted that the convergence rates are affected by the initial population [36]. To overcome such limitations the use of a multi-phase GA method is proposed [37], which runs individual GA in each phase, as depicted in Figures 6.7 a and b. Each phase is initialized with a set of best individuals from the previous phase and a random set of other individuals. The multiple phases are introduced to realize the effect of multiple initializations. The good performances of MPGA are due to the mix of randomness and better characteristics of the previous generations.

The number of phases n_{ph} in the MPGA are decided on the basis of the maximum number of generations and the population size, to be more precise as a ratio of them. The initial population of the first phase is randomly chosen and the MPGA proceeds until it reaches a specified number of generations. The number of generations for each phase, $n_{g/ph}$, is calculated by equally dividing the maximum number

of generations, $n_{ph,Max}$, among the phases:

$$n_{g/ph} = \frac{n_{ph,Max}}{n_{ph}} \tag{6.21}$$

In more details, each phase, for $j_{ph} = 1, ..., n_{ph}-1$, is initialized with a percentage of random individuals and with the best individuals of the previous phase. The performance of the MPGA is influenced by the level of the mixing factor L: the new population is initialized with the L portion of individuals of previous phase and $(1 - L)$ portion of random individuals, with $0 \leqslant L \leqslant 1$. When L is zero the population becomes a random set of individuals. Since the MPGA uses the output of a previous phase in the current phase, the best characteristics of the previous phases are propagated to the next phases and the random individuals introduced in each phase act as a mutation operator and help GA to climb different peaks. Moreover, in the last phase a genetic-inoculations technique is used, that provides a way to incorporate such knowledge to speed up the convergence of the MPGA algorithm to a sub-optimal and consistent solution.

An important factor in the successful application of evolutionary techniques to real-world problems is the incorporation of domain knowledge. One form such knowledge often takes is the possession of one or more high-quality solutions. Non-random initialization, or inoculation, of the population in an evolutionary algorithm provides a way to incorporate such knowledge. A body of folklore about the methods and results of such initialization techniques exists, but is largely unwritten and unquantified [38].

To achieve this, we have employed the solutions derived from the two common strategies, sequential strategy and symmetric strategy, for a set of n-parallel chillers with m-discrete capacity steps system. These strategies are coded into phenotypes; furthermore, phenotypes are decoded into genotypes and are used for initialize, at the last n_{ph} phase, a portion of individuals by mixing factors L_1 and L_2, both greater than or equal to zero and smaller than or equal to one (Tab. 6.2).

By using this formulation, with data from experimental tests and chiller's working curves, MPGA algorithm can be usefully employed to solve the unconstrained minimization problem 6.14. The formulation of the common genetic algorithm relays on a binary encoding of the solutions, i.e. the chromosomes consist of a string of 0s and 1s. Hence, each chiller PLR_i and $status_i$ is translated into a binary string and all of them are connected into a long string, as shown in Tab. 6.3.

The MPGA operates in phases, as described above. During each phase, standard GAs are employed. The algorithm works on a problem solution until a convenient end condition is satisfied, then it stops and returns the best solution evaluated. From best PLR_i and $status_i$, the set-point, T_{sp_iGA} , for the i - th chiller can be

Table 6.2: Mixing factors.

Portion of individuals			
phase $j_{ph} = 1...n_{ph} - 1$			
L	best of previous phase		
$(1-L)$	random		
phase $j_{ph} = n_{ph}$			
L	best of previous phase		
$(1-L)$	$(1-L)L_1$	$(1-L)L_1L_2$	SS
		$(1-L)L_1(1-L_2)$	MS
	$(1-L)(1-L_1)$	random	

Table 6.3: Chromosome example: PLR and status of chillers are encoded into a binary string of $(10+1) \cdot n$ bits.

$PLR_1^{(1)}$	...	$PLR_1^{(10)}$	$status_1$	... ...	$PLR_n^{(1)}$	...	$PLR_n^{(10)}$	$status_n$

estimated as:

$$T_{sp_iGA} = \hat{T}_{P,i} - PLR_i \cdot \Delta T\,, \tag{6.22}$$

with:

$$\hat{T}_{P,i} = T_{P,o} + P\hat{L}R_{tot} \cdot \Delta T\,, \tag{6.23}$$

$$P\hat{L}R_{tot} = \frac{\hat{Q}_L}{Q_{Max}}\,, \tag{6.24}$$

where ΔT is a fixed water temperature differential[4], $\hat{Q}_L$ is the estimated cooling energy and Q_{Max} is nominal design cooling capacity on the time step.

6.6 PID

To solve the OCL-OCS problems, the MPGA makes use of $Y_{curve} - Z_{curve}$ curves. These curves give an approximation of chiller performance at part load conditions, therefore an error between water supply temperature and its set-point can occur. In order to reduce this effect a standard Proportional-Integrative-Derivative (PID) controller is implemented at supervisor level.

The PID controller job is to maintain $T_{L,i}$ at a certain level so that the error ($e_{T_{sp}}$), between the process variable and the set-point $\bar{T}_{L,i_{sp}}$, is bounded. The chiller set-points are modified by:

$$T_{sp_i} = T_{sp_iGA} + K_p e_{T_{sp}} + K_d \frac{de_{T_{sp}}}{dt} + K_i \int e_{T_{sp}} dt \tag{6.25}$$

where $e_{T_{sp}} = \bar{T}_{L,i_{sp}} - T_{L,i}$. PID parameters have been tuned using SIMULINK™ optimization tools.

6.7 Remark: on suboptimality of the GA approach

The main advantages of Genetic Algorithms are:

- They efficiently search the model space, so they are more likely (than local optimization techniques) to converge towards a global minimum.
- Can escape local minimum.
- Easy to parallelize.
- There is no need for linearization of the problem.

[4]The water temperature differential is defined as a difference between the chillers water-supply and the water-return temperatures, at nominal design cooling capacity.

- There is no need to compute partial derivatives.
- More probable models are sampled more frequently than less probable ones.
- Works on a wide range of problems.

The disadvantages of Genetic Algorithms result as a:

- Need of much more function evaluations than linearized methods.
- No guaranteed convergence even to local minimum.
- Necessity to discretize the parameter space.

In the context of optimal chiller problems, the advantages of GAs seem much more valuable than disadvantages. About the possible suboptimality of the heuristic approach decribed above, the GA method is compared with an exact method, related to simple case, to solve optimal chiller loading problem for fixed load condition.

In a simplified hypotesis, the electric power consumption of a chiller (kW), can be expressed as a concave function of its PLR for a given wet-bulb temperature[5]. The kW_i function of i-th chiller unit is represented as a second order polynomial of PLR_i:

$$kW_i = a_i + b_i PLR_i + c_i PLR_i^2 \,, \tag{6.26}$$

where a_i, b_i, c_i are coefficients of kW-PLR curve of i-th chiller. The OCL problem is to find a set of chiller output which does not violate the operating limits while minimizing the objective function:

$$J = \sum_{i=1}^{I} KW_i \,, \tag{6.27}$$

where I, is the number of chillers.

Simultaneously, the balance equation must be satisfied:

$$\sum_{i=1}^{I} PLR_i \cdot CC_i = CL \,, \tag{6.28}$$

where CC_i is the capacity of i-th chiller and CL the system cooling load.

To solve OCL problem, the Lagrangian method has been adopted, based on the convex function of the kW–PLR curve. By combining the objective function

[5]Really, as assumed in the Chapter 5, the input power of the chiller depends of water return temperature, external air temperature (for example in air condensed chillers) and water mass flow rate. Moreover, in order to carry out a correct energy analysis of the HVAC plant an evaluation of the effect of operating at part load conditions is required.

(6.27) with the balance equation (6.28) multiplied by a Lagrangian multiplier λ, the Lagrangian function is expressed as:

$$\mathcal{L} = \sum_{i=1}^{I} KW_i + \lambda \left[CL - \sum_{i=1}^{I} PLR_i \cdot CC_i \right] . \tag{6.29}$$

The optimum chiller loading is achieved by taking the derivative of $\mathcal{L}$ with respect to PLR_i and the PLR_i of i-th unit can be expressed as:

$$PLR_i = \frac{\lambda CC_i - b_i}{2c_i} . \tag{6.30}$$

The system cooling load is expressed by the sum over all chiller units as:

$$\sum_{i=1}^{I} PLR_i \cdot CC_i = \lambda \sum_{i=1}^{I} \frac{CC_i^2}{2c_i} - \sum_{i=1}^{I} \frac{b_i}{2c_i} CC_i \tag{6.31}$$

By substituting Equation (6.28) into Equation (6.31) and rearranging, the Lagrangian multiplier can be rewritten as:

$$\lambda = \frac{2CL + \sum_{i=1}^{I} \frac{b_i}{c_i} CC_i}{\sum_{i=1}^{I} \frac{\mathrm{CC}_i^2}{c_i}} . \tag{6.32}$$

For a system cooling load CL, the Lagrangian multiplier λ can be evaluated and the cooling load of each unit is acquired from Equation (6.30). The solution steps are stated as follows:

1. Read in system information including CC_i, CL and coefficients a_i , b_i and c_i.
2. Calculate Lagrangian multiplier by Equation (6.32).
3. Calculate PLR_i by Equation (6.30).
4. If any unit violates its operating limit, then fix PLR_i at this very limit and go to step 2 to recalculate other chillers' outputs. Otherwise, go to step 5.
5. Output results.

Owing to the maximal output of a chiller being its design capacity, the upper limit of PLR_i is equal to 1.

With the Lagrangian method the kW-PLR curve must be convex[6] and there is need to compute partial derivatives. Moreover, the method using a lambda iteration technique, may cause the side effect of not reaching convergence at low demand [5].

[6]Really, the $kW - PLR$ can include convex and nonconvex pieces.

Table 6.4: Chillers parameters.

Chiller	a_i	b_i	c_i	$CC_i[kW]$
1	220.28	-445.28	569.30	1583
2	263.06	-561.00	665.70	1583
3	370.38	-703.68	1028.20	3517
4	1453.30	-4387.20	4215.2	3517

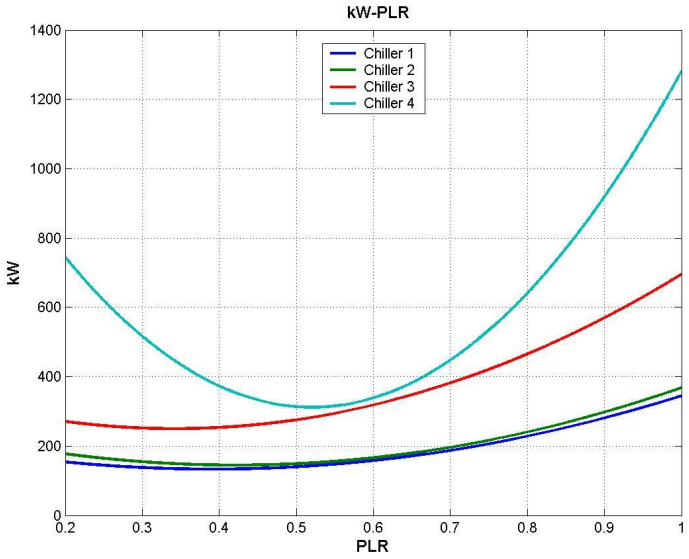

Figure 6.8: Chillers type: kW-PLR curves.

Next examples solve the same OCL problem by using Lagrangian method and by using GA to overcome these shortcomings. After an extensive number of experiments, GA produced high accuracy.

6.7.1 Simulation examples

The examples consider four type of chillers. The electric power consumption of a chiller i-th can be calculated by Equation (6.26). Table 6.6 shows the assigned value of parameters when OCL is executed in GA (Tables 6.5 shows the control parameters) and Lagrangian method (LGM). Under the GA method, the solution is very close to optimal. Also, the discrepancy is small. Then, it can be concluded then, that GA is a highly recommendable method for this type of problem.

Table 6.5: Control parameters by GA.

Population size	100
Generation number	100
String length	10
Crossover probability	0.6
Mutation probability	0.01

Table 6.6: Simulation results. Cooling powers are expressed in Tons of Refrigeration (1 TR = 3517 W).

Load [RT]	Method	LGM			GA		
		COP	CC_i [TR]	kW	COP	CC_i [TR]	kW
2175 (75%)	Chiller 1	1.586	356.11	224.43	1.6112	346.80	215.24
	Chiller 2	1.541	343.65	222.87	1.5190	352.41	232.00
	Chiller 3	1.671	834.70	499.39	1.6784	829.67	494.32
	Chiller 4	1.719	640.54	372.58	1.7078	646.04	378.28
			2175	1319.27		2174.9	1318.84
1450 (50%)	Chiller 1	1.5786	218.18	138.22	1.5700	216.31	137.78
	Chiller 2	1.5132	225.70	149.15	1.4912	220.80	148.07
	Chiller 3	1.7354	457.57	263.67	1.8010	491.50	272.90
	Chiller 4	1.7410	548.55	315.08	1.6725	521.41	311.75
			1450	866.12		1450	870.5
725 (25%)	Chiller 1	0.5048	80.26	158.97	0.5225	82.46	157.80
	Chiller 2	0.6456	107.75	166.90	0.5377	94.05	174.89
	Chiller 3	0.2510	80.44	320.42	0.5209	150.00	287.96
	Chiller 4	1.3880	456.56	328.93	1.0641	398.44	374.45
			725	975.22		724.9	995.10

7 Implementation and results

The performance of the algorithm illustrated in the above chapters is evaluated by resorting to a dynamic simulation environment developed in MATLAB™ and SIMULINK™, where the multiple chiller system with primary-secondary architecture (Figure 4.1) plant dynamics are accurately described. In fact, the MCM optimized method works dynamically, therefore it has been developed and tested under dynamic plant operation. Given the versatility of MATLAB™ high-level language, problem can be coded in m-files in a fraction of the time that it would take to create *C* or *Fortran* programs for the same purpose. Moreover, SIMULINK™provides an interactive graphical environment and a customizable set of block libraries that let design, simulate, implement, and test the whole system. Furthermore, in order to implement GA functions under MATLAB™ , the Genetic Algorithm Toolbox (GATBX) is used (see Appendix A).

7.1 System modelling

The plant, and the two-level control structure are modelled. As concern with the plant and the low-level controller the sample time is T_{sam}, while for the high-level controller the sample time is T_{sup}, with $T_{sup} > T_{sam}$. With reference to the examples considered in Section 7.2 results: $T_{sam} = 60$ s and $T_{sup} = 600$ s. An example of basic overall scheme is illustrated in Figure 7.2.

7.1.1 Plant

The modelled components of the multiple chiller system with primary-secondary architecture results:

1. Chillers.

2. Collector.

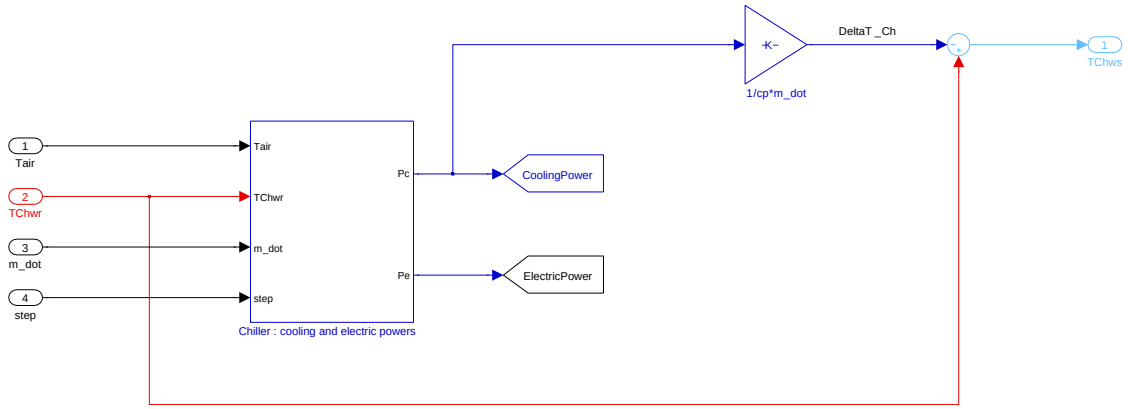

Figure 7.1: Basic chiller scheme.

3. Bypass.

4. Water-Tank.

5. Loads.

6. Piping.

A particular of a basic chiller scheme is depicted in Figure 7.1 where the cooling power and electric power are calculated by polynomial function 5.7. The chiller water sent temperature results:

$$T_{Chws} = T_{Chwr} - P_c \frac{1}{c_p \dot{m}_{ch,o}} \tag{7.1}$$

7.1.2 Low level controller

The relay control law with virtual tank, mentioned before in Section 6.2.1, is modelled.

7.1.3 Supervisor: MCM

The structure of the supervisor is illustrated in Scheme 6.2. In particular the GATBX toolbox functions are used.

The GATBX uses MATLAB matrix functions to build a set of versatile tools for implementing a wide range of genetic algorithm methods. The Genetic Algorithm Toolbox is a collection of routines, written mostly in m-files, which implement the most important functions in genetic algorithms. However, in order to realize a genetic inoculation that provides a way to incorporate such knowledge to speed up the convergence of the MPGA algorithm, a function for mapping genotypes into phenotypes is required. In the Genetic Algorithm Toolbox there isn't a similar

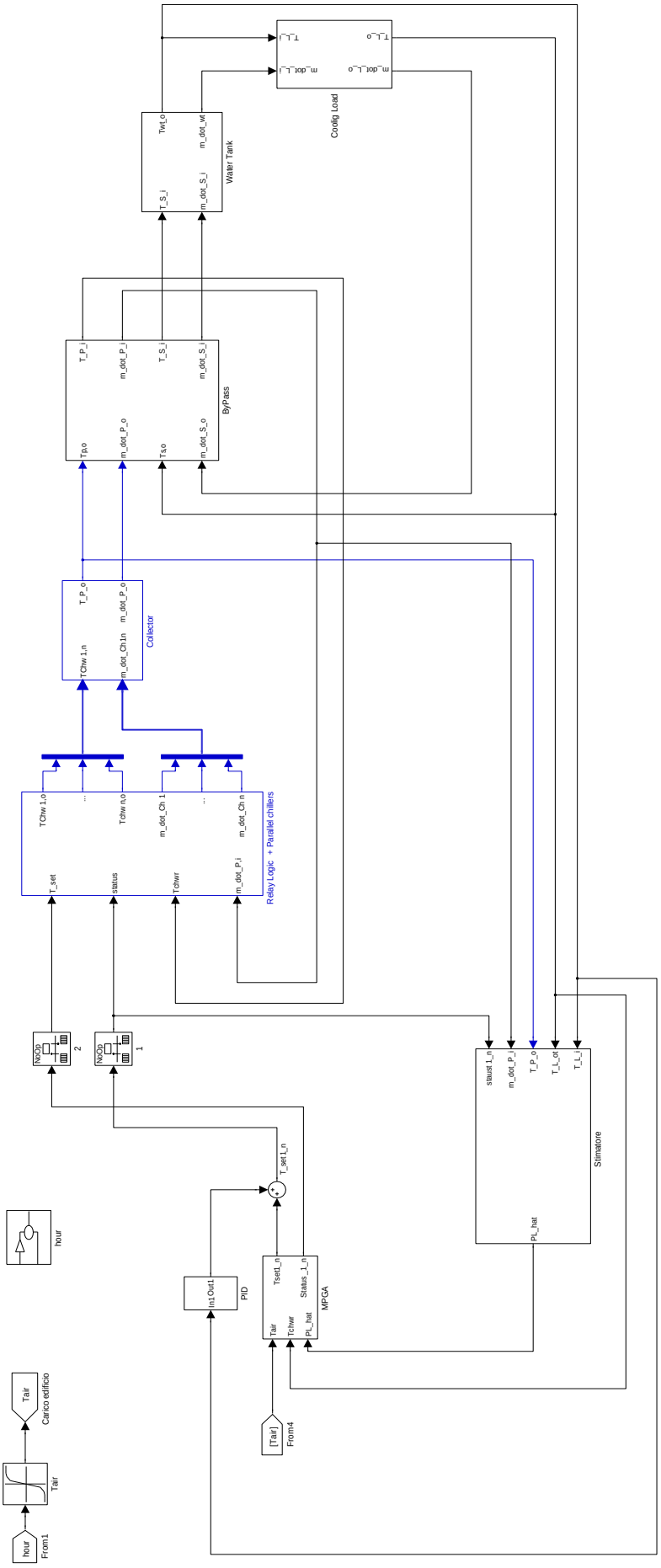

Figure 7.2: Basic chiller scheme.

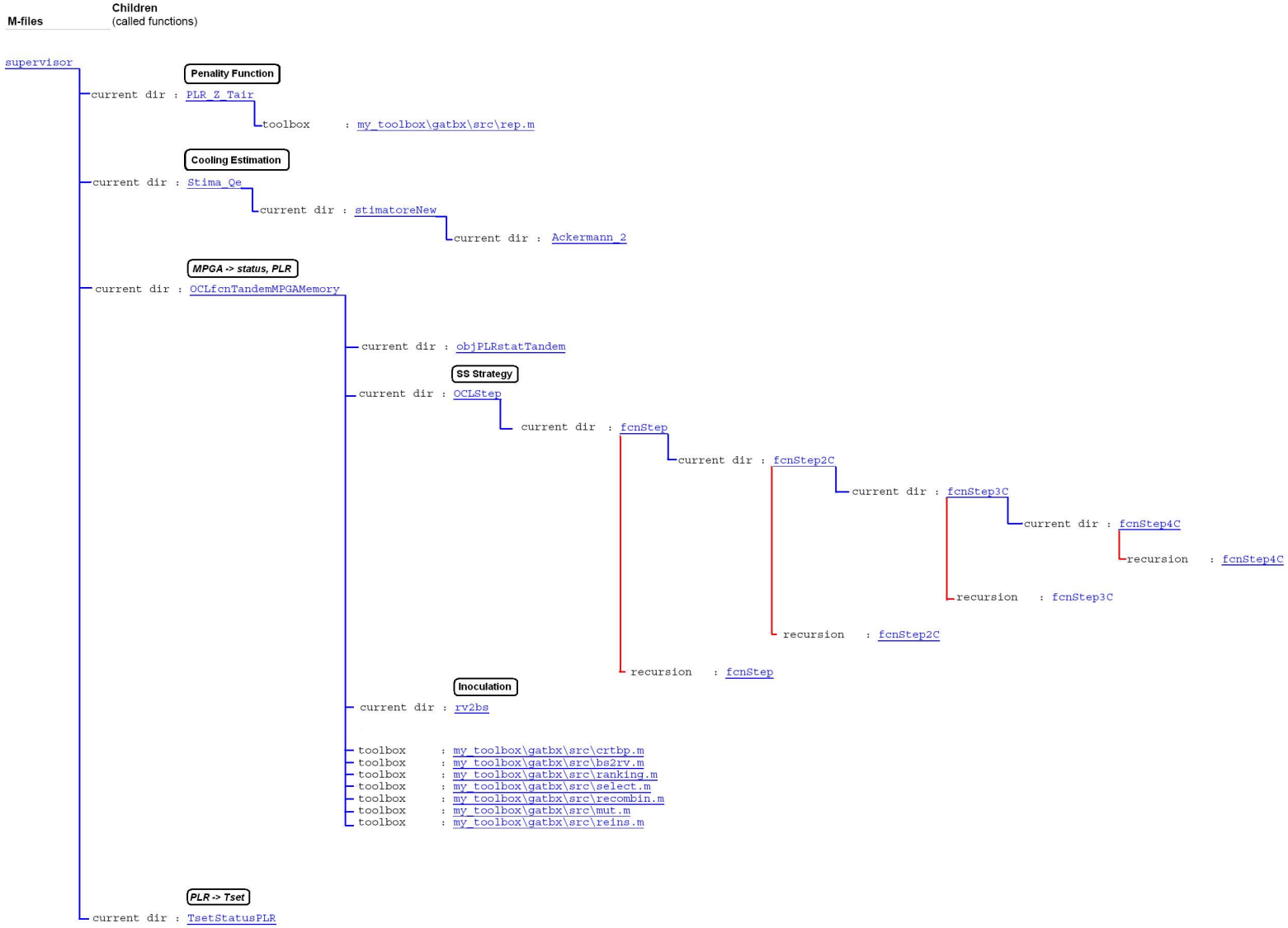

Figure 7.3: Supervisor: architecture dependent functions.

function, therefore, a MATLAB™ function *rv2bs.m* (see Appendix A.8) is developed: this function decodes vectors of reals (phenotype) into genotype.

A basic example of architecture dependent functions of high-level supervisor MCM (with Load estimation and MPGA algorithms) is illustrated in Figure 7.3.

7.2 Examples

Extensive simulations are used to estimate and illustrate the dynamic of the system (Figure 4.1) over the time and to evaluate the system's energy consumption and performance. The MCM algorithm is compared with SS and MS strategies results.

Table 7.1: Target chiller data in the following conditions: $T_{air} = 35\,°C$ and $T_{water} = 12\,°C$.

Chiller model	TCAE 4320	TCAVBZ 2600
Nominal cooling power	316.2 [kW]	607.4 [kW]
Absorbed power	120.9 [kW]	215.9 [kW]
EER	2.62	2.67
a_c	317.9	607.5
a_e	121.4	217.4
b_c	7.70	18.16
b_e	0.08	2.52
c_c	-3.29	-5.48
c_e	2.22	3.11
d_c	0.38	0.79
d_e	0.01	0.10

A case study of a Milan's directional building (Northern Italy) on a typical

Table 7.2: Case studies.

	Case 1	Case 2	Case 3
Chiller model	TCAE4320	TCAVBZ2600	TCAVBZ2600 + TCAE4320
Number of chillers	6	3	2 + 2
Nominal cooling capacity	1897.2 [kW]	1822.2 [kW]	1847.2 [kW]
Plant water content	2 [l/kW]	2 [l/kW]	2 [l/kW]
Temperature differential	1 [°C]	1 [°C]	1 [°C]
Supply water temperature	7 [°C]	7 [°C]	7 [°C]

cooling season ranging from April to September was analysed. The building load demand profile was calculated by an EnergyPlus simulation model with a 10 minutes time step [39].

Three case studies are analysed: six multi-scroll chillers, three multi-screw chillers and mixed two multi-scroll and two multi-screw chillers in parallel (Tab. 7.2). The experimental data of Rhoss TCAE 4320 (a four scroll compressors, two refrigerant circuit unit) and of Rhoss TCAVBZ 2600 (a two screw compressor, two refrigerant circuit unit) packaged aircooled water chillers are used. In Figures 7.4a and 7.4b, Y and Z curves for the two chiller models are plotted as a function of the PLR_i and air temperature.

It is worth noting that for the scroll unit (Figure 7.4a) there are four different capacity steps:

1. four compressors on;
2. three compressors on;
3. two compressors on two different refrigerant circuits;
4. one compressor on.

The screw unit is equipped with compressors having a capacity regulation slide valve with four discrete steps (100%, 75%, 50%, 25% capacity respectively), the six steps that may be seen in Figure 7.4b are obtained as follows:

1. two compressors at 100%;
2. one compressor at 100% and one at 75%;
3. one compressor at 100% and one at 50%;
4. one compressor at 100%;
5. one compressor at 75%;
6. one compressor at 50%.

As shown in Figure 7.4, it is clear that at part load condition the system with scroll compressors behaves much better than the one with screw compressors, due to the effect of the capacity control on isentropic compression efficiency. To control capacity, the scroll unit switches on-off the compressors, which operate at nearly constant isentropic efficiency. The system takes advantage from switching off one compressor per circuit since heat exchangers perform at lower thermal load. On the other hand, the screw unit regulates the compressors sliding valves at part load

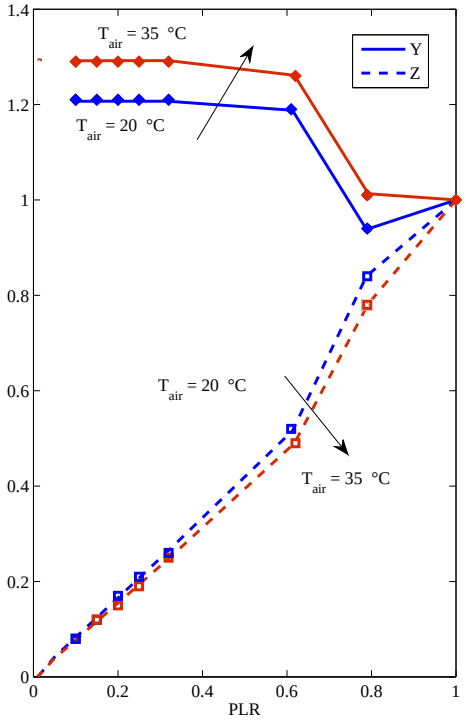

(a) TCAE 4320, scroll unit.

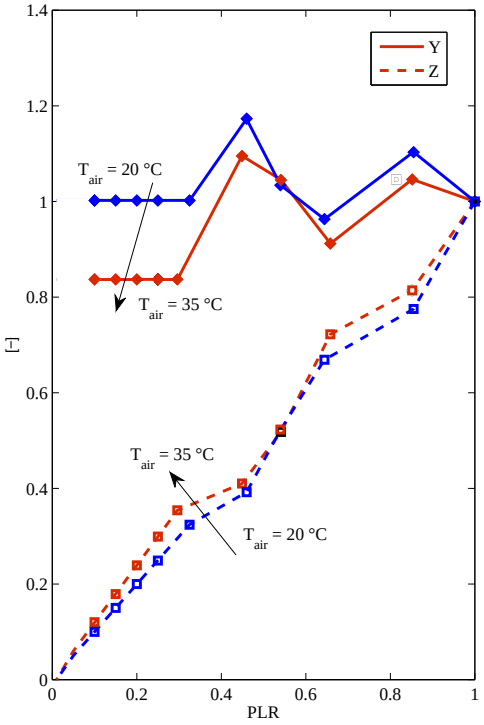

(b) TCAVBZ 2600, screw unit.

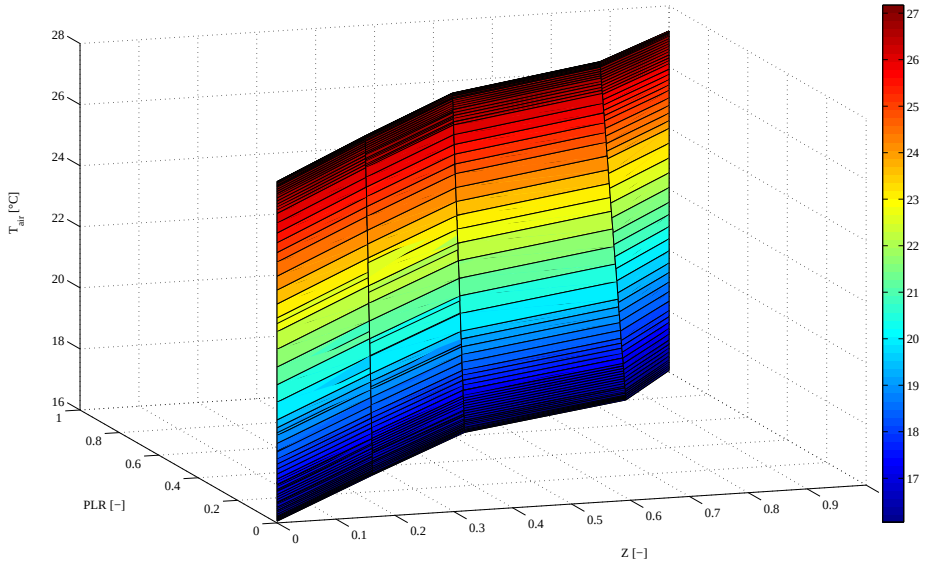

(c) TCAE 4320, scroll unit.

Figure 7.4: Y and Z curves.

Table 7.3: MPGA control parameters.

Population size	100	Mixing factor L_1	0.5
Generation number	500	Mixing factor L_2	0.5
String length	11	h_{obj}	10÷20
n_{ph}	5	ν_{obj}	1
$n_{g/ph}$	100	h_{err}	5÷10
Crossover probability	0.6	ν_{err}	2
Mutation probability	0.03	h_{reg}	1÷5e4
Selection method	rws	ν_{reg}	1
Mixing factor L	0.5	k_i	0.2÷0.5

condition. This lowers their isentropic efficiency since the intrinsic volume tends to the unity when the capacity reaches its minimum and the vapour is more an more undercompressed when discharged. This penalization becomes more severe as the condensing pressure increases.

In Tab. 7.2, the chiller model and number, cooling capacity at 35°C external air temperature, plant water content, and supply water set-point are shown for each test case. It is worth noting that the plant water content considered in the examples is quite low compared to real plants (common values can be between 5÷15 l/kW). However, such a choice yields a system with faster dynamics.

The set of control parameters for MPGA is reported in Table 7.3.

7.2.1 Case 1: six scroll chillers

The MCM algorithm is compared to the SS strategy in presence of multi-scroll chillers in parallel. The SS strategy is the most commonly implemented law in this kind of system. In fact, as it is evident from the shape of the Y-curve of Figure 7.4a, the most favorable condition for a multi-scroll chiller is to work at low part-load. In Figure 7.5a, 7.5b, 7.6 and 7.7, cooling capacity and EER, water supply temperature and the chiller switching are plotted for the 15-th of July. With respect to SS strategy it can be observed that the MCM offer similar trends but slightly lower fluctuations water supply temperature with decreasing load. In Tab. 7.4 the monthly and seasonal integrated values of cooling capacity and efficiency ratio, EER, are reported for both MCM and SS strategies. The MCM method exhibits a 3.23% seasonal improvement with respect to SS strategy. In Table 7.5 the mean, the variance and the standard deviation of the cooling load error $P_{CL} - \hat{P}_{CL}$ are calculated for MCM and SS strategies.

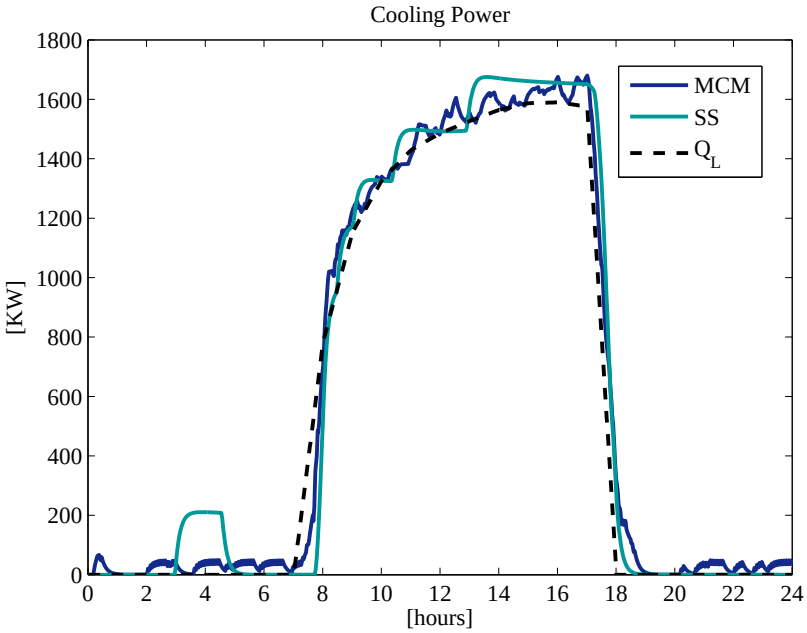

(a) case 1, cooling power.

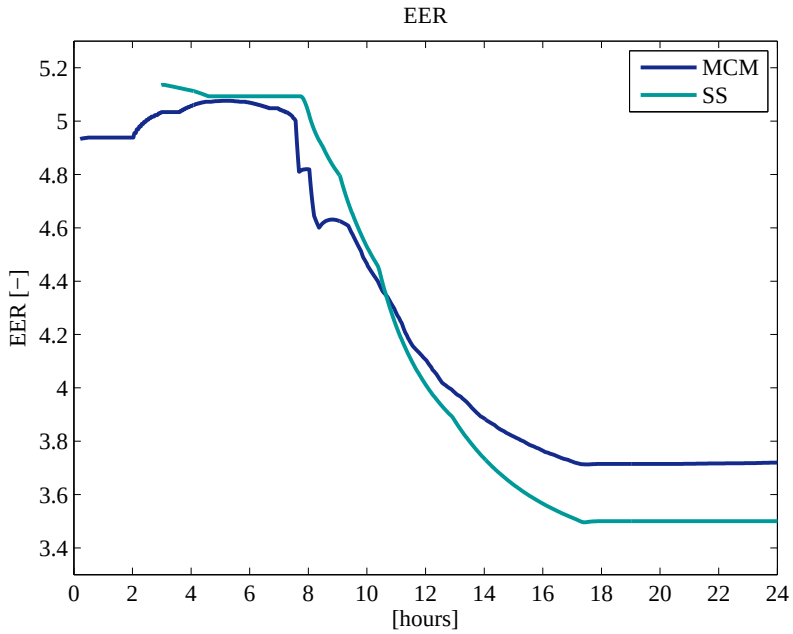

(b) Energy Efficiency Ratio.

Figure 7.5: case 1, cooling power and EER.

Table 7.4: seasonal performances, typical day on month, MPGA vs SS strategies, case 1.

	Apr.	May	June	July	Aug.	Sept.	seasonal
Cooling energy SS [kWh]	4397	8972	12237	14893	13348	10230	64077
Cooling energy MCM [kWh]	4330	8772	11923	14513	12925	10030	62493
EER SS	5.224	4.789	4.355	3.502	3.796	4.503	4.116
EER MCM	5.238	4.793	4.438	3.704	3.975	4.573	4.249
ΔEER (MCM-SS) %	0.27	0.09	1.91	5.78	4.72	1.55	3.23

Table 7.5: case 1, load profile following, MPGA vs SS strategies.

	$E\left[P_{CL}-\hat{P}_{CL}\right]$	$Var\left[P_{CL}-\hat{P}_{CL}\right]$	$\sigma\left[P_{CL}-\hat{P}_{CL}\right]$
SS	37.6 kW	15352 kW^2	123.9 kW
MCM	33.1 kW	$5554kW^2$	74.5 kW

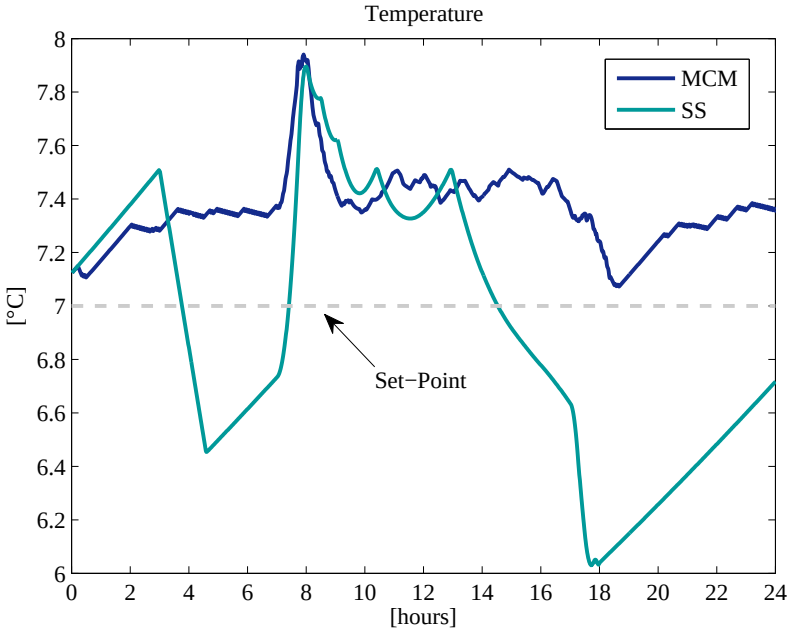

Figure 7.6: case 1, inlet water temperature.

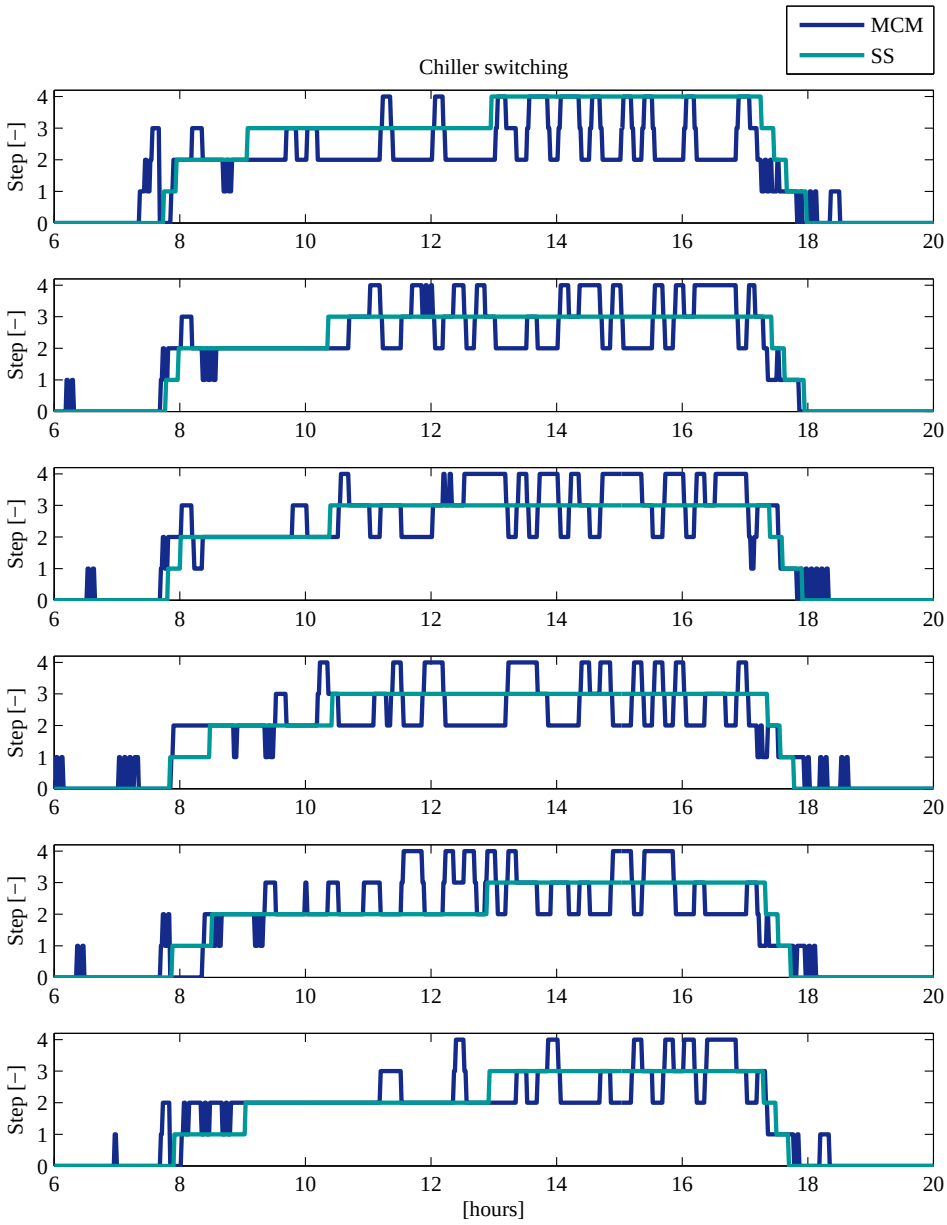

Figure 7.7: case 1, chillers steps switching.

Table 7.6: seasonal performances, typical day on month, MPGA vs MS strategies, case 2.

	Apr.	May	June	July	Aug.	Sept.	seasonal
Cooling energy MS [kWh]	4183	8473	11528	14022	12482	9862	60550
Cooling energy MCM [kWh]	4133	8415	11385	13870	12350	9605	59758
EER MS	4.461	4.110	3.882	3.485	3.627	3.860	3.787
EER MCM	4.633	4.176	3.967	3.558	3.744	4.039	3.893
ΔEER (MCM-MS) %	3.84	1.61	2.20	2.09	3.24	4.63	2.79

Table 7.7: case2, load profile following, MPGA vs MS strategies.

	$E\left[P_{CL}-\hat{P}_{CL}\right]$	$Var\left[P_{CL}-\hat{P}_{CL}\right]$	$\sigma\left[P_{CL}-\hat{P}_{CL}\right]$
MS	33.5 kW	11086 kW^2	105.3 kW
MCM	31.2 kW	5529 kW^2	74 kW

7.2.2 Case 2: three screw chillers

The MCM method is compared to the MS strategy in presence of multi-screw chillers in parallel. The MS strategy is the most commonly implemented law in this kind of system although it is not close to the optimal one. In fact, as it is evident from Figure 7.4b, the shape of Y curve is characterized by lower and upper peaks while the MS strategy tends to make each chiller work at full-load. In Figure 7.8a, 7.8b, 7.9 and 7.10, cooling capacity and power absorption, supply water temperature and the chiller switching are plotted for the 15-th of July. With respect to MS strategy it can be observed that the MCM allows lower fluctuations of the cooling power and water supply temperature. In Tab. 7.6 the monthly and seasonal integrated values of cooling capacity and efficiency ratio, EER, are reported for both MCM and MS strategies. The MCM exhibits a 2.79% seasonal improvement with respect to MS strategy. In Table 7.7 the mean, the variance and the standard deviation of the cooling load error $P_{CL}-\hat{P}_{CL}$ are calculated for MCM and MS strategies.

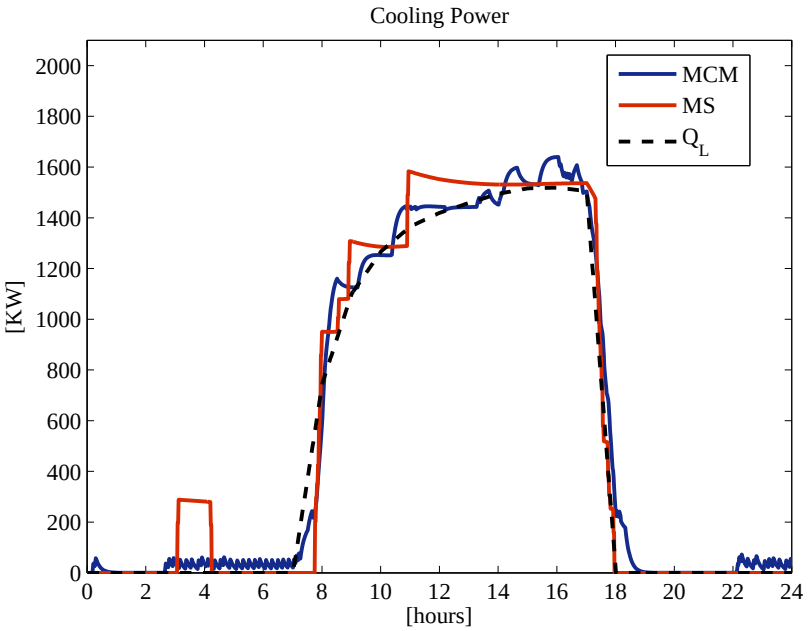

(a) cooling power.

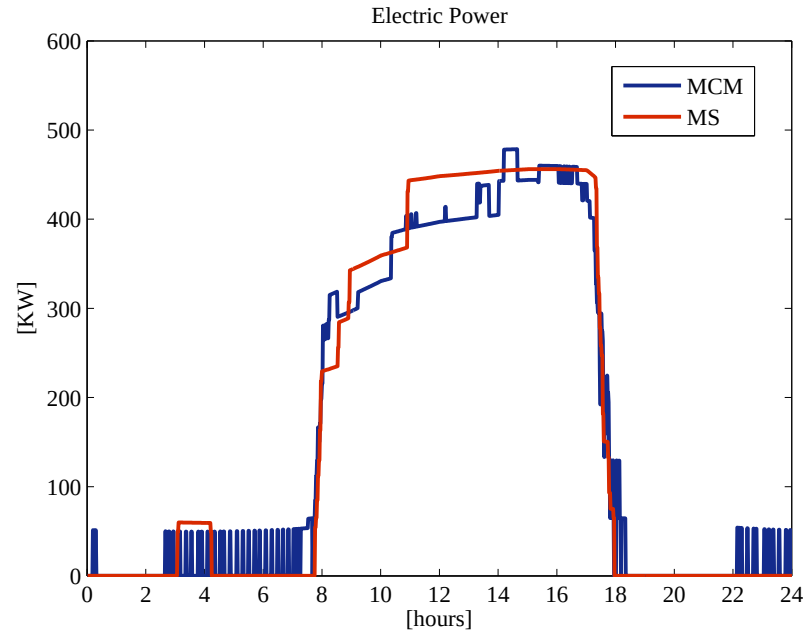

(b) electric power.

Figure 7.8: case 2, cooling and electric powers.

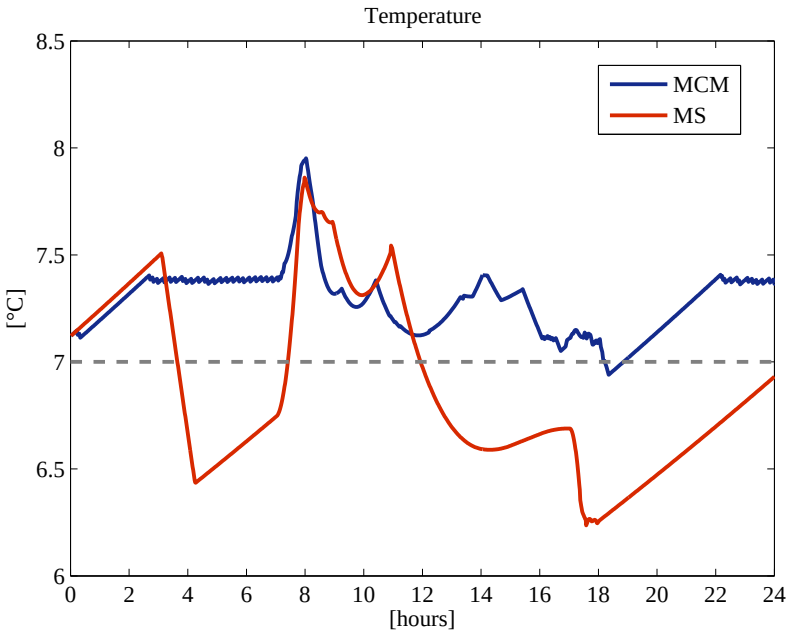

Figure 7.9: case2, inlet water temperature.

7.2.3 Case 3: two screw and two scroll chillers

An interesting feature of the MCM is that it can be applied to mixed multi-scroll and multi-screw chillers system. Considering the different shapes of the Y-curve for the two refrigerating units, it would be hard to define *a priori* a strategy for the optimal system management. In fact, in real life, it's hard to find such mixed systems, that could be on the other side very interesting for their flexibility, modularity and improved part load efficiency. A mixed system is simulated and MCM performance compared to both SS and MS laws. For the latter, the two screw units are switched on before the scroll ones. In Figures 7.11a, 7.11b, 7.12 and 7.13, cooling capacity and EER , supply water temperature and the chiller switching are plotted for the 15-th of July. With respect to MS and SS strategies it can be seen that the MCM allows lower fluctuations of the cooling power and water supply temperature. In Tab. 7.8 the monthly and seasonal integrated values of cooling capacity and efficiency ratio, EER, are reported for MCM, MS and SS strategies. The MCM exhibits a seasonal 4.19% seasonal improvement with respect to MS strategy and 2.01% with respect to SS strategy. In Table 7.9 the mean, the variance and the standard deviation of the cooling load error $P_{CL} - \hat{P}_{CL}$ are calculated for all three strategies.

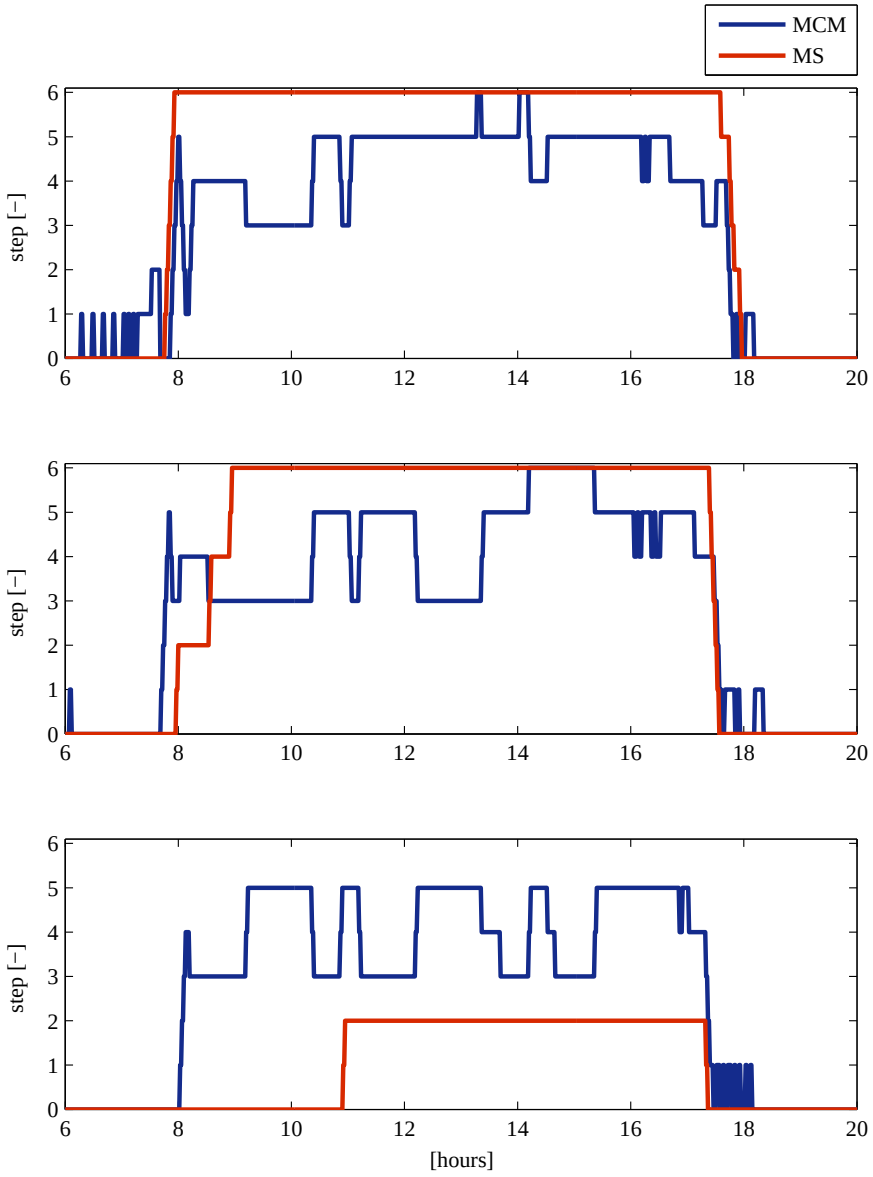

Figure 7.10: case 2, chiller steps switching.

Table 7.8: seasonal performances, typical day on month, MCM vs MS and SS strategies, case 3.

	Apr.	May	June	July	Aug.	Sept.	seasonal
Cooling energy MS [kWh]	4233	8612	11642	14315	12897	9973	61672
Cooling energy SS [kWh]	4242	8558	11620	14240	12545	9787	60992
Cooling energy MCM [kWh]	4123	8057	11535	14093	12548	9700	60057
EER MS	4.465	4.104	3.876	3.472	3.619	3.819	3.772
EER SS	4.451	4.341	3.871	3.560	3.626	4.008	3.853
EER MCM	4.611	4.395	4.036	3.611	3.700	4.044	3.931
ΔEER (MCM-MS) %	3.28	7.08	4.11	4.00	2.22	5.91	4.19
ΔEER (MCM-SS) %	3.61	1.24	4.25	1.42	2.04	0.91	2.01

Table 7.9: case 3, load profile following, MPGA vs SS and MS strategies.

	$E\left[P_{CL}-\hat{P}_{CL}\right]$	$Var\left[P_{CL}-\hat{P}_{CL}\right]$	$\sigma\left[P_{CL}-\hat{P}_{CL}\right]$
MS	53.7 kW	24170 kW^2	155.5 kW
SS	34.1 kW	8459 kW^2	92.0 kW
MCM	31.9 kW	6648 kW^2	81.6 kW

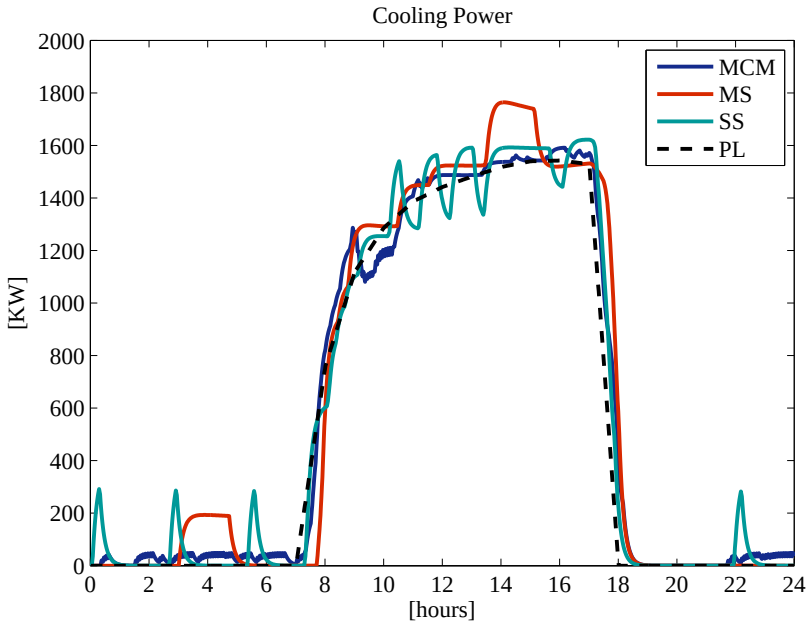

(a) case 3, cooling power.

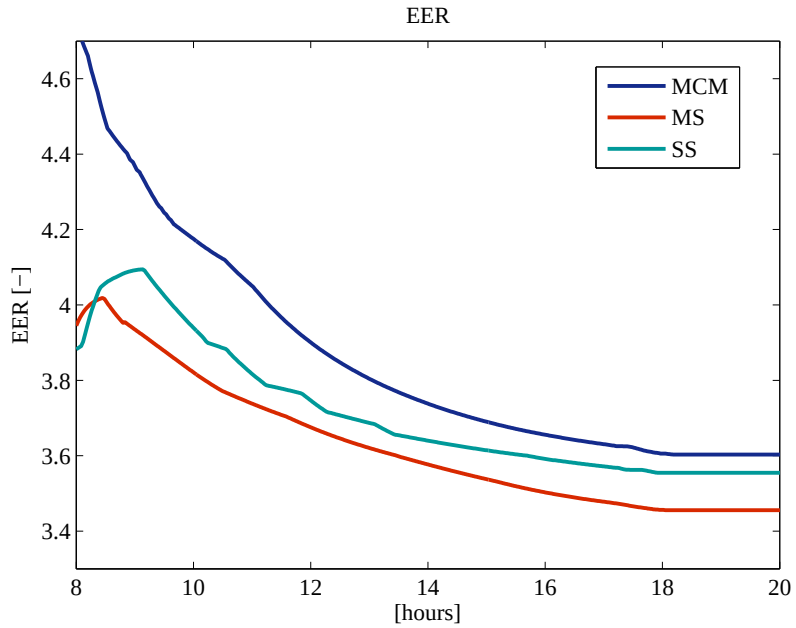

(b) Energy Efficiency Ratio.

Figure 7.11: case 3, cooling power and EER.

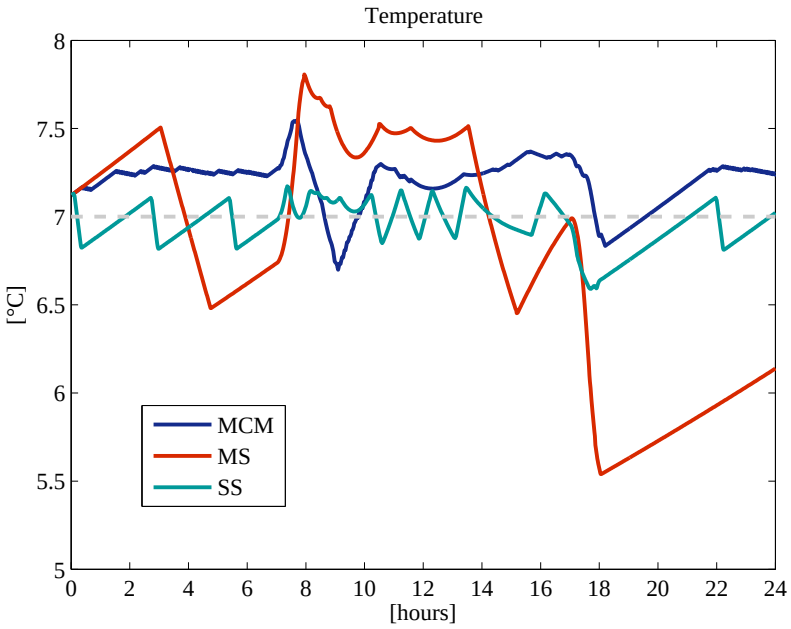

Figure 7.12: case 3, inlet water temperature.

7.2.3.1 Floating Set-Point

The estimated cooling load of the building allows even to introduce, in the MCM algorithm, strategies for the adjustment of the building delivery systems water temperature, this to issue the real needs of ambients to be conditioned. It is known ([4]) that acting on the value of the going out water set-point according to actual load conditions, increasing it if the degree of choking is reduced, increases the thermodynamic efficiency of vapor compression cycles of the different chillers connected to system. In this example, the same system described in the previous example has been simulated, but now by setting a supply water set point which is variable linearly between 14°C and 7°C depending on the degree of total choking between 30% and 100%, see Figure 7.14a. In Figure 7.14b, the supply water temperature and its set-point for MS and MCM_{Flt} strategies are depicted. In Table 7.10 is shown the (integrated) monthly and seasonal cooling energy values and EER, in relation to different strategies. The MCM method with floating set- point MCM_{Flt} exhibits a seasonal improvement of 9.37% compared to the MCM strategy, of 11.64% compared to the SS strategy and of 14.04% against the MS strategy.

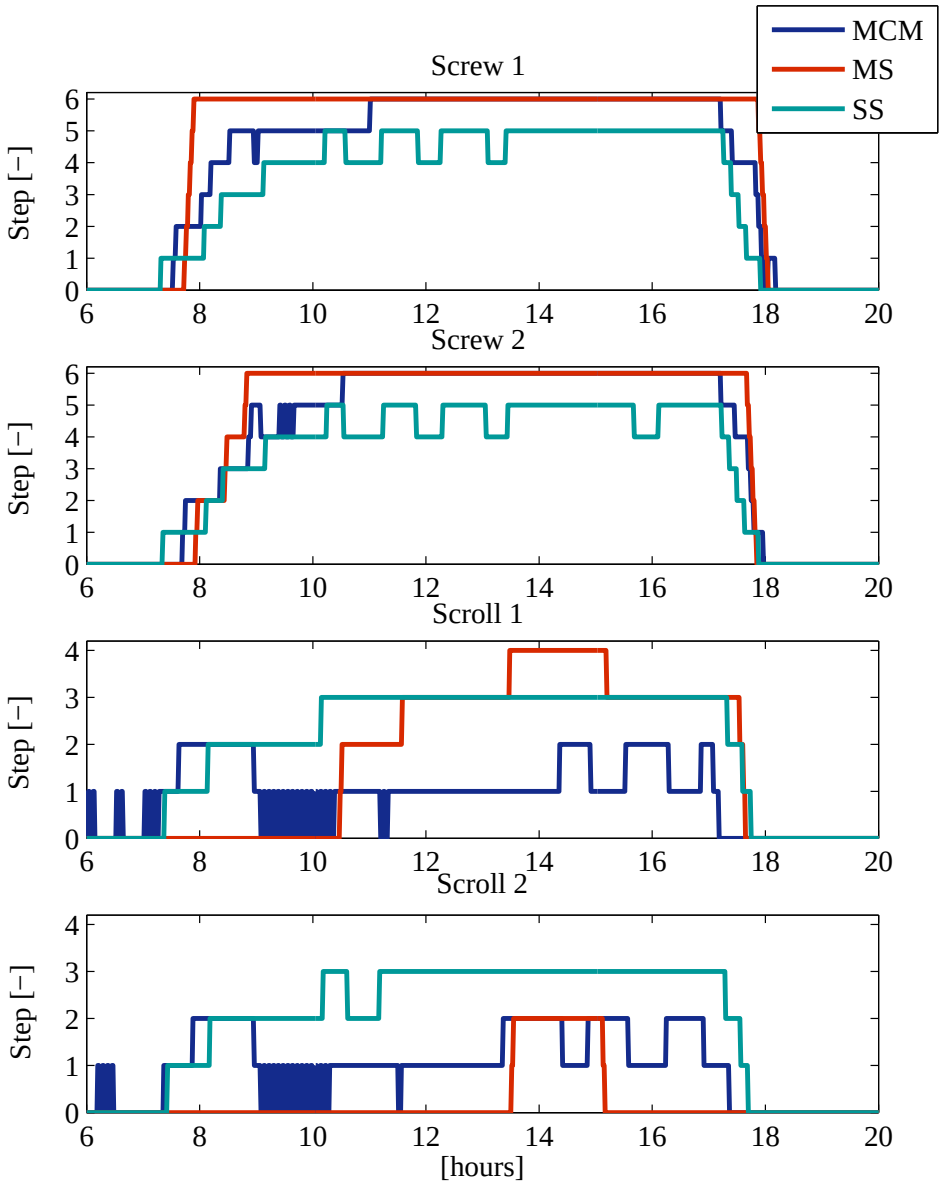

Figure 7.13: case 3, chiller steps switching.

Table 7.10: seasonal performances, typical day on month, MCM_{Flt} vs MCM, MS and SS strategies, case 3.

	Apr.	May	June	July	Aug.	Sept.	seasonal
Cooling energy MCM_{Flt} [kWh]	4482	8928	1228	15093	13397	10233	64362
EER MCM_{Flt}	5.671	4.835	4.407	3.811	4.051	4.498	4.302
ΔEER $(MCM - MS)$ %	25.81	17.81	13.68	9.79	11.94	17.79	14.04
ΔEER $(MCM - SS)$ %	26.21	11.38	13.83	7.06	11.74	12.22	11.64
ΔEER $(MCM_{Flt} - MCM)$ %	21.81	10.02	9.19	5.56	9.50	11.22	9.37

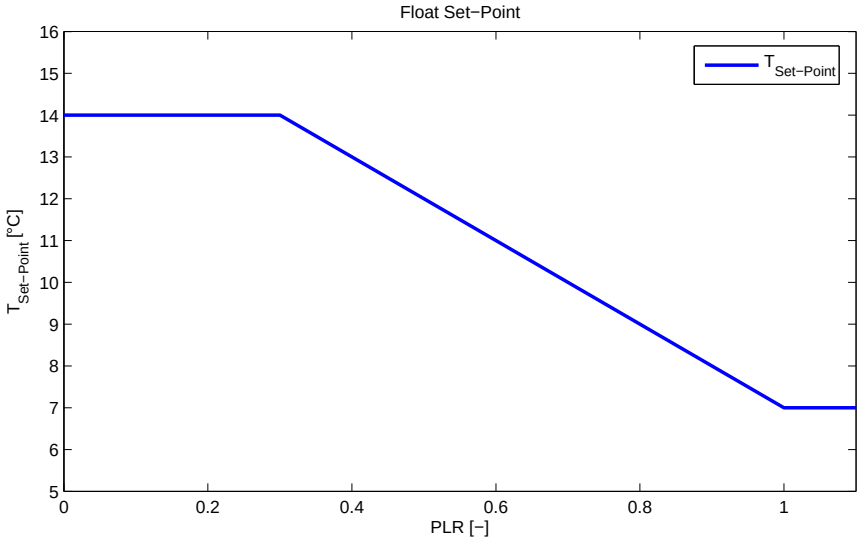

(a) floating set-point.

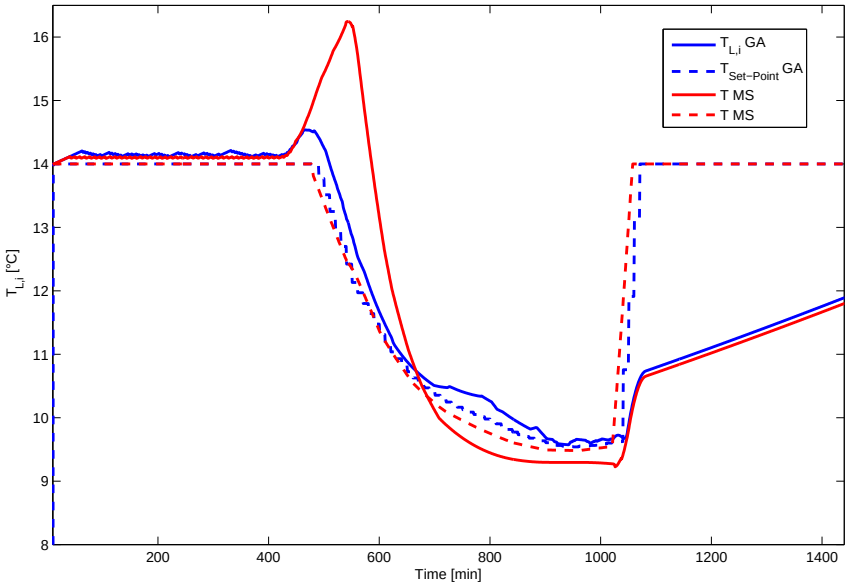

(b) supply water temperature.

Figure 7.14: Floating Set-Point.

7.3 Computational performance

In order to quantify the complexity of the proposed supervisor, an analysis of complexity of MPGA algorithm, in the form of the computational time, is carried out. Although the computational time cannot characterize the true computational complexity, it captures the order of the computation load. The computational complexity of proposed MPGA algorithm mainly comes from steps of:

- initialization;
- inoculation.
- selection;
- reproduction;
- termination;

The tests are carried out for a configuration of n-chillers, scroll type, in parallel. Fixed cooling load initial conditions are assumed. The indipendet variables are:

1. n, number of chillers.
2. population size

In Figures 7.15 and 7.16 the MPGA average elapsed time in function of number of chillers and population size are reported. In FIgure 7.17 the MPGA average memory request in function of number of chillers and population size is depicted. The simulations were run on conventional PC equipped with an Intel®Pentium 4 processor and 2GB of RAM.

It is worth noting that for a realistic number of chillers (1-10) the computations required by the optimization process are well performed within a time length of ten minutes on a personal computer, thus granting an on-line implementation.

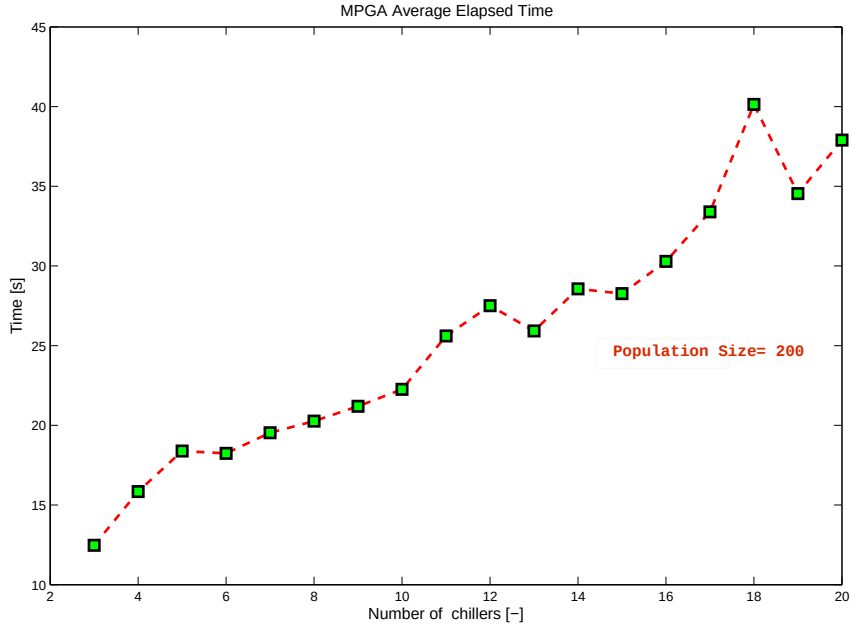

Figure 7.15: MPGA average elapsed time in function of number of chillers for a fixed population size.

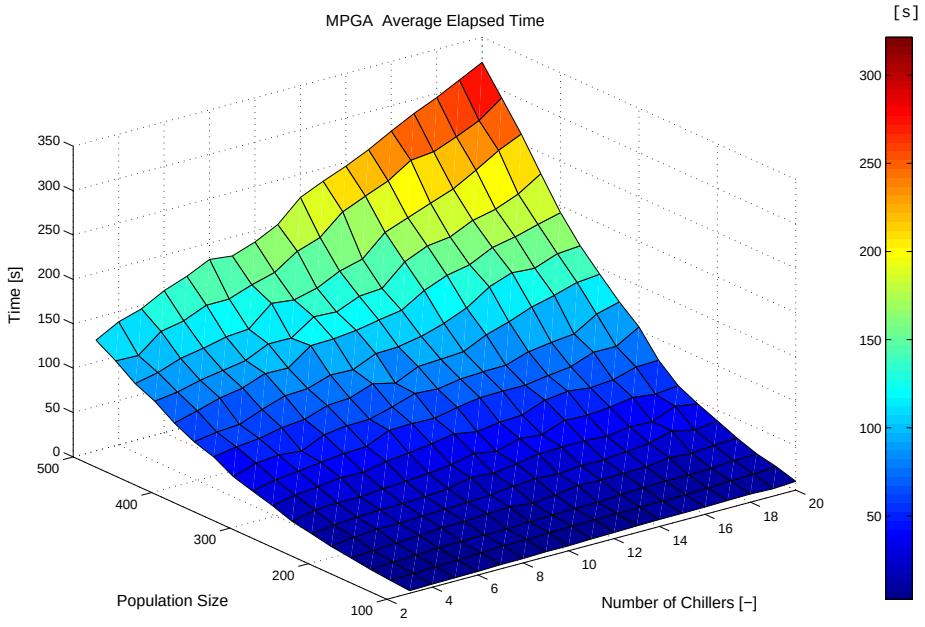

Figure 7.16: MPGA average elapsed time in function of number of chillers and population size.

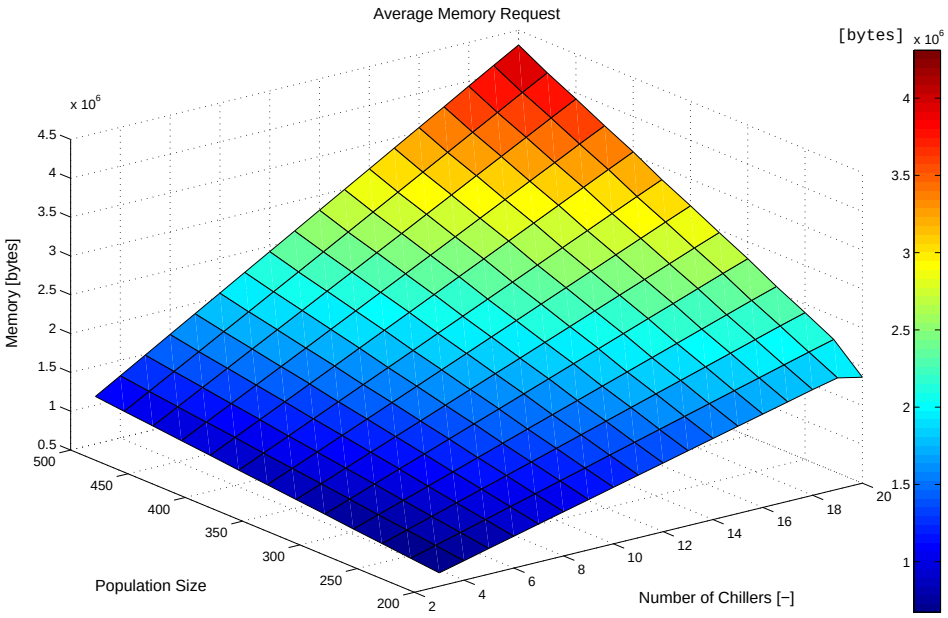

Figure 7.17: MPGA average memory request in function of number of chillers and population size.

Conclusion

In this Thesis the problem of optimizing the operation of multi-chiller systems has been addressed. To achieve optimal performance in terms of reducing both power consumption and operative costs, as well as granting good load tracking properties, it is necessary to solve simultaneously the OCL and OCS problems, making use of information on the actual thermal load applied to the plant. Such information is gained from plant measurements by means of a linear observer, which is designed on the basis of a dynamic model describing the load time behavior. Once an estimate of the load is available, it is possible to optimize the system operation by minimizing the energy consumption under the constraint that the cooling demand be satisfied. The resulting nonlinear, constrained, combinatorial optimization with both continuous and discrete variables has been successfully solved by using a multi-phase genetic algorithm. There are several advantages associated with this choice, such as the computational efficiency which grants real-time implementation over commercial platforms as well as the possibility of easy extensions of the approach by inserting extra penalty terms in the performance index. The method can also be extended in order to include the management of more complex systems, comprising air handling units and radiant and fan coil systems. Furthermore, information from load forecasting models for the energy and economic management of thermal storages could be easily exploited by simple modifications of the load estimation scheme and performance index. The performance of the algorithm has been evaluated by means of simulations performed with a dynamic model of the plant, so that all the actual operational conditions have been taken into consideration. The results show that it is possible to achieve substantial energy savings while granting good satisfaction of the cooling demand, if compared with standard MCM algorithms. Implementation of the algorithm on a commercial supervisory system is presently under development.

A

Genetic Algorithm

The GA is a stochastic global search method that mimics the metaphor of natural biological evolution. GAs operate on a population of potential solutions applying the principle of survival of the fittest to produce (hopefully) better and better approximations to a solution. At each generation, a new set of approximations is created by the process of selecting individuals according to their level of fitness in the problem domain and breeding them together using operators borrowed from natural genetics. This process leads to the evolution of populations of individuals that are better suited to their environment than the individuals that they were created from, just as in natural adaptation. Individuals, or current approximations, are encoded as strings, chromosomes, composed over some alphabet(s), so that the genotypes (chromosome values) are uniquely mapped onto the decision variable (phenotypic) domain. The most commonly used representation in GAs is the binary alphabet {0, 1} although other representations can be used, e.g. ternary, integer, real-valued etc.

Examining the chromosome string in isolation yields no information about the problem we are trying to solve. It is only with the decoding of the chromosome into its phenotypic values that any meaning can be applied to the representation. However, as described below, the search process will operate on this encoding of the decision variables, rather than the decision variables themselves, except, of course, where real-valued genes are used. Having decoded the chromosome representation into the decision variable domain, it is possible to assess the performance, or fitness, of individual members of a population. This is done through an objective function that characterises an individual's performance in the problem domain. In the natural world, this would be an individual's ability to survive in its present environment. Thus, the objective function establishes the basis for selection of pairs of individuals that will be mated together during reproduction. During the reproduction phase, each individual is assigned a fitness value derived from its raw performance measure given by the objective function. This value is used in the selection to bias towards

more fit individuals. Highly fit individuals, relative to the whole population, have a high probability of being selected for mating whereas less fit individuals have a correspondingly low probability of being selected. Once the individuals have been assigned a fitness value, they can be chosen from the population, with a probability according to their relative fitness, and recombined to produce the next generation. Genetic operators manipulate the characters (genes) of the chromosomes directly, using the assumption that certain individual's gene codes, on average, produce fitter individuals. The recombination operator is used to exchange genetic information between pairs, or larger groups, of individuals. The simplest recombination operator is that of single-point crossover.

A further genetic operator, called mutation, is then applied to the new chromosomes, again with a set probability, Pm. Mutation causes the individual genetic representation to be changed according to some probabilistic rule. In the binary string representation, mutation will cause a single bit to change its state, $0 \Rightarrow 1$ or $1 \Rightarrow 0$.

Mutation is generally considered to be a background operator that ensures that the probability of searching a particular subspace of the problem space is never zero.

This has the effect of tending to inhibit the possibility of converging to a local optimum, rather than the global optimum. After recombination and mutation, the individual strings are then, if necessary, decoded, the objective function evaluated, a fitness value assigned to each individual and individuals selected for mating according to their fitness, and so the process continues through subsequent generations. In this way, the average performance of individuals in a population is expected to increase, as good individuals are preserved and bred with one another and the less fit individuals die out. The GA is terminated when some criteria are satisfied, e.g. a certain number of generations, a mean deviation in the population, or when a particular point in the search space is encountered.

A.1 GAs versus traditional methods

From the above discussion, it can be seen that the GAs differ substantially from more traditional search and optimization methods. The four most significant differences are:

- GAs search a population of points in parallel, not a single point.
- GAs do not require derivative information or other auxiliary knowledge; only the objective function and corresponding fitness levels influence the directions of search.
- GAs use probabilistic transition rules, not deterministic ones.

- GAs work on an encoding of the parameter set rather than the parameter set itself (except in where real-valued individuals are used).

It is important to note that the GA provides a number of potential solutions to a given problem and the choice of final solution is left to the user. In cases where a particular problem does not have one individual solution, for example a family of Pareto-optimal solutions, as is the case in multiobjective optimization and scheduling problems, then the GA is potentially useful for identifying these alternative solutions simultaneously.

A.1.1 Population representation and initialization

GAs operate on a number of potential solutions, called a population, consisting of some encoding of the parameter set simultaneously. Typically, a population is composed of between 30 and 100 individuals.

The most commonly used representation of chromosomes in the GA is that of the single-level binary string. Here, each decision variable in the parameter set is encoded as a binary string and these are concatenated to form a chromosome. The use of Gray coding has been advocated as a method of overcoming the hidden representational bias in conventional binary representation as the Hamming distance between adjacent values is constant [40]. Empirical evidence of Caruana and Schaffer [41] suggests that large Hamming distances in the representational mapping between adjacent values, as is the case in the standard binary representation, can result in the search process being deceived or unable to efficiently locate the global minimum.

Whilst binary-coded GAs are most commonly used, there is an increasing interest in alternative encoding strategies, such as integer and real-valued representations. For some problem domains, it is argued that the binary representation is in fact deceptive in that it obscures the nature of the search.

The use of real-valued genes in GAs offer a number of advantages in numerical function optimization over binary encodings. Efficiency of the GA is increased as there is no need to convert chromosomes to phenotypes before each function evaluation; less memory is required as efficient floating-point internal computer representations can be used directly; there is no loss in precision by discretisation to binary or other values; and there is greater freedom to use different genetic operators.

Having decided on the representation, the first step in the SGA is to create an initial population. This is usually achieved by generating the required number of individuals using a random number generator that uniformly distributes numbers in the desired range. For example, with a binary population of N_{ind} individuals whose chromosomes are Lind bits long, $N_{ind} \times L_{ind}$ random numbers uniformly distributed from the set $0, 1$ would be produced.

A.2 The objective and fitness functions

The objective function is used to provide a measure of how individuals have performed in the problem domain. In the case of a minimization problem, the most fit individuals will have the lowest numerical value of the associated objective function. This raw measure of fitness is usually only used as an intermediate stage in determining the relative performance of individuals in a GA. Another function, the fitness function, is normally used to transform the objective function value into a measure of relative fitness, thus:

$$F(x) = g(f(x)) \,, \tag{A.1}$$

where$f(\cdot)$ is the objective function, $g(\cdot)$ transforms the value of the objective function to a non-negative number and $F(\cdot)$ is the resulting relative fitness. This mapping is always necessary when the objective function is to be minimized as the lower objective function values correspond to fitter individuals. In many cases, the fitness function value corresponds to the number of offspring that an individual can expect to produce in the next generation. A commonly used transformation is that of proportional fitness assignment . The individual fitness, $F(xi)$, of each individual is computed as the individual's raw performance, $f(xi)$, relative to the whole population, i.e.:

$$F(x_i) = \frac{f(x_i)}{\sum_{i=1}^{N_{ind}} f(x_i)} \,, \tag{A.2}$$

where N_{ind} is the population size and x_i is the phenotypic value of individual i. Whilst this fitness assignment ensures that each individual has a probability of reproducing according to its relative fitness, it fails to account for negative objective function values. A linear transformation which offsets the objective function is often used prior to fitness assignment, such that:

$$F(x) = af(x) + b \,, \tag{A.3}$$

where a is a positive scaling factor if the optimization is maximizing and negative if we are minimizing. The offset b is used to ensure that the resulting fitness values are non-negative.

The linear scaling and offsetting outlined above is, however, susceptible to rapid convergence. The selection algorithm (see below) selects individuals for reproduction on the basis of their relative fitness. Using linear scaling, the expected number of offspring is approximately proportional to that individuals performance. As there is no constraint on an individual's performance in a given generation, highly fit individuals in early generations can dominate the reproduction causing rapid con-

vergence to possibly sub-optimal solutions. Similarly, if there is little deviation in the population, then scaling provides only a small bias towards the most fit individuals.

Limiting the reproductive range, so that no individuals generate an excessive number of offspring, prevents premature convergence. Individuals are assigned a fitness according to their rank in the population rather than their raw performance. One variable, MAX, is used to determine the bias, or selective pressure, towards the most fit individuals and the fitness of the others is determined by the following rules:

- $MIN = 2.0 - MAX$
- $INC = 2.0 \times (MAX - 1.0)/Nind$
- $LOW = INC/2.0$

where MIN is the lower bound, INC is the difference between the fitness of adjacent individuals and LOW is the expected number of trials (number of times selected) of the least fit individual. MAX is typically chosen in the interval $[1.1, 2.0]$. Hence, for a population size of $Nind = 40$ and $MAX = 1.1$, we obtain $MIN = 0.9$, $INC = 0.05$ and $LOW = 0.025$. The fitness of individuals in the population may also be calculated directly as:

$$F(x_i) = 2{-}MAX + 2(MAX{-}1)\frac{x_i - 1}{N_{ind} - 1}\,, \tag{A.4}$$

where x_i is the position in the ordered population of individual i. It should be noted that the linear scaling function is not suitable for use with objective functions that return negative fitness values.

A.3 Selection

Selection is the process of determining the number of times, or trials, a particular individual is chosen for reproduction and, thus, the number of offspring that an individual will produce. The selection of individuals can be viewed as two separate processes:

1. determination of the number of trials an individual can expect to receive;
2. conversion of the expected number of trials into a discrete number of offspring.

The first part is concerned with the transformation of raw fitness values into a realvalued expectation of an individual's probability to reproduce and is dealt with in the previous subsection as fitness assignment. The second part is the probabilistic selection of individuals for reproduction based on the fitness of individuals relative to one another and is sometimes known as sampling.

The measures of performance for selection algorithms is given by three properties:

- **Bias:** defined as the absolute difference between an individual's actual and expected selection probability. Optimal zero bias is therefore achieved when an individual's selection probability equals its expected number of trials.

- **Spread:** is the range in the possible number of trials that an individual may achieve.

- **Efficiency:** to evaluate the computational complexity of the algorithm.

It has been shown in the literature that the other phases of a GA (excluding the actual objective function evaluations) are O(Lind.Nind) or better time complexity, where Lind is the length of an individual and Nind is the population size. The selection algorithm should thus achieve zero bias whilst maintaining a minimum spread and not contributing to an increased time complexity of the GA.

A.3.1 Roulette wheel selection methods

Many selection techniques employ a "roulette wheel" mechanism to probabilistically select individuals based on some measure of their performance. A real-valued interval, Sum, is determined as either the sum of the individuals' expected selection probabilities or the sum of the raw fitness values over all the individuals in the current population. Individuals are then mapped one-to-one into contiguous intervals in the range$[0, Sum]$. The size of each individual interval corresponds to the fitness value of the associated individual. To select an individual, a random number is generated in the interval $[0, Sum]$ and the individual whose segment spans the random number is selected. This process is repeated until the desired number of individuals have been selected.

The basic roulette wheel selection method is stochastic sampling with replacement (SSR). Here, the segment size and selection probability remain the same throughout the selection phase and individuals are selected according to the procedure outlined above. SSR gives zero bias but a potentially unlimited spread. Any individual with a segment size > 0 could entirely fill the next population.

A.3.2 Stochastic universal sampling

Stochastic universal sampling (SUS) is a single-phase sampling algorithm with minimum spread and zero bias. Instead of the single selection pointer employed in roulette wheel methods, SUS uses N equally spaced pointers, where N is the number of selections required. The population is shuffled randomly and a single random

number in the range [0 Sum/N] is generated, ptr. The N individuals are then chosen by generating the N pointers spaced by 1, $[ptr, ptr+1, ..., ptr+N-1]$, and selecting the individuals whose fitnesses span the positions of the pointers.

The roulette wheel selection methods can all be implemented as $O(N \log N)$ although SUS is a simpler algorithm and has time complexity $O(N)$.

A.4 Crossover (Recombination)

The basic operator for producing new chromosomes in the GA is that of crossover. Like its counterpart in nature, crossover produces new individuals that have some parts of both parent's genetic material. The simplest form of crossover is that of single-point crossover, described above The other forms results:

- **Multi-point Crossover** For multi-point crossover, m crossover positions,$k_i \in \{1, 2, ..., l-1\}$, where k_i are the crossover points and l is the length of the chromosome, are chosen at random with no duplicates and sorted into ascending order. Then, the bits between successive crossover points are exchanged between the two parents to produce two new offspring. The section between the first allele position and the first crossover point is not exchanged between individuals.

- **Uniform Crossover** Single and multi-point crossover define cross points as places between loci where a chromosome can be split. Uniform crossover generalises this scheme to make every locus a potential crossover point. A crossover mask, the same length as the chromosome structures is created at random and the parity of the bits in the mask indicates which parent will supply the offspring with which bits.

Uniform crossover, like multi-point crossover, has been claimed to reduce the bias associated with the length of the binary representation used and the particular coding for a given parameter set. This helps to overcome the bias in single-point crossover towards short substrings without requiring precise understanding of the significance of individual bits in the chromosome representation.

There are other crossover operators as: Intermediate Recombination and Line Recombination.

A.5 Mutation

In natural evolution, mutation is a random process where one allele of a gene is replaced by another to produce a new genetic structure. In GAs, mutation is randomly applied with low probability, typically in the range 0.001 and 0.01, and modifies elements in the chromosomes. Usually considered as a background operator, the role

of mutation is often seen as providing a guarantee that the probability of searching any given string will never be zero and acting as a safety net to recover good genetic material that may be lost through the action of selection and crossover. The binary mutation flips the value of the bit at the loci selected to be the mutation point. Given that mutation is generally applied uniformly to an entire population of strings, it is possible that a given binary string may be mutated at more than one point.

With non-binary representations, mutation is achieved by either perturbing the gene values or random selection of new values within the allowed range.

For codings more complex than binary, high mutation rates can be both desirable and necessary and show how, for a complex combinatorial optimization problem, high mutation rates and non-binary coding yielded significantly better solutions than the normal approach.

Moreover Mutation prevents the algorithm to be trapped in a local minimum. If crossover is supposed to exploit the current solution to find better ones, mutation is supposed to help for the exploration of the whole space. Mutation helps escape form local minimum's trap and maintains diversity in the population.

A.6 Reinsertion

Once a new population has been produced by selection and recombination of individuals from the old population, the fitness of the individuals in the new population may be determined. If fewer individuals are produced by recombination than the size of the original population, then the fractional difference between the new and old population sizes is termed a generation gap. In the case where the number of new individuals produced at each generation is one or two, the GA is said to be steady-state or incremental. If one or more of the most fit individuals is deterministically allowed to propagate through successive generations then the GA is said to use an elitist strategy.

To maintain the size of the original population, the new individuals have to be reinserted into the old population. Similarly, if not all the new individuals are to be used at each generation or if more offspring are generated than the size of the old population then a reinsertion scheme must be used to determine which individuals are to exist in the new population. An important feature of not creating more offspring than the current population size at each generation is that the generational computational time is reduced, most dramatically in the case of the steady-state GA, and that the memory requirements are smaller as fewer new individuals need to be stored while offspring are produced. When selecting which members of the old population should be replaced the most apparent strategy is to replace the least fit

members deterministically.

Termination of the GA

Because the GA is a stochastic search method, it is difficult to formally specify convergence criteria. As the fitness of a population may remain static for a number of generations before a superior individual is found, the application of conventional termination criteria becomes problematic. A common practice is to terminate the GA after a prespecified number of generations and then test the quality of the best members of the population against the problem definition. If no acceptable solutions are found, the GA may be restarted or a fresh search initiated.

Table A.1: M-File list.

bs2rv	BS2RV.m	Binary string to real vector
crtbase	CRTBASE.m	Create base vector
crtbp	CRTP.m	Create an initial population
crtrp	CRTRP.m	Createe an initial Real-value Population
migrate	MIGRATE.m	Migration of individuals between subpopulations
mpga	MPGA.m	Multi population genetic algorithm
mut	MUT.m	Mutates each element with given probability
mutate	MUTATE.m	Mutation high-level function
mutbga	MUTBGA.m	Real-value mutation like Breeder Genetic Algorithm
objfun1	OBJFUN1.m	Objective function for De Jong's FUNction 1
objharv	OBJHARV.m	Objective function for HARVest problem
ranking	RANKING.m	Rank-based fitness assignment
recdis	RECDIS.m	Recombination discrete
recint	RECINT.m	Recombination extended intermediate
reclin	RECLIN.m	Recombination extended line
recmut	RECMUT.m	Line recombination with mutation features
recombin	RECOMBIN.m	Recombination high-level function
reins	REINS.m	Re-insertion of offspring in population replacing parents
resplot	RESPLOT.m	Result ploting
rws	RWS.m	Roulette Wheel Selection
scaling	SCALING.m	Linear fitness scaling
select	SELECT.m	Universal selection
sus	SUS.m	Stochastic Universal Sampling
xovdp	XOVDP.m	Crossover Double Point
xovdprs	XOVDPRS.m	Crossover Double-Point with Reduced Surrogate
xovmp	XOVMP.m	Multi-point crossover
xovsh	XOVSH.m	Crossover Shuffle
xovshrs	XOVSHRS.m	Crossover Shuffle with Reduced Surrogate
xovsp	XOVSP.m	Crossover Single-Point
xovsprs	XOVSPRS.m	Crossover Single-Point with Reduced Surrogate

A.7 GA Toolbox

Version 1.2 15-Apr-94. Department of Automatic Control and Systems Engineering. University of Sheffield, England. List of m-function, Table A.1.

A.8 Function MATLAB™ rv2bs

```
function genot = rv2bs(var,fieldD)
%
% This function decodes vectors of reals (phenotype) into genotype. The
% chromosomes are made of binary strings of given
% length using ONLY standard binary (NO Gray decoding).
% The real numbers must given in a specified interval.
%
% INPUT:
%
% var: matrix containing in each row the vector of reals of the current
%      population.
% fieldD: matrix describing the length and how to decode each substring
%         in the chromosome. It has the following structure:
%
%   [len;        (num)
%    lb;         (num)
%    ub;         (num)
%    code;       (0=binary     | 1=gray)
%    scale;      (0=arithmetic | 1=logarithmic)
%    lbin;       (0=excluded   | 1=included)
%    ubin];      (0=excluded   | 1=included)
%
%   where
%   len: row vector containing the length of each substring in Chrom.
%        sum(len) should equal the individual length.
%   lb, ub: lower and upper bounds for each coded variable.
%   code: row vector indicating how each substring is to be decoded.
%         ONLY BINARY is allowed
%   scale: binary row vector indicating where to use arithmetic
%          and/or logarithmic scaling. ONLY ARITHMETIC is allowed
%   lbin, ubin: binary row vectors indicating whether or not to include
%               each bound in the representation range
%
% OUTPUTS:
%
% genot: matrix containing in each row the individual's concatenated
%        binary string representation.
%        Leftmost bits are MSb and  rightmost are LSb.

%
% Author: Marco Bertinato and Mirco Rampazzo
% Date: 20/09/09

% Identify the population size (Nind)
%      and the number of variable (Nvar)
[Nind,Nvar] = size(var);

% Identify the number of decision variables (Nvar)
[seven,NvarF] = size(fieldD);

if Nvar ≠ NvarF
    error('var must have the number of variables described in fieldD.');
end
if seven ≠ 7
    error('fieldD must have 7 rows.');
end

% Get substring properties
len = fieldD(1,:);
lb = fieldD(2,:);
ub = fieldD(3,:);
code = ¬(¬fieldD(4,:));
scale = ¬(¬fieldD(5,:));
lin = ¬(¬fieldD(6,:));
uin = ¬(¬fieldD(7,:));
% number of bit each genotypic representation
Lind = sum(len);
```

```
% preallocating for speed
genot = zeros(Nind,Lind);
% vector with the index of last bit for each variables
lf = cumsum(len);
% vector with the index of first bit for each variables
li = cumsum([1 len]);

% for logarithmic scaling
logsgn = sign(lb(scale));
lb(scale) = log( abs(lb(scale)) );
ub(scale) = log( abs(ub(scale)) );
Δ = ub − lb;

% vector with the quantum for the representation of each variables
Prec = .5 .^ len;
%       = quantum if lb is not included
% num
%       = 0       if lb is included
num = (¬lin) .* Prec;
%       = quantum  if lb and ub are included
% den   = −quantum if neither lb nor up are included
%       = 0        if lb is icluded && ub not or viceversa
den = (lin + uin − 1) .* Prec;
% initializing at zero evry bit of genotype
genDec = zeros(Nind,Nvar);
for i = 1:Nvar,
    % scaling of the real values of each variables into [0 1]
    % for all the row of var matrix
    genDec(:,i) = (var(:,i)−lb(i))./Δ(i) − num(i) ./ (1−den(i));
    for n = 1:Nind
        for b = 1:len(i)
            % performing consecutive divisions to convert the rv
            % into binary representation.
            if ( genDec(n,i)/(.5^b) ) ≥ 1
                % put 1 in correct position in genot: LSB @ li(i)
                % MSB at lf(i)
                genot(n,b+li(i)−1) = 1;
                genDec(n,i) = genDec(n,i) − .5^b;
            end
        end
    end
end
```

B

Constrained optimization

A constrained optimization problem is usually written as a nonlinear optimization problem of the following form:

$$\begin{aligned} &\arg_{(x \in F \subseteq S \subseteq \mathbb{R}^n)} \min f(x)\,, \\ &\text{subjected to:} \\ &g_i(x) \leq 0 \qquad\qquad i = 1, ..., q\,; \\ &h_j(x) \qquad\qquad j = q+1, ..., m\,; \end{aligned} \tag{B.1}$$

where x is the vector of solutions, F is the feasible region and S is the whole search space. There are q inequality and $m - q$ equality constraints. $f(x)$ is usually called the objective function or criterion function. Objective function and constraints could be linear or nonlinear in the problem. Vector $\bar{x}$ that satisfies all the constraints is a feasible solution of the problem. All of the feasible solutions constitute the feasible region. Inequality constraints that satisfy$g_i(x) = 0$ are called active at x. Using these definitions, nonlinear programming problem is to find a point $x^* \in F$ such that $f(x^*) \leq f(x)$ for all $x \in F$.

B.1 Constraint handling in GAs

There are several approaches proposed in GAs to handle constrained optimization problems:

- Method based on penalty functions.
- Methods based on a search of feasible solutions.
- Methods based on preserving feasibility of solutions.

- Hybrid methods.

Here, a penalty functions approach is considerated.

B.2 Penalty Functions

Penalty method transforms constrained problem to unconstrained one in two ways. The first way is to use additive form as follows:

$$eval(x) = \begin{cases} f(x)\,, & \text{if } x \in F \\ f(x) + p(x)\,, & \text{otherwise.} \end{cases} \tag{B.2}$$

where $p(x)$ presents a penalty term. If no violation occurs, $p(x)$ will be zero and positive otherwise. Under this conversion, the overall objective function now is $eval(x)$ which serves as an evaluation function in GAs. Second way is to use multiplicative form,

$$eval(x) = \begin{cases} f(x)\,, & \text{if } x \in F \\ f(x) \cdot p(x)\,, & \text{otherwise.} \end{cases} \tag{B.3}$$

For minimization problems, if no violation occurs $p(x)$ is one and bigger than one, otherwise. The additive penalty type has received much more attention than the multiplicative type in the GA community. In classical optimization, two types of penalty function are commonly used: interior and exterior penalty functions. In GAs exterior penalty functions are used more than interior penalty functions. The main reason of this, there is no need to start with a feasible solution in exterior penalty functions. Because finding a feasible solution in many GAs problems is a NP- hard itself. The general formulation of an exterior penalty function is:

$$\varphi(x) = f(x) + \left[\sum_{i=1}^{q} r_i G_i + \sum_{j=q+1}^{m} c_j L_j\right]\,, \tag{B.4}$$

where $\varphi(x)$ indicates the new objective function to be optimized. G_i and L_j are the functions of $g_i(x)$ and $h_j(x)$ constraints respectively, and r_i and c_j are penalty parameters. General formulas of G_i and L_j are,

$$G_i = \max\left[0,\, g_i(x)\right]^{\beta}\,, \tag{B.5}$$

$$L_j = |h_j(x)|^{\gamma}\,, \tag{B.6}$$

where β and γ are commonly 1 or 2. If the inequality is hold, $g(x) \leq 0$ and $\max\left[0,\, g_i(x)\right]$ will be zero. Therefore the constraint does not effect $\varphi(x)$. If the constraint is violated that means $g_i(x) > 0$ or $h_j(x) \neq 0$, a big term will be added to $\varphi(x)$ function such that the solution is pushed back towards to the feasible region.

The severeness of the penalty depends on the penalty parameters r_i and c_j. If either the penalty is too large or too small, the problem could be very hard for GAs. A big penalty prevents to search unfeasible region. In this case GA will converge to a feasible solution very quickly even if it is far from the optimal. A pretty small penalty will cause to spend so much time in searching an unfeasible region; thus GA would converge an unfeasible solution.

C

Common Strategies Algorithms

C.1 Simmetric Strategy

In order to simulate the function and performance of the (SS) of an array of parallel N_{ch}, a specific function has been built: the input are cooling load Q_L and T_{air} air temperature on the work point. The output of this function there will be $PLRs$ and ON/OFF states to be imposed on machines; it has to be reminded that the machines functioning is managed by a local chiller controller, on the basis of the fraction of the load provided by the supervisor. A recursive function has been chosen to be developed, so as being totally flexible on the variation of the number of machines and being terminated as soon as possible, without performing uselss iterations (how would happen by the means of a for cycle, instead). The SS function as a pseudo-code is reported on the the Algorithm 1 for chillers with two (1C and 2C) capacity steps.

Algorithm 1 SS

1: $\{\mathbf{status}, \mathbf{PLR}, \mathbf{Q}, \mathbf{P_e}, \mathbf{E}\}$ = `SS` (Q_L, T_{air})
2: $CumP_f := 0$ ▷ Cooling power supply
3: $\{\}$ = `fcnStep1C`$(CumP_f, 1)$ ▷ from the Algorithm 2
4: **end** `SS`

It has to be noted that the SS call the function fncStep1C only one time: other calls will be nested inside the fcnStep1C itself; when all the chillers are being activated on 1C capacity step, the procedure will call the analogue function (look at Algorithm 3) for activation of the 2C capacity step.

Algorithm 2 Ignition of 1C capacity step, i-th chiller

1: $\{\}$ = `fcnStep1C` $(cumP_f, i)$
2: **if** $cumP_f + P_{f,i}^{(1C)} > Q_L$ **then** ▷ with the ignition of i-th chiller, the request is subsided
3: $status_i = 1$
4: $Q_i = Q_L - cumP_f$ ▷ with this chiller the remaining load part is being supplied
5: $PLR_i = Q_i / P_{f,i}^{(2C)}$
6: $\overline{PLR}_i = PLR_i / PLR_i^*$
7: Calculation of $k_{F,i}^*$, $P_{e,i}$, E_i
8: $status_{i+1} = \ldots = status_{N_{ch}} = 0$ ▷ successive chillers are remaining switched-off
9: $Q_{i+1} = \ldots = Q_{N_{ch}} = P_{e,i+1} = \ldots = P_{e,N_{ch}} = E_{i+1} = \ldots = E_{N_{ch}} = 0$
10: **else**
11: $status_i = 1$
12: $PLR_i = PLR_i^*$ ▷ ignition on the maximum partialisation 1C
13: $Q_i = P_{f,i}^{(1C)}$ ▷ maximum chiller power in 1C
14: Calculation of $P_{e,i}$, E_i
15: **if** $i < N_{ch}$ **then**
16: $\{\} =$ `fcnStep1C`$(CumP_f + Q_i, i+1)$ ▷ the function itself is being called recursively, adding to the accumulator the chiller power here activated
17: **else**
18: $\{\} =$ `fcnStep2C`$(CumP_f + Q_i, 1)$ ▷ restart to ignition of the 2C of the first chiller
19: **end if**
20: **end if**
21: **end** `fcnStep1C`

C.2 Sequential Strategy

The function MS for the Sequential Strategy control is mostly analogue to the Algorithm 1. Instead, is different the function called: fcnMach, reported on the Algorithm 4.

Algorithm 3 Ignition of the 2C capacity step of , i-th chiller

1: $\{\}$ = `fcnStep2C` $(cumP_f, i)$
2: $cumP_f = cumP_f - P_{f,i}^{(1C)}$ ▷ if this function is being called it means that the chiller (already ON) has to go on 2C, therefore the power due to the 1C has to be subtracted
3: **if** $cumP_f + P_{f,i}^{(2C)} > Q_L$ **then** ▷ with the i-th chiller on 2C, the request is subsided
4: $Q_i = Q_L - cumP_f$ ▷ with this chiller the remaining load part is being supplied
5: $PLR_i = Q_i / P_{f,i}^{(2C)}$
6: Calculation $k_{F,i}$, $P_{e,i}$, E_i
7: **else**
8: $PLR_i = 1$ ▷ maximum ignition of 2C
9: $Q_i = P_{f,i}^{(2C)}$ ▷ maximum chiller power
10: Calculation $P_{e,i}$, E_i
11: **if** $i < N_{ch}$ **then**
12: $\{\}$ = `fcnStep2C`$(CumP_f + Q_i, i+1)$ ▷ the function itself is being called recursively, adding to the accumulator the chiller power here activated
13: **else** ▷ are already all active on 2C: the production cannot satisfy the load
14: **end if**
15: **end if**
16: **end** `fcnStep2C`

Algorithm 4 Ignition, i-th chiller

1: $\{\}$ = `fcnMach` $(cumP_f, i)$
2: **if** $cumP_f + P_{f,i}^{(2C)} > Q_L$ **then** ▷ with the i-th chiller ignition, the request is subsided
3: $status_i = 1$
4: $Q_i = Q_L - cumP_f$ ▷ with this chiller the remaining load part is being supplied
5: $PLR_i = Q_i / P_{f,i}^{(2C)}$
6: **if** $PLR_i \leq PLR_i^*$ **then**
7: $\overline{PLR}_i = PLR_i / PLR_i^*$
8: Calcolo $k_{F,i}^*$, $P_{e,i}$, E_i ▷ on 1C functioning!
9: **else**
10: Calcolo $k_{F,i}$, $P_{e,i}$, E_i ▷ on 2C functioning!
11: **end if**
12: $status_{i+1} = \ldots = status_{N_{ch}} = 0$ ▷ successive chillers are remaining switched-off
13: $Q_{i+1} = \ldots = Q_{N_{ch}} = P_{e,i+1} = \ldots = P_{e,N_{ch}} = E_{i+1} = \ldots = E_{N_{ch}} = 0$
14: **else**
15: $status_i = 1$ ▷ the chiller is not enough: ignition anyway!
16: $PLR_i = 1$
17: $Q_i = P_{f,i}^{(2C)}$ ▷ maximum chiller power on 2C
18: Calculation $P_{e,i}$, E_i
19: **if** $i < N_{ch}$ **then**
20: $\{\} =$ `fcnMach`$(CumP_f + Q_i, i+1)$ ▷ the function itself is being called recursively, adding to the accumulator the chiller power here activated
21: **else**▷ they are all already active on 2C: the plant cannot satisfy the load
22: **end if**
23: **end if**
24: **end** `fcnMach`

D

Regulation of Electronic Expansion Valve for Evaporator Control

Finned-coiled evaporators are used in many industrial vapour compression refrigeration systems including aircooled display cabinets for commercial applications. Nowadays, a standard approach to the control of the mass flow rate of the refrigerant through such an evaporator is that of resorting to an Electronic Expansion Valve (EEV), which, on the basis of measurements of the evaporator outlet pressure and temperature, regulates the degree of outlet superheat at a given set-point value. An EEV-controlled evaporator operates in a transient manner during start-up and shut-down of the cabinet. In addition, the system undergoes dynamic changes in response to changes in the temperature and humidity of the supply air from the cabinet, which is also affected by disturbances from the external environment. Other disturbances are caused by frost formation on the finned-coil and variation on the operational setup (such as during night operation). In the case of cabinets installed in centralized refrigeration plants, another source of dynamic changes is the pressure variation in the main suction line due to compressor cycling and on/off operation of other units (cabinets or cold rooms). While transients associated with start-up and shut-down are factors that determine the system performance in terms of energy efficiency and power consumption, the dynamic behavior of the evaporator due to changes in the load conditions is important from the point of view of control system design and stability.

An EEV-controlled finned-coiled evaporator is shown schematically in Figure D.1. For the safe operation of the compressor, the EEV has to ensure that refrigerant leaving the evaporator is in a superheated state. Moreover, a superheat value close to 0 K leads to instability, since the temperature measurements are heavily affected by the proximity to the refrigerant liquid/vapour transition plane. However, an excessive degree of superheat at the outlet would lower the effectiveness of the evaporator by reducing the area available for refrigerant evaporation. In practice,

a 5±10 K superheat constitutes a reasonable compromise. Classical control techniques such as Proportional-Integral-Derivative (PID) controllers are widely used for regulating EEVs, due to their low cost and ease of tuning and operation. However, more advanced control systems, such as predictive or adaptive controllers, can provide better performance since they can adapt the control action to the (widely) varying operational conditions. Moreover, since the same EEV can be interfaced with many different display cabinets, auto-tuning techniques can greatly ease the task of setting up the control system.

D.1 Auto-tuning regulator (ATR)

Proportional-Integral-Derivative (PID) controllers have been the most commonly used controllers in process industries for over 50 years, due to their versatility and ease of operation. However, proper tuning of the PID parameters is crucial for achieving the desired response characteristics. The tuning procedure, if done manually, is tedious and time consuming. The resulting system performance mainly depends on the experience and the process knowledge of the field engineers. However, with the advent of the auto-tuning of PID controller concept, this problem has been solved to a considerable extent [42]. Development of a control system involves many tasks such as modeling, design of a control law, implementation, and validation. The auto-tuning regulator (ATR) attempts to automate several of these tasks. The goal of this work is to give a simple, auto-tuning scheme for high-performance, robust control algorithm for EEVs to be used for controlling the superheat temperature of finned coil evaporators[43]. The control scheme can be thought of as being composed of two loops (Figure D.2). The inner loop consists of the process and a PID controller. It is assumed that the structure of a process model is given but its parameters are unknown. In the outer loop, model parameters identification and design calculation are performed. The PID parameters can then be re-tuned on-line to better fit the operative conditions and improve the overall close-loop performance.

D.2 System modeling and closed-loop identification

Dry-expansion refrigerant evaporators have been widely used in the air conditioning and refrigeration industry. Because of two-phase evaporating flow inside coils and air dehumidification outside tubes, the local heat transfer coefficients vary over a great range at different locations and time, which results in uneven air distribution inside the evaporator. In order to fully simulate the heat transfer processes and air temperature and other parameter distributions inside the coil, distributed parameter models have gained popularity [44], [45], [46].

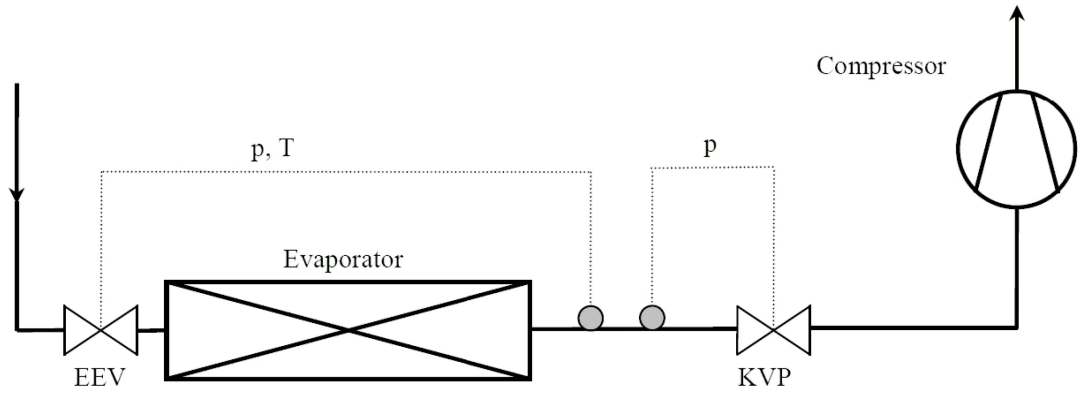

Figure D.1: Schematic representation of the modeled system. The system consists of a finned-coil evaporator, a step motor electronic expansion valve (EEV), the EEV temperature probe, a back-pressure valve (KVP) at the evaporator outlet, and a compressor.

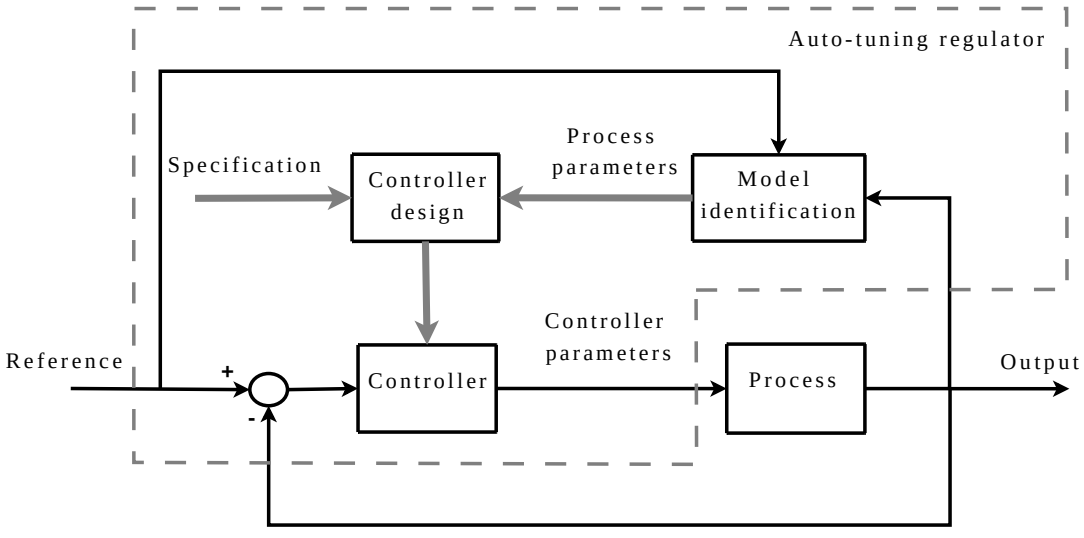

Figure D.2: Auto-tuning regulator.

The modeled system consists of a finned-coil evaporator, a step motor EEV, the EEV temperature probe, a back-pressure valve (KVP) at the evaporator outlet, and a compressor. The scheme of the system is shown in Figure D.1.

The assumptions made in the analysis are the following:

1. The refrigerant mass flow rate is uniform in each circuit and the heat conduction between each circuit is neglected.
2. The two-phase evaporating flow inside the tube is simplified as a one-dimensional flow. The refrigerant vapor and liquid are incompressible and in thermal equilibrium condition.
3. The heat transfer coefficients on the air side are uniform in either dry or wet coil region.
4. The axial heat conduction of the pipe wall can be ignored.
5. The air is incompressible, i.e., no mass and energy accumulation occurs.

In [47], on the basis of the above assumptions and by applying the conservation equations of mass, momentum, and energy on the refrigerant, air and tube wall, a differential algebraic equations (DAE) system has been derived, thus obtaining a detailed model that has been implemented in a dedicated simulation environment. The model has been extensively validated on an experimental test facility, see for instance Figure D.3 for a comparison (model and experimental data) of the time behavior of superheat and evaporation temperature after cabinet startup.

To obtain a low-order approximation of the process model, we resort to a first order plus dead-time (FOPDT) model, following a common practice in process control. For most processes, in fact, the use of the FOPDT model is adequate for control system design. Although a FOPDT model does not capture all the features of a high order process, it often reasonably describes the process gain, overall time constant, and effective dead time [48]. Typically, the FOPDT model of the process is estimated from the process reaction curve obtained from open-loop step responses, with the risk of process runaway. So, it is often appropriate to perform the model identification by operating the system in close-loop with a feedback controller. This is particularly relevant if safety issues are a concern or when it is expensive to take the plant offline for testing. By using the virtual prototyping environment described in [47], the procedure suggested in [49] is adopted for estimating a FOPDT model of the system shown in Figure D.1 in closed-loop with a PI controller. Choice of the PI controller parameters can be done on the basis of previous knowledge of the plant behavior. For instance, if the plant is normally operated with a PID controller, the test PI controller can be simply chosen by switching off the derivative action.

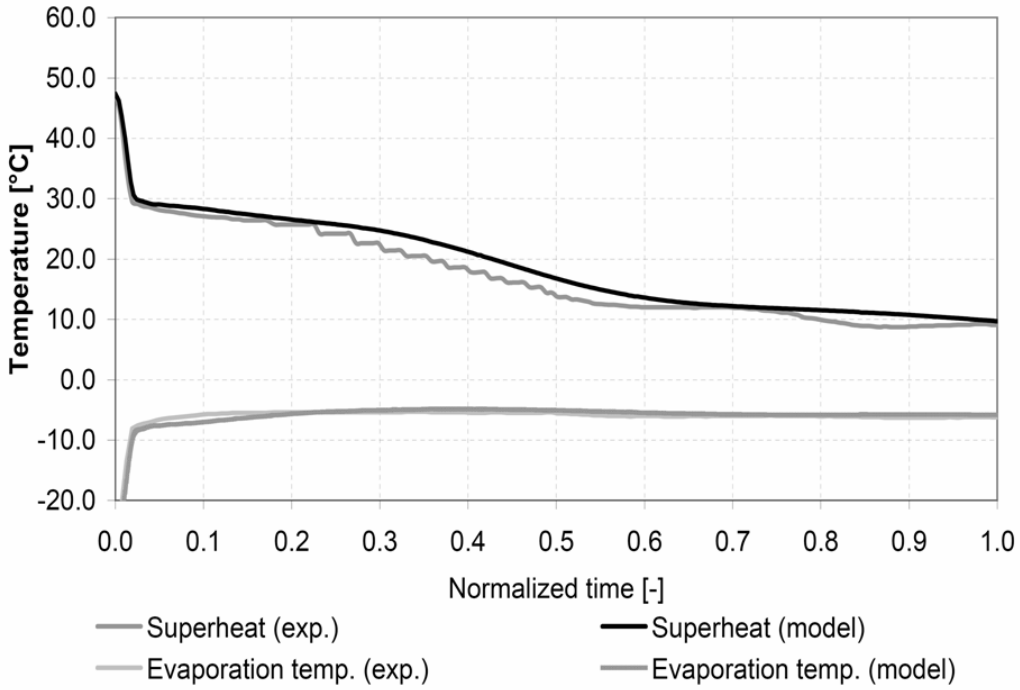

Figure D.3: Model and experimental superheat and evaporation temperature trends comparison after the cabinet startup. The test was carried out at a 19 °C ambient temperature and 40% relative humidity with 10 K superheat set-point.

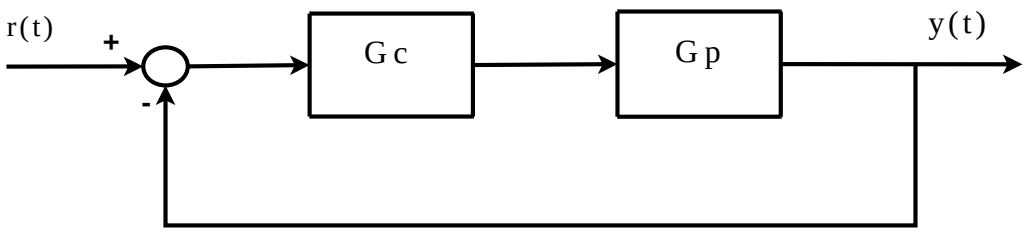

Figure D.4: Block diagram of standard feedback control system.

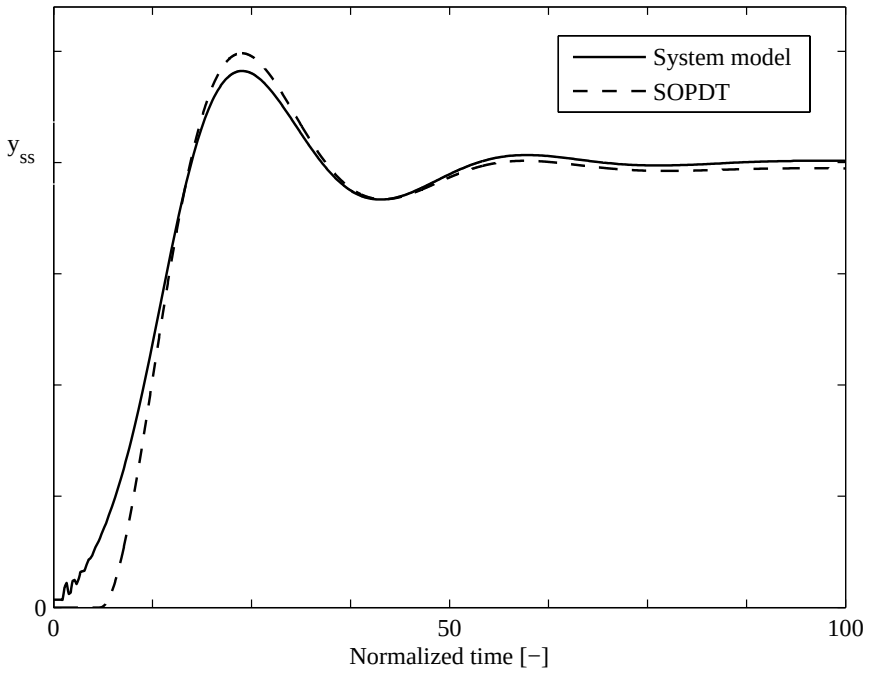

Figure D.5: Closed-loop SOPDT approximation, step response.

A standard closed-loop control structure is shown in Figure D.4, where $G_c(s)$ is the PI controller transfer function and $G_p(s)$ is the FOPDT process model to be identified:

$$G_c(s) = K_c \left(1 + \frac{1}{T_i s}\right) , \tag{D.1}$$

$$G_p(s) = \frac{K_p e^{-d_p s}}{1 + \tau_p s} . \tag{D.2}$$

For appropriate values of K_c and T_i, the step response of the closed-loop system exhibits an under-damped oscillatory mode, which can be suitably approximated by a second-order system plus delay (SOPDT) as shown in Figure D.5,

$$G_{cl}(s) = \frac{Y(s)}{R(s)} = \frac{K e^{-ds}}{\tau^2 s^2 + 2\zeta\tau s + 1} . \tag{D.3}$$

By writing the time domain solution of (D.3) and using the method proposed in [49] (see remark D.5), the values of K_p, d_p and τ_p can be obtained.

D.3 Model based controller design

Once the parameters of the FOPDT system (D.2) have been obtained, the PID parameters can be set by using well-known tuning formulas (e.g. Ziegler-Nichols [50], Cohen and Coon [51], Shinskey [52] , Silva et al. [53], CHR [54]). In the

Table D.1: Zhuang and Atherton PID tuning formulas, $0.1 < d_p/\tau_p < 1$.

PID parameters	ISE set-point change	ISTE load disturbance
K_c	$\frac{1.048}{K_p}\left(\frac{d_p}{\tau_p}\right)^{-0.897}$	$\frac{1.468}{K_p}\left(\frac{d_p}{\tau_p}\right)^{-0.970}$
T_i	$\frac{\tau_p}{1.195 - 0.368 \cdot d_p/\tau_p}$	$\frac{\tau_p}{0.942}\left(\frac{\tau_p}{d_p}\right)^{-0.725}$
T_d	$0.489\tau_p\left(\frac{d_p}{\tau_p}\right)^{0.888}$	$0.443\tau_p\left(\frac{d_p}{\tau_p}\right)^{0.939}$

next examples, the optimum setting algorithms proposed by Zhuang and Atherthon [55] have been adopted. The method is based on the minimization of the following performance index:

$$J_n(\theta) = \int_0^\infty \left[t^n e(\theta, t)\right]^2 dt\Big], \tag{D.4}$$

where $e(\theta, t)$ is the error signal which enters the controller, and θ the PID parameter vector. $J_n(\theta)$ corresponds to the well-known ISE and ISTE criteria for n=0 and 1, respectively. For the system structure shown in Figure D.4, two parameter setting strategies are proposed: one for set-point change and the other for load disturbance rejection (see Tab. D.1).

D.4 Simulation examples

The auto-tuning regulator has been implemented in the virtual prototyping environment where all the system constraints are considered. The controller has then been digitally implemented using an incremental form, due to the advantages of such formulation in terms of integrator wind-up and robustness in controller switching (as required, for instance, at start up) [42]. Simulations are performed to compare the performance of the proposed auto-tuning regulator with another one, based on a standard relay feedback method with a frequency domain approach, and that is presently implemented on board of the commercial EEV considered in the work. Two examples are described in the following to illustrate the performance of the proposed control algorithm.

D.4.1 Example 1

In the first example, the system is operated as follows. The superheat set-point is 10 K (Figure D.6). The system is first taken from startup to steady state by a PID controller, with parameters set based on the standard relay feedback method (PID_{RM} in Tab. D.2). At normalized time t=100 and t=600, two set-point vari-

Table D.2: FOPDT model parameters obtained by Mamat-Fleming procedure and PID parameters.

	FOPDT		PID_{RM}	PI_{id}	PID_{ZA_S}
K_p	1.27	K_c	3.5	2.2	2.5
d_p	29	T_i	97	110	92
τ_p	100	T_d	12		16

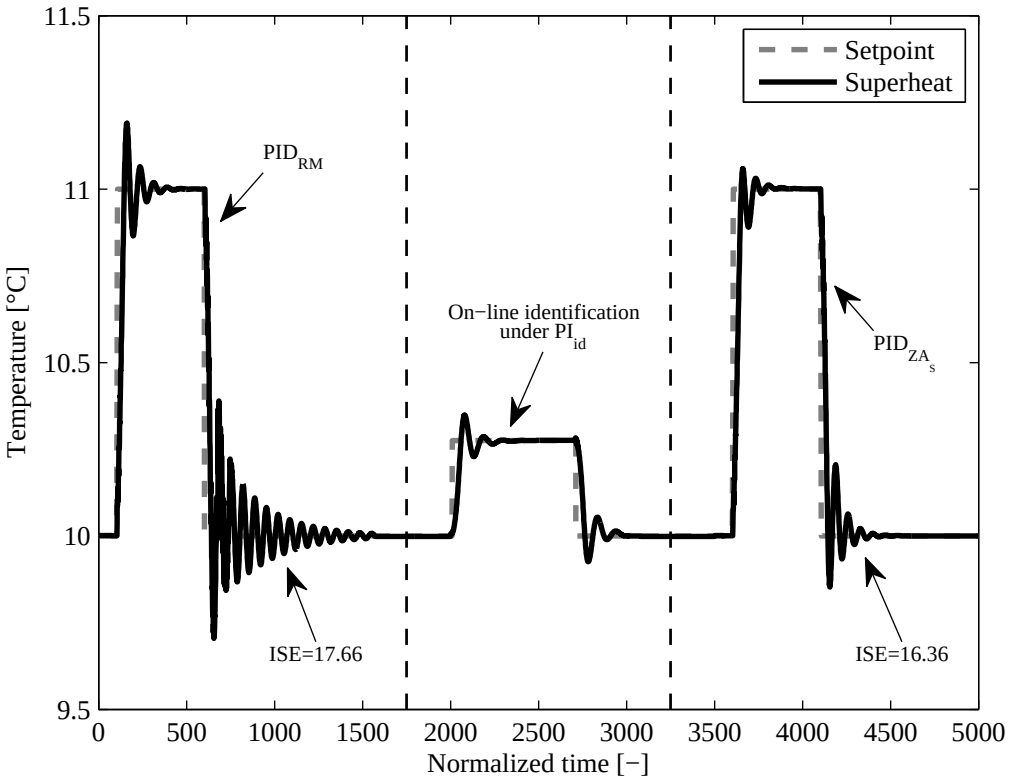

Figure D.6: Auto-tuning regulator; the test was carried out at a 19 °C ambient temperature and 40% relative humidity.

ations are requested. It can be seen that the system response exhibits a strong oscillatory behaviour , with settling time to within 5% of about 500 and ISE=17.66. At normalized time t=2000 the on-line identification process is activated to re-tune the controller. The PI controller with PI_{id} parameters in Tab. D.2 is used. At the end of the on-line identification phase, the closed-loop system is approximated by SOPDT model and the FOPDT model parameters are obtained. Then, a new set of controller parameters (PID_{ZA_S} Tab. D.2) is chosen by using the Zhaung-Atherton formula in table D.1 (ISE set-point change). It is worth noticing that the system response to the same change in the set-point operated before is now much better (settling time to within 5%, of about 200 and ISE=16.36), as can be seen in Figure D.6.

Table D.3: Integral Squared Time weighted Error (ISTE).

Case	1	2	3
ISTE PID_{RM}	$4.4 \cdot 10^7$	$2.3 \cdot 10^9$	$1.9 \cdot 10^7$
ISTE PID_{ZA_L}	$2.1 \cdot 10^7$	$4.6 \cdot 10^8$	$8.1 \cdot 10^6$

D.4.2 Example 2

The load disturbance rejection properties are particularly relevant for the regulation algorithms in the control process area. In this example, after the on-line identification of the FOPDT, the PID parameters set, PID_{ZA_L} ($Kc = 3.8$, $T_i = 43$ and $T_d = 14$), is obtained by using the ISTE load disturbance rejection formula in Tab. D.1. The performances of the two set parameters, PID_{RM} and PID_{ZA_L}, have been compared with reference to the three case studies:

1. influence of external load disturbances;
2. influence of evaporator inlet air temperature change, from start-up condition;
3. influence of evaporator inlet air temperature rapid change, from steady state condition.

The results of simulations are shown in Figure D.7, D.8 and D.9. In Tab. D.3, the ISTE values are reported for the case studies. It is worth noticing that PID_{ZA_L}, exhibits much better performance, in term of disturbance rejection, with respect to the PID_{RM} obtained by the relay feedback method.

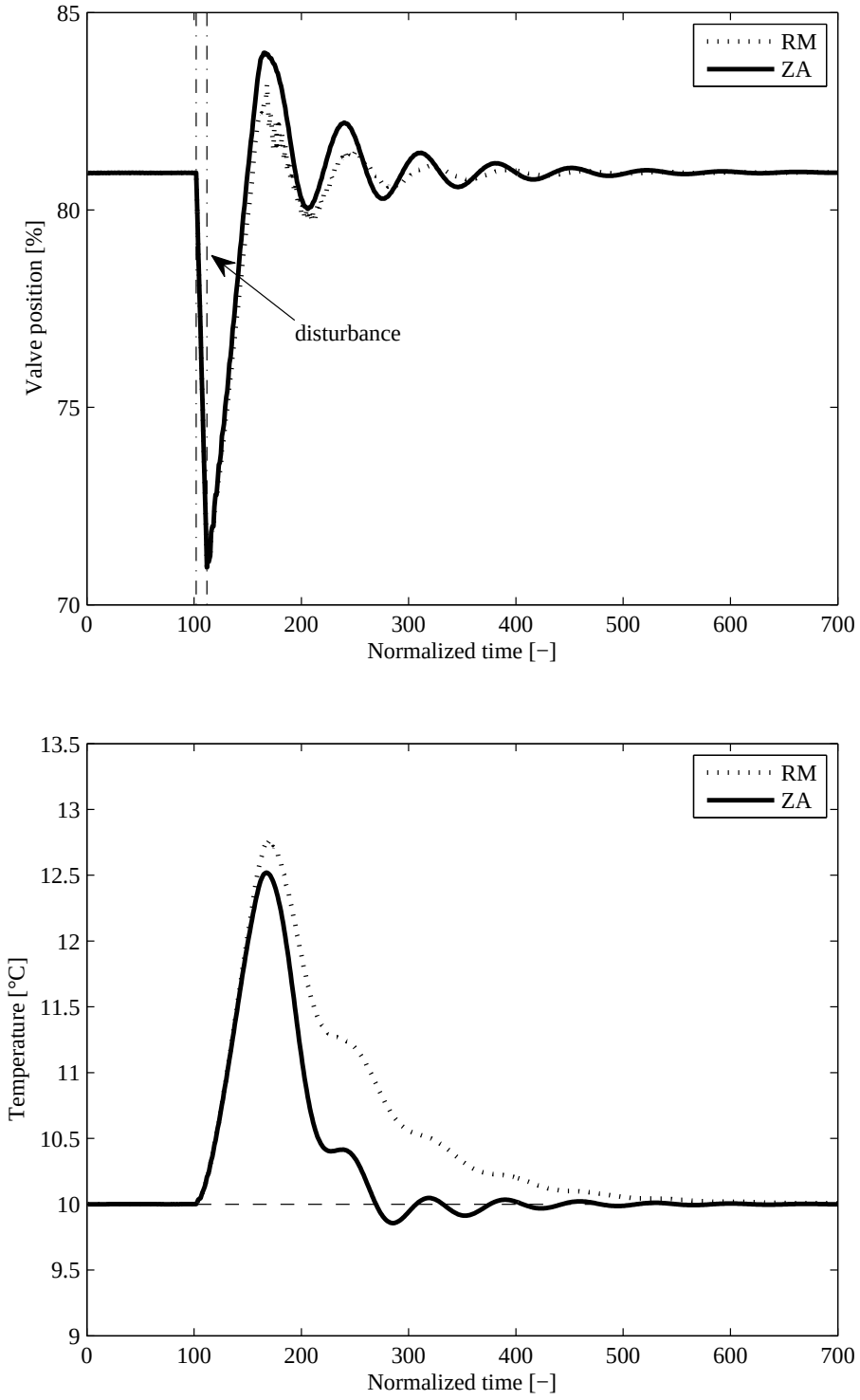

Figure D.7: Case 1, valve position [%] and superheat temperature under influence of external disturbances; the test was carried out at a 19 °C ambient temperature and 40% relative humidity with 10 K superheat set-point. PID_{RM}: $Kc = 3.5$, $T_i = 97$ and $T_d = 12$; PID_{ZA_L}: $Kc = 3.8$, $T_i = 43$ and $T_d = 14$.

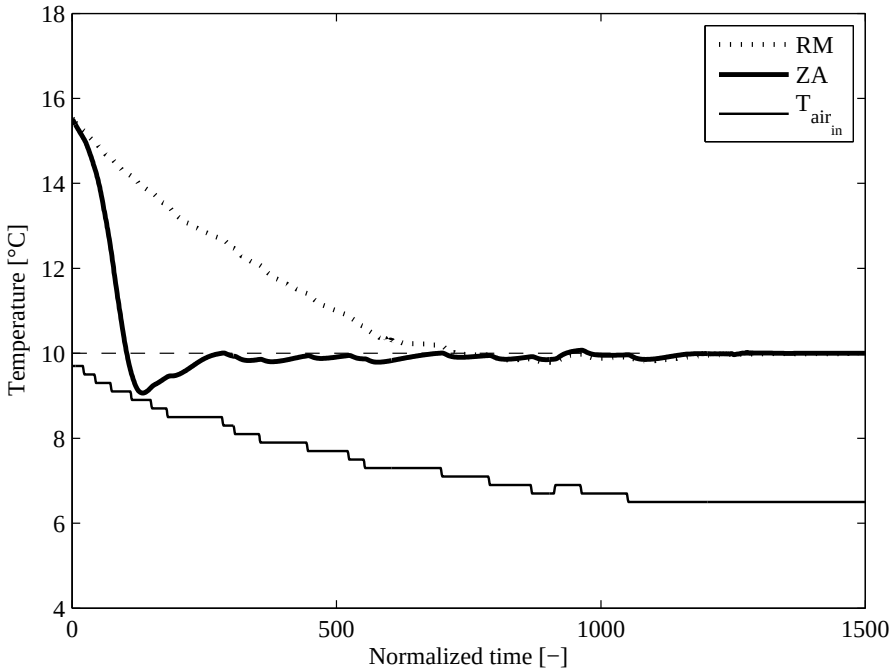

Figure D.8: Case 2, superheat temperature under influence of evaporator inlet air temperature change (values were taken from experimental data), from start-up condition; the test was carried out at 40% relative humidity with 10 K superheat set-point.

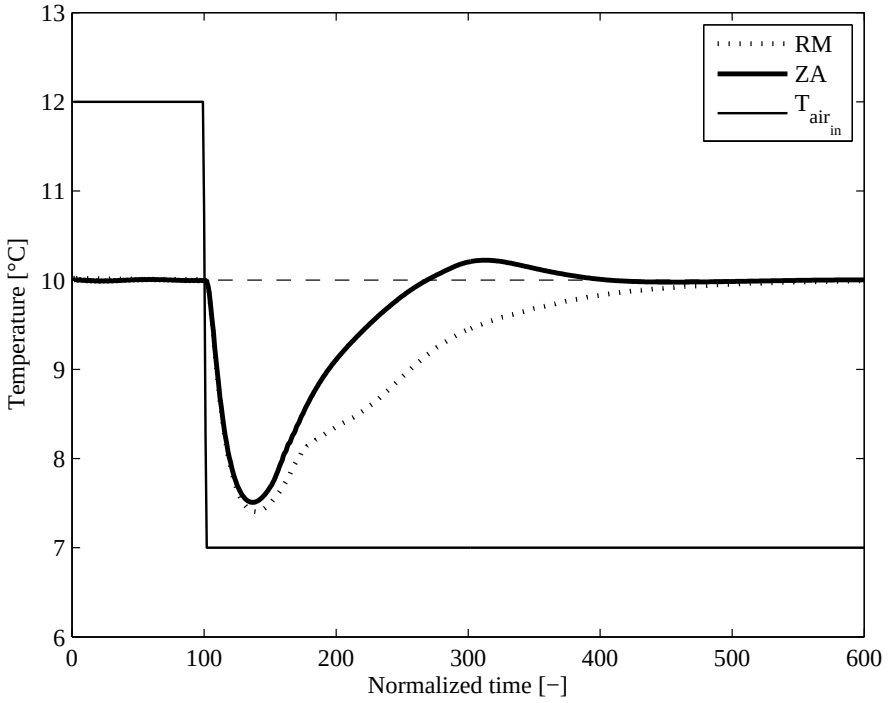

Figure D.9: Case 3, superheat temperature under influence of evaporator inlet air temperature rapid change (12-7 °C), from steady state condition; the test was carried out at 40% relative humidity with 10 K superheat set-point.

D.5 Remark

Consider the typical under-damped closed-loop response to a step-set-point change sketched in Figure D.10. The system with such behavior can be approximated by a second order plus dead-time transfer function:

$$G_{cl}(s) = \frac{Y(s)}{R(s)} = \frac{Ke^{-ds}}{\tau^2 s^2 + 2\zeta\tau s + 1}\,, \tag{D.5}$$

From the time domain solution of equation (D.5), it can be shown that:

$$K = \frac{y_{ss}}{r_r}\,, \tag{D.6}$$

$$\rho = -\frac{1}{2\pi}\ln\left[\frac{y_{p2} - y_{ss}}{y_{p1} - y_{ss}}\right]\,, \tag{D.7}$$

$$\zeta = \sqrt{\frac{\rho^2}{1+\rho^2}}\,, \tag{D.8}$$

$$\tau = \frac{(t_{p2} - t_{p1})\sqrt{1-\zeta^2}}{2\pi}\,, \tag{D.9}$$

$$d = \frac{S_c}{y_{ss}} - 2\zeta\tau\,, \tag{D.10}$$

where y_{ss}, y_{p1}, y_{p2}, t_{p1} and t_{p2} are defined in Figure D.10. The magnitude of the set-point change is indicated by r_r, and S_c is the characteristic area defined by:

$$S_c = \int_0^{+\infty} [y_{ss} - y(t)]dt\,, \tag{D.11}$$

From the values of K, ζ, τ and d, the frequency response of the closed-loop system, $G_{cl}(j\omega)$, can be determined. Knowing the dynamics of the closed-loop system $G_{cl}(j\omega)$ and the dynamics of the controller $G_c(j\omega)$, the open-loop dynamics of the process $G_p(j\omega)$ can be determined by separating the dynamics of the controller from the closed-loop dynamics [49].

The critical frequency of the closed-loop system ω_c can be obtained by solving the following equation:

$$-d\omega_c - \arctan\frac{2\zeta\tau\omega_c}{1-\tau^2\omega_c^2} = -\pi\,, \tag{D.12}$$

Moreover, if $|G_{cl}(j\omega_c)|$ denotes the closed-loop magnitude ratio (MR) at the crossover frequency, then the open-loop MR at ω_c is given from:

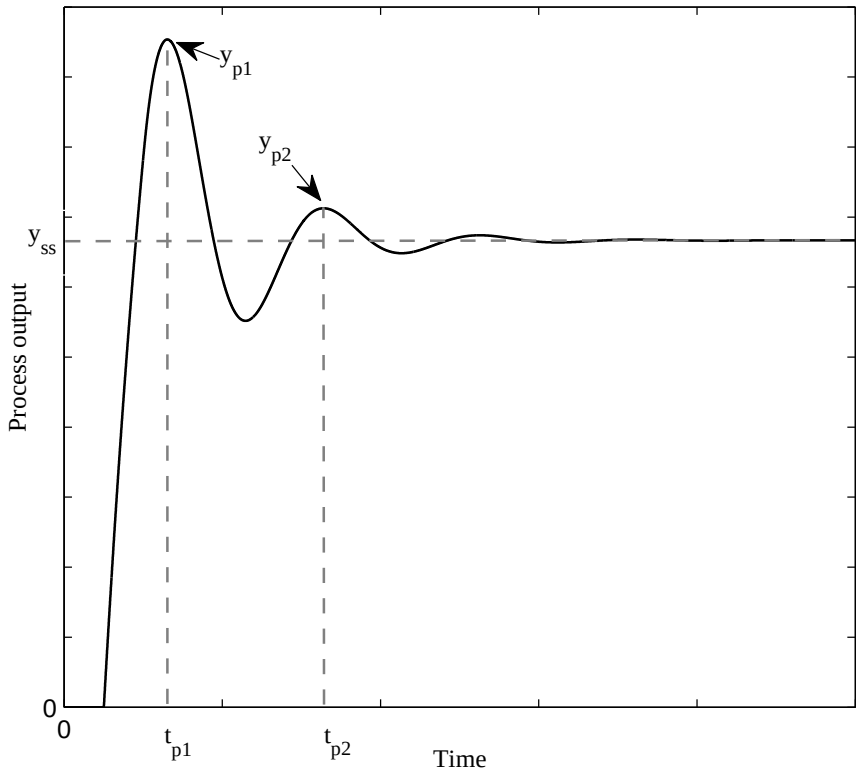

Figure D.10: Typical under-damped closed-loop response to a step-set-point change.

$$|G_c(j\omega_c)G_p(j\omega_c)| = \frac{|G_{cl}(j\omega_c)|}{1+|G_{cl}(j\omega_c)|}\,. \tag{D.13}$$

The corresponding closed-loop magnitude is determined from:

$$|G_{cl}(j\omega_c)| = M = \frac{K}{\sqrt{\left(1-\tau^2\omega_c^2\right)^2+\left(2\tau\zeta\omega_c\right)^2}}\,, \tag{D.14}$$

The parameters of the FOPDT model are given by:

$$K_p = \frac{T_i}{K_c S_c} y_{ss}\,, \tag{D.15}$$

$$\tau_p = \frac{\sqrt{\left(K_cK_p\right)^2\left(1+T_i^2\omega_c^2\right)\left(1+M\right)^2-\left(MT_i\omega_c\right)^2}}{M\omega_c^2T_i}\,, \tag{D.16}$$

$$d_p = \frac{1}{\omega_c}\left[\arctan\left(T_i\omega_c\right)+\arctan\left(\frac{1}{\tau_p\omega_c}\right)\right]\,, \tag{D.17}$$

where equations (D.16) and (D.17) are corrected version of the equations given by Mamat and Fleming [49].

Bibliography

[1] Mick Schwedler. *Applications Engineering Manual. Multiple-Chiller-System Design and Control.* TRANE, 2001.

[2] ASHRAE. *ASHRAE Handbook - HVAC Systems and Equipment. American Society of Heating, Refrigerating and Air-Conditioning Engineers.* Atlanta (Chapter 42), 2008.

[3] R.J. Hackner, J.W. Mitchell, and W.A. Beckman. Hvac system dynamics and energy use in buildings - part i. *ASHRAE Trans*, 90(213):523–35, 1984.

[4] ASHRAE. *ASHRAE Handbook - HVAC Applications. American Society of Heating, Refrigeration and Air Conditioning Engineers.* Atlanta (Chapter 41), 2007.

[5] Y.C. Chang, J.K. Lin, and M.H. Chuang. Optimal chiller loading by genetic algorithm for reducing energy consumption. *Energy and Buildings*, 37(2):147–155, 2005.

[6] Y.C. Chang. An innovative approach for demand side management-optimal chiller loading by simulated annealing. *Energy*, 31:1883–1896, 2006.

[7] Y.C. Chang, F.A. Lin, and C.H. Lin. Optimal chiller sequencing by branch and bound method for saving energy. *Energy Conversion and Management*, 46:2158–2172, 2005.

[8] Y.C. Chang. An outstanding method for saving energy-optimal chiller operation. *IEEE J EC*, 21(2):527–532, 2006.

[9] Nassif N., S. Kajl, and R. Sabourin. Optimization of hvac control system strategy using two-objective genetic algorithm. *HVAC&R Research*, 11(3):459–86, 2005.

[10] L. Lu and W. Cai. Application of genetic algorithms for optimal chiller selection in hvac systems. In *13th Int. Conference on Process Control. Strbské Pleso, Slovakia, June 11-14*, 2001.

[11] Steve Doty Wayne C. Turner. *Energy Management Handbook.* The Fairmont Press, Inc, 2006.

[12] Chris P. Underwood. *HVAC Control Systems Modelling, Analysis and Design.* Spon Press, 1999.

[13] Bela Liptak. *Optimization of Unit Operations.* Chilton Book Company, 1987.

[14] B. Atanasiu and P. Bertoldi. Electricity consumption and efficiency trends in the enlarged european union - status report. *JRC*, 2006.

[15] J. Adnot and et al. Energy efficiency and certification of central air conditioners (eeccac). *Study for the D.G. Transportation-Energy (DGTREN) of the Commission of the E.U. - Final report*, 2003.

[16] http://www.mtprog.com/.

[17] MTP. Energy consumption of air conditioning systems. *Market Transformation Programme - UK*, 2006.

[18] www.eurovent-association.eu/.

[19] Herbert W. Stanford III. *Hvac Water Chillers And Cooling Towers: Fundamentals, Applications And Operation.* Marcel Dekker, Inc, 2007.

[20] G.L. Morini and S. Piva. The simulation of transients in thermal plant. part i: Mathematical model. *Appl. Therm. Eng*, 27(11-12):2138–2144, 2007.

[21] W.L. Jian and M. Zaheeruddin. Sub-optimal on-off switching control strategies for chilled water cooling systems with storage. *Appl. Therm. Eng.*, 18 (6):369–386, 1998.

[22] M. Albieri, A. Beghi, C. Bodo, and L. Cecchinato. Advanced control systems for single compressor chiller units. *International Journal of Refrigeration*, 32(5):1068 –1076, 2009.

[23] E.W. Lemmon, M.O. McLinden, and M.L. Huber. Nist reference fluid thermodynamic and transport properties refprop 7.0. Technical report, NIST Std. Database, 2002.

[24] Rishel. Control of variable speed pumps for hvac water systems. *Ashrae Trans*, 109(1):380–392, 2003.

[25] Avery. Controlling chillers in variable flow systems. *Ashrae Journal*, 40(2):42–47, 1998.

[26] Air Conditioning & Refrigeration Institute ARI. Unitary air-conditioning and air-source heat pump equipment, standard 210/240, arlington virginia. Technical report, 1989.

[27] UNI-10963:2001. Air conditioners, liquid chilling packages and heat pumps - performance tests at part load. Italy, 2001.

[28] E. Bettanini, A. Gastaldello, and L. Schibuola. Simplified models to simulate part load performances of air conditioning equipments. In *Eighth International IBPSA Conference Eindhoven, Netherlands*, August 11-14, 2003.

[29] C. Bodo. Algoritmo di supervisione e controllo per macchine frigorifere (in italian). Master's thesis, University of Padova, 2006.

[30] M. Bertinato. Algoritmi genetici per l'ottimizzazione di sistemi di supervisione per impianti hvac (in italian). Master's thesis, University of Padova, 2008.

[31] A. Beghi, M. Bertinato, L. Cecchinato, and M. Rampazzo. A multi-phase genetic algorithm for the efficient management of multi-chiller systems. In *Proceedings of the 7th Asian Control Conference, Hong Kong, China*, August 27-29, 2009.

[32] P.O. Fanger. *Thermal Comfort*. PhD thesis, Copenhagen: Danish Technical, 1970.

[33] ISO 7730:2005. Ergonomics of the thermal environment – analytical determination and interpretation of thermal comfort using calculation of the pmv and ppd indices and local thermal comfort criteria. Technical report, ISO, 2005.

[34] T. Kailath. *Linear Systems*. Englewood Cliffs, NJ: Prentice Hall, 1979.

[35] J. Kautsky and N.K. Nichols. Robust pole assignment in linear state feedback. *Int. J. Control*, 41:1129–1155, 1985.

[36] Y.R. Tsoy. The influence of population size and search time limit on genetic algorithm. In *Proc. 7th Korea-Russia International Symposium on Science and Technology KORUS*, volume 3, pages 181–187, 28 June–6 July 2003.

[37] G.A. Jayalakshmi, K. Srinivasan, and R. Rajaram. Performance analysis of a multi-phase genetic algorithm in function optmization. *IE(I) Journal-CP*, Vol 85, 2004.

[38] P. Surry and N. Radcliffe. Inoculation to initialize evolutionary search. *In Evolutionary Computing: AISB workshop*, LNCS 1141, 1996.

[39] EnergyPlus. *http://www.energyplus.gov*, 2003.

[40] R.B. Holstien. *Artificial Genetic Adaptation in Computer Control Systems, PhD Thesi.* PhD thesis, Department of Computer and Communication Sciences, University of Michigan, Ann Arbor, 1971.

[41] R.A. Caruana and J.D. Schaffer. Representation and hidden bias: Gray vs. binary coding. In *Proc. 6th Int. Conf. Machine Learning*, pages 153–161, 1988.

[42] K.J. Astrom and T. Hagglund. *PID controllers: Theory, Design and Tuning.* Instrument Society of America, North Carolina, 1995.

[43] A. Beghi, L. Cecchinato, and M. Rampazzo. On-line, auto-tuning regulation of electronic expansion valve for evaporator control. In *7th IEEE International Conference on Control & Automation (ICCA'09), Christchurch, New Zealand*, December 9-11, 2009.

[44] J. Chi and D.A. Didion. Simulation model of the transient performance of a heat pump. *Int J. Refrig.*, 5:176–180, 1982.

[45] J.W. MacArthur. Transient heat pump behavior: a theoretical investigation. *Int. J. Refrig.*, 7:123–132, 1984.

[46] H. Wang and S.Touber. Distributed and non-steady-state modeling of an air cooler. *Int. J. Refri.*, 14:98–111, 1991.

[47] A. Beghi and L. Cecchinato. A simulation environment for dry-expansion evaporators with application to the design of autotuning control algorithms for electronic expansion valves. *International Journal of Refrigeration*, 32(7):1765 – 1775, 2009.

[48] D. Dougherty and D. Cooper. A practical multiple model adaptive strategy for single-loop mpc. *Control Engineering Practice*, 11:141–159, 2003.

[49] R. Mamat and P.J. Fleming. Method for on-line identification of a first order plus dead-time process model. *Electronic Letters*, 31(15):1297–1298, 20th July 1995.

[50] J.G. Ziegler and N.B. Nichols. Optimum settings for automatic controllers. *Trans. ASME*, 65:433–444, 1943.

[51] G.H. Cohen and G.A. Coon. Theoretical considerations of retarded control. *Trans. ASME*, 75:827–834, 1953.

[52] F.G. Shinskey. *Process Control Systems: Applications, Design and Adjustment.* McGraw-Hill, New York, 1988.

[53] G.J. Silva, A. Datta, and S.P. Bhattacharya. Pi stabilization of first order systems with time delay. *Automatica*, 37:2025–2031, 2001.

[54] K.L. Chien, J.A. Hrones, and J.B. Reswick. On the automatic tuning of generalized passive systems. *Trans. ASME*, 74:175–185, 1952.

[55] M. Zhuang and D.P. Atherton. Automatic tuning of optimum pid controllers. *IEE Proceedings of Control Theory and Applications*, 140:216–224, 1993.